PHILOSOPHICAL TRANSACTIONS OF THE ROYAL SOCIETY A MATHEMATICAL, PHYSICAL & ENGINEERING SCIENCES

The Fermi Surfaces of Copper, Silver and Gold I. The de Haas-van Alphen Effect

D. Shoenberg

Phil. Trans. R. Soc. Lond. A 1962 **255**, 85-133
doi: 10.1098/rsta.1962.0011

THE FERMI SURFACES OF COPPER, SILVER AND GOLD

I. THE DE HAAS–VAN ALPHEN EFFECT

By D. SHOENBERG, F.R.S.
The Royal Society Mond Laboratory, University of Cambridge

(*Received* 12 *March* 1962)

[Plates 1 and 2]

CONTENTS

Following the discovery of the effect in copper, silver and gold by the impulsive high-field method, a study of the variation of the oscillatory frequency (which is proportional to the extremal area of cross-section of the Fermi surface by planes normal to the field) with the direction of the magnetic field relative to the crystal axes has made possible a detailed determination of the Fermi surfaces of these metals. As well as high-frequency oscillations associated with major ('belly') sections of the Fermi surface, low frequency oscillations are observed for the field in the [111] direction, which can be associated with the 'necks' in which the Fermi surface makes contact with the hexagonal faces of the Brillouin zone, as suggested by Pippard. The general topology of Pippard's model is confirmed by the existence of medium frequencies for the field along [100] and [110], which can be associated with 'hole' sections having the shape of a 'rosette' and a 'dog's bone', respectively. By making the high-frequency belly oscillations beat with the oscillations from a reference specimen, it has proved possible to measure the small variations of the belly frequency with field direction, which amount to only a few parts per cent, with an accuracy of a few parts per cent. These variations and the neck frequency have been fitted by Roaf to an analytical representation of the Fermi surface in the form of a Fourier series for each metal as explained in the accompanying paper, and the calculated surfaces are found to give the correct frequency for every direction studied. The surfaces have been chosen to have a volume exactly half that of the Brillouin zone, and the fact that the absolute values of the frequencies predicted by Roaf's formulae agree within experimental error with the observed frequencies confirms the validity of the assumption that these metals have exactly one electron per atom. It shows also that electron interaction effects do not modify appreciably the theoretical relation between frequency and area which was derived by Onsager without taking such effects into account.

From the variation of the amplitude of the oscillations with temperatures and field, information is deduced about cyclotron masses and electron relaxation times. The absolute amplitude of the oscillations is found to agree in order of magnitude with theoretical prediction, but to explain the very strong harmonic content of the oscillations, it is necessary to invoke a new mechanism. This is the frequency modulation of the applied field caused by the oscillations of the magnetization, the contribution of which to the local field is appreciable when the differential susceptibility is, as here, comparable to $1/4\pi$, but is neglected in the theory as usually developed. It is shown that this frequency modulation effect can account in order of magnitude for the harmonic content and is probably also responsible for certain anomalies observed in the field and temperature variation. The paper concludes with a discussion of a number of effects which can appreciably reduce the observed amplitude. These are field inhomogeneity, specimen imperfections such as bending and random substructure, inhomogeneity of field due to eddy currents, and various possible heating effects which can raise the temperature of the specimen above that of the bath. In many of the experiments resonant amplification is used and the rapid passage through resonance ('gliding tone' effect) which is relevant to various of the amplitude problems, is discussed in an appendix.

Introduction

The importance of the de Haas–van Alphen effect (the oscillatory dependence on magnetic field of the magnetic properties of metal single crystals at low temperatures) as a tool in the investigation of the electron structure of metals, arises mainly from the formula (Onsager 1952)

$$F = chA/4\pi^2 e, \tag{1}$$

which relates the frequency F (defined as the reciprocal of the periodic interval P, in $1/H$)* and the extremal area A of cross-section of the Fermi surface by planes normal to the field direction. By observing how F, and therefore A, varies with the direction of H, valuable information about the size and shape of the Fermi surface can be inferred. Other interesting information can in principle, and to some extent in practice, be obtained from the temperature and field variation of the amplitude of the oscillations: the former gives the cyclotron mass and the latter information about the relaxation time.

From the point of view of simplicity of interpretation it would evidently be best to study monovalent metals, since for them the Fermi surface should consist of a single sheet whose volume should be just half that of the fundamental zone. In fact, however, until recently, the de Haas–van Alphen effect was observed only in polyvalent metals. The early experiments (see, for example, Shoenberg 1952*a*) in which the torque on a single crystal was observed, could indeed hardly have shown up the oscillations characteristic of a large sheet of Fermi surface (such as that of a monovalent metal) because of the insufficient magnitude of the magnetic field used. The actual field interval ΔH of one oscillation is just H^2/F, and a limit to the frequency which can be measured is set by the unsteadiness of the field in time and inhomogeneity over the specimen. In the conditions of these early experiments H was of order 10^4 G and the unsteadiness and inhomogeneity was of order 10 G, so it is clear that frequencies much higher than $F = 10^7$ G would have been beyond the resolution of the experiments; this is still only one-fiftieth of $F = 5\times 10^8$ G, the frequency expected

* In previous papers on the de Haas–van Alphen effect it has been usual to discuss the results in terms of P, but in fact $F = 1/P$ is rather more convenient both because F is directly proportional to A and because it lends itself better to discussion of beats.

to be typical of a monovalent metal. Even if the resolution were greatly improved by better stabilization and homogeneity, the amplitude of the oscillations would be extremely small because of the factor $\exp(-4\pi^3 mckT/ehH)$ which enters into the theoretical formula for the amplitude. This is about e^{-20} for $T = 1°K$ and $H = 10^4$ G if m, the cyclotron mass, is assumed to be just the ordinary electronic mass. It is only because the small sheets of Fermi surface characteristic of polyvalent metals have low values of m that appreciable amplitudes do in fact show up in experiments at low fields.

To observe large areas of Fermi surface it is necessary to go to much higher fields and a method (Shoenberg 1952*b*, 1953) was developed in which fields of order 10^5 G were produced impulsively by discharging a condenser through a coil, and observing the de Haas–van Alphen effect by the oscillatory e.m.f. produced in a pick-up coil surrounding the specimen as the field varied. Although this method was successful in showing up in various polyvalent metals much larger pieces of Fermi surfaces than had been observed in lower fields, no effect was found in any monovalent metal for several years. It was gradually realized that the observation of oscillations with F as high as 5×10^8 G would make great demands on the homogeneity not only of the field over the specimen but of the specimen itself. The phase of the oscillations is $2\pi F/H$ and even with H as high as 10^5 G this is $10^4\pi$ for $F = 5 \times 10^8$ G so that H and F cannot be allowed to vary by much more than 1 part in 10^4 if the amplitude is not to be seriously reduced. Since F is orientation-dependent, a possible source of trouble is a slight variation of crystal orientation through the specimen. This effect would clearly be least serious for H along a symmetry direction (where F must be maximum or minimum) and the idea of using copper whiskers suggested itself. Not only do these usually grow with a symmetry axis along the axis of figure (so that a whisker can be set with the field along a symmetry direction, merely by alining the whisker axis with the field), but they grow just about thin enough to avoid difficulties due to eddy currents in the specimen. It was in fact in copper whiskers that the de Haas–van Alphen effect was first observed in a monovalent metal (Shoenberg 1959).

A few months later the effect was found in silver and gold single crystals grown from the melt and an important step forward was the discovery that for certain crystallographic directions oscillations occurred of other and lower frequencies than those associated with major sections of the Fermi surface. It soon became apparent (Shoenberg 1960*a*) that the results for all three metals were consistent with a model of the Fermi surface similar in character to that proposed by Pippard (1957) for copper on the basis of experiments on the anomalous skin effect. Essentially, this is a sphere distorted so much that it makes contact with the hexagonal faces of the Brillouin zone; in the repeated zone scheme this has the appearance illustrated schematically, in figure 1. It can be seen that in this model there are several kinds of extremal areas: (*a*) round the 'belly' of the Fermi surface (maxima),* (*b*) round the 'neck' (minima) joining the surfaces in adjacent zones, and (*c*) round various hole sections, such as the 'dog's bone' and the 'four-cornered rosette' (figure 2). Oscillations of frequencies corresponding very plausibly in magnitude to most of these extremal areas were indeed observed for the field along the appropriate symmetry directions, thus definitely establishing the general form of the Fermi surfaces and

* The distortion from a sphere is, however, so severe that the (111) belly section proves to be a minimum rather than a maximum.

PHILOSOPHICAL TRANSACTIONS OF THE ROYAL SOCIETY A MATHEMATICAL, PHYSICAL & ENGINEERING SCIENCES

approximately confirming that the volumes of the surfaces were those appropriate to 1 free electron per atom.

It still remained, however, to determine the precise shapes and sizes of the surfaces. To do this it was necessary to measure accurately the small variations (only a few parts per cent) of belly frequency with field direction over as wide as possible a range of directions and to work out an inversion procedure for converting such measurements (and those on neck areas) into a precise analytical specification of the Fermi surface. The

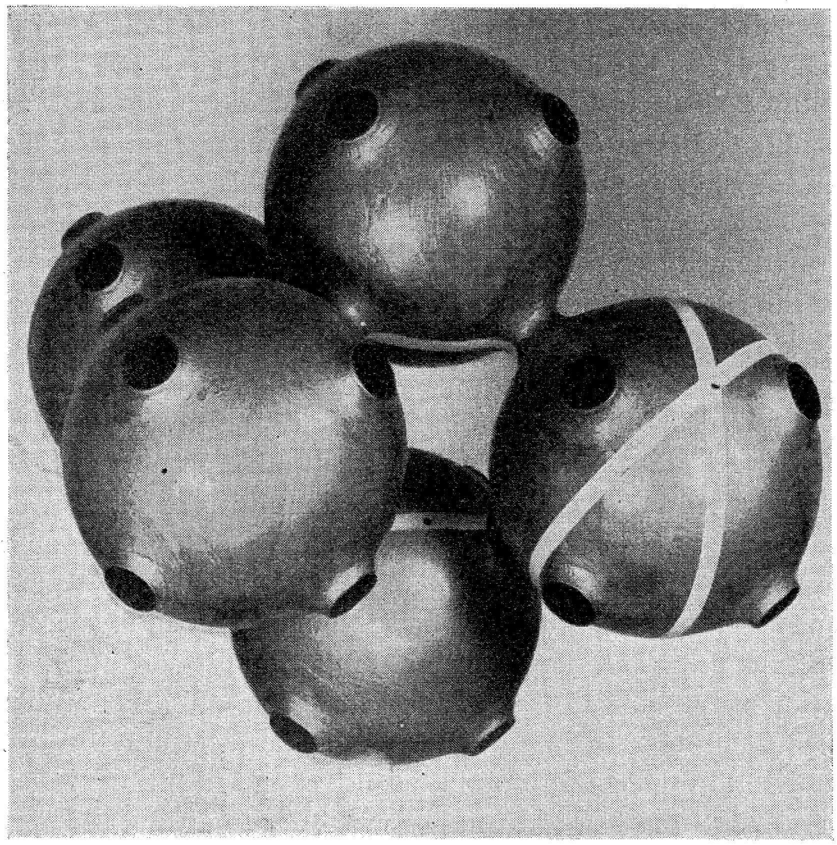

FIGURE 1. Schematic model of Fermi surface; the real surfaces are much less spherical (a photograph showing the shape of the gold surface appears in Shoenberg (1962) and sections of the various surfaces are shown in figure 3 of II). The white bands pick out the (100) and (111) 'belly' sections (vertical and oblique, respectively), and part of the 'four-cornered rosette'.

experimental problem was solved by exploitation of the beat method, in which the oscillations from the specimen are made to beat against those from a reference specimen whose orientation is fixed, so that the slight changes of frequency as the specimen is rotated relative to the field show up as much larger changes of beat frequency.

The inversion procedure, by which the raw material of the frequency data was converted into analytical formulae describing the Fermi surfaces, was worked out by Mr D. J. Roaf, as described in the accompanying paper (II). Essentially what he has done is to fit to the experimental data for each metal a Fourier expansion with a small number of adjustable coefficients by a process of trial and error in which extremal areas for each trial surface were calculated by the electronic computer EDSAC II. The coefficients were chosen in

PHILOSOPHICAL TRANSACTIONS OF THE ROYAL SOCIETY A MATHEMATICAL, PHYSICAL & ENGINEERING SCIENCES

the first place to fit only a small number of experimental features, and the formulae proved in fact to fit the experimental values of F surprisingly well over the whole range studied. Finally, the formulae were 'trimmed' slightly to improve their fit with the anomalous skin effect data of Pippard (1957) for copper and Morton (1960) for silver, while leaving their fit with the de Haas–van Alphen data almost unimpaired. It is not unreasonable to claim that the Fermi surfaces as described by the final formulae have now been determined to an accuracy of order 1 % in radius vector.

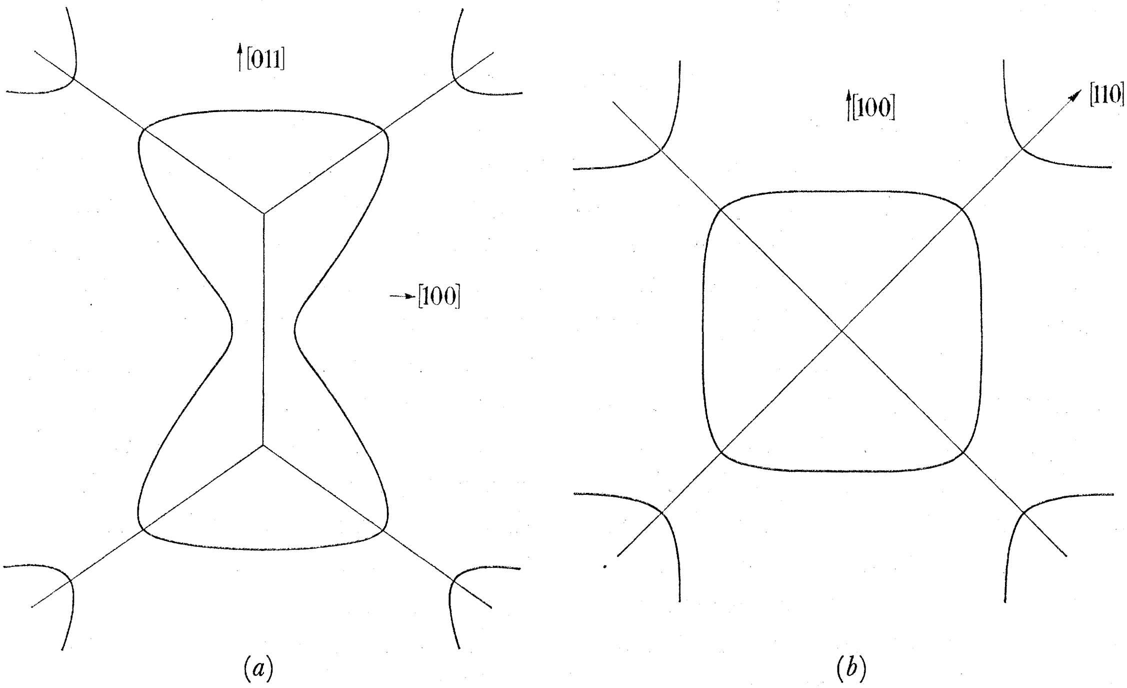

FIGURE 2. (*a*) The dog's bone (*b*) the four-cornered rosette. Both sketches are based on Roaf's Au IV formula and are drawn a little schematically but to the same scale; the straight lines show the intersections of each section with the Brillouin zone and the beginnings of the neighbouring orbits are indicated. In gold the surface is so distorted from a sphere that the rosette no longer has the appearance which originally suggested its name. (It should be noted that the sketch of the rosette for gold in Shoenberg (1962) is incorrect.)

Following an account of the experimental techniques, the main theme of the paper is the presentation of the frequency measurements and their comparison with Roaf's formulae. Some results on the temperature variation of amplitude (from which cyclotron masses can be deduced), on the field variation of amplitude and on other amplitude questions (absolute size, orientation dependence, strengths of harmonics) will also be described.

EXPERIMENTAL TECHNIQUE

The general principles of the high field method have already been sufficiently described (Shoenberg 1953, 1957; Gold 1958) and only those aspects will be described here which are particularly relevant.

The high-field installation

The first successful results on whiskers were obtained using the installation in the form described by Gold (1958) in which discharge of a 2000 μF condenser charged to 1700 V produced a field rising to a peak of $0{\cdot}8\times10^5$ G in 11 ms in a magnet coil cooled in liquid nitrogen. Shortly afterwards a new installation was used in which the capacity of the condenser bank and the magnet coil characteristics were about the same as before, but voltages up to 2500 V were used giving peak fields up to about $1{\cdot}1\times10^5$ G. Still later the capacity of the condenser bank was raised to 4000 μF and this increased the peak field to about $1{\cdot}35\times10^5$ G and the rise time to about 15 ms. A few measurements were made also with two other magnet coils in each of which a field of about $1{\cdot}9\times10^5$ G rising to its peak in 7 ms was obtained by discharging 4000 μF charged to 2300 V.

The pick-up coil system

To eliminate most of the e.m.f. induced directly in the pick-up coil by the varying field a second pick-up coil is connected in series opposition. In these experiments this balancing coil was arranged in a novel way; instead of being side by side or in line with the pick-up coil which contains the specimen it was wound *around* it but with a considerably smaller number of turns chosen so that the area-turns just blanced those of the specimen coil. This somewhat reduced sensitivity, since the effective number of turns linked to the specimen is now the *difference* between the numbers of turns in the two coils, and typically this reduction was by 30% or so, but the arrangement has the advantage of compactness. Moreover, detailed consideration shows that any movement of such a balanced pair in a slightly inhomogeneous field produces less change of flux linkage than for other dispositions in which the centres of gravity of the two coils are separated. In principle then, this system should produce less 'noise' due to mechanical vibration, though it is not certain that this source of 'noise' was in fact ever an important one.

The problem of varying the orientation of the specimen with respect to the field and of knowing this orientation accurately is complicated by the smallness of the space available; essentially it involves rotation about a horizontal axis within a vertical cyclinder of 11 mm diameter (the bottom end of the liquid-helium Dewar vessel), and the rotation must be operated from outside, some 60 cm above the specimen. A further difficulty is that the whole assembly must be made of insulating materials in order to avoid field distortion by eddy currents. Because of the small space it is not practicable to rotate the specimen (usually 5 mm long) within its pick-up coil and it is necessary to rotate the pair of pick-up coils together with the specimen as a unit.

The orientation of the coil axis was accurately determined by a method suggested by Professor A. B. Pippard. A 'monitor' coil wound on a hoop of diameter 70 cm and fed with 1 kc/s a.c. was set up outside the apparatus and rotated about a horizontal axis passing through the specimen and perpendicular to the specimen coil axis, until the e.m.f. induced in the specimen coil disappeared. In this position of zero mutual inductance, which was indicated by a pointer on an angular scale, the plane of the monitor coil is parallel to the axis of the specimen coil. In this way angular *differences* between settings of the specimen coil (and therefore of the specimen) could be determined to better than $\frac{1}{2}°$, but because of slightly imperfect geometry and small stray e.m.fs. in the circuit, there was usually a zero error of as much as 2° in the orientation indicated by the pointer. Fortunately the true zero could usually be fixed from the symmetry of the frequency variation, so that the accurately determined angular differences were sufficient.

The method of rotating the specimen coil described by Gold (1958) had certain drawbacks and two new arrangements were tried. In the first (which was used only in the early exploratory experiments) the coil assembly was suspended from three equal threads about 2 cm long which were attached to three long rods coming out at the top of the apparatus, and whose relative heights could be delicately controlled by screws. This had the theoretical advantage that the specimen could be rotated in any plane during the same experiment. In practice, however, this extra degree of freedom complicated the monitoring procedure and was not of great value, since a proper study of the variation in any one plane of rotation usually required a whole helium experiment; also the range of angular variation could not be made greater than about 20°.

The second arrangement, which was used in all the definitive experiments, was suggested and worked out in detail by Mr H. L. Davies. The specimen coil was mounted in a wheel of diameter 10 mm which carried two sets of teeth on its circumference and could be turned through nearly 90° in either sense by pushing on a spade-ended rod which could be made to engage with the appropriate set of teeth at the appropriate place. This simple arrangement has worked very reliably in many experiments and has the advantage over Gold's winch arrangement and the trifilar suspension, that once the spade is withdrawn, the wheel is not subject to rotational drift, such as occurred in the other arrangements because of thermal expansion in the strings or rods, as the liquid helium level fell. The effective plane of rotation of the field with respect to the specimen can be varied in between helium experiments by rotating the specimen mounting about the specimen coil axis through known angles. Because of the miniature scale of the specimen mount and inaccuracies in the X-ray determination of the specimen orientation, some uncertainty of the plane of rotation was difficult to avoid, but probably this uncertainty rarely exceeded a few degrees. As far as possible the planes of rotation were chosen to be in or near symmetry planes so that slight departures from them would have little effect (since frequencies should have extremal values with respect to departures from symmetry planes).

For the beat method it was necessary to have a second pair of pick-up coils containing the 'reference' specimen and this second pair was mounted with its centre 1 cm below the axis of rotation of the specimen coil pair. The homogeneity of the magnet coils used was just good enough to tolerate this separation of 1 cm, the minimum compatible with free movement of the rotating coil, and the field variation over each specimen was less than 1 part in 10^4;* even so, this slight inhomogeneity is probably responsible for an appreciable diminution of amplitude (see p. 119).

The detection system

The oscilloscope used was a twin-beam Nagard DT 103. The output from the pick-up coils was passed through a high-pass filter, cutting off below about 1 kc/s, to eliminate the residual out-of-balance e.m.f. induced by the varying field (which otherwise swamped the amplifier) and then applied to the amplifier of the c.r.o. In some of the early experiments auxiliary amplifiers were also used. The detecting circuit could be made resonant by

* In the magnet coil which gave $1{\cdot}9\times10^5$ G, however, the homogeneity may have been as poor as 1 part in 2000 over the specimen in some circumstances.

TABLE 1

no.	orientation of specimen axis	source	method	length (mm)	diam. (mm)	R(20 °C)/R(4·2 °K)	
Cu 35				7·3	0·26		
Cu 41				5·4	0·14		
Cu 43	[111]			4·3	0·18	135	
Cu 46				6·5	0·15		
Cu 47				3·6	0·11		
Cu 48				3·5	0·20		
Cu 38		G.E. whiskers		7·5	0·16 × 0·16	390	(170)
Cu 45				3·0	0·11 × 0·13		
Cu 49	[100]			3·6	0·08 × 0·18		
Cu 51				3·6	0·08 × 0·08		
Cu 52				3·5	0·09 × 0·10		
Cu 42	[110]			5·0	0·05 × 0·14		
Cu 44				5·0	0·05 × 0·20		
Cu 68	11° off [111]	I	(a)	3·4	0·16	11	
Cu 72	5° off [111]	B		6·2	0·20	1520	
Cu 73	7° off [111]		(b)	3·5	0·14	670	
Cu 75	3° off [111]	J.M. 4234		4·0	0·13	87	
Ag 7	28° off [100]			6·0	0·16	92	
Ag 8	19° off [100]			4·5	0·17		
Ag 15	18° off [111]	H	(a)	2·6	0·35		(60)
Ag 19	12° off [110]			4·5	0·16		
Ag 21	13° off [100]			2·6	0·17	48	
Ag 27	3° off [111]			3·4	0·30		
Ag 28	4° off [111]	M	(b)	3·6	0·30	105	
Ag 30	2° off [100]			5·0	0·20		
Au 7	14° off [100]			3·2	0·13		
Au 8	8° off [111]			3·2	0·24		
Au 9	18° off [110]			4·5	0·30		
Au 16	7° off [111]	H	(a)	3·6	0·27		(12, 19, 40)
Au 21	2° off [110]			4·1	0·50		
Au 29	17° off [100]			2·5	0·35		
Au 31	8° off [111]			4·1	0·28	18	
Au 36	1° off [100]	J.M. 3226	(b)	4·3	0·29	95	(71)
Au 37	4° off [111]			6·2	0·30		
Ag–Au 17	5° off [111]	J.M. 1761 (0·31 % Ag)	(a)	3·1	0·36		(15·3, 13·7)

Notes. The orientations given are intended only as rough indications. Many of the specimens were not exact cylinders, and the diameters quoted indicate rough averages. The whiskers, however, had fairly regular cross-sections, hexagonal for the [111] and rectangular for the [100] and [110] whiskers; the figures for [111] whiskers are the diagonals across opposite corners, and for the other whiskers the sides of the rectangles (accuracy ~ 10 %). The code letters for source have the following meanings: G.E., General Electric Co., Schenectady (see text), I, Illinois; the crystal was grown from wire drawn down from an ingot of very pure copper kindly supplied by Dr J. S. Koehler of the University of Illinois. B, Bell Telephone Laboratories; the crystal was spark cut from a large single crystal ingot kindly supplied by Dr J. E. Kunzler. H, Heraeus; pre-war stock of unknown purity. M, Dr A. R. Mackintosh who prepared a large single crystal silver ingot of fairly high purity but unknown origin, from which these crystals were spark cut. J.M., Johnson, Matthey and Co., Ltd (the number following is their laboratory report number). The methods of preparation (*a*) and (*b*) are those explained in the text. The measurements of residual resistance were made only after the main experiments had been completed and only some of the specimens actually used were measured; the figures in brackets are for other specimens prepared from the same material by similar methods and give some idea of the variability. It should be noted that no allowance has been made for mean-free path effects; in Cu 72 and 73 the real resistivity is probably considerably lower than that indicated since the mean free path is of the same order as the specimen diameter. It seems that method (*a*), of growing a thin crystal in a graphite mould, introduces more impurity than (*b*), where an ingot of much larger diameter is melted; presumably this is because the larger surface to volume ratio of a thin specimen favours absorption of impurities from the graphite. Nearly all the specimens listed are mentioned in the text in connexion with particular experiments; Cu 35 and Au 7 are included as the specimens in which the de Haas–van Alphen effect was first observed in these metals; Cu 42 and 44 were used in unsuccessful attempts to find the dog's bone oscillations in copper and Cu 63, 72, 73 and 75 were used in unsuccessful attempts to observe the de Haas–van Alphen effect in copper crystals grown from the melt.

PHILOSOPHICAL TRANSACTIONS OF THE ROYAL SOCIETY A MATHEMATICAL, PHYSICAL & ENGINEERING SCIENCES

connecting a small condenser across the pick-up coil system (see p. 95); one of the pick-up coil systems used, however, had sufficient self capacity to resonate at 80 kc/s without any external condenser.

The specimens and their mounting

The specimens for which results are quoted in this paper are listed in table 1; many others were produced in unsuccessful attempts to achieve particular orientations or were used in preliminary experiments which for a variety of reasons were partly or wholly unsuccessful.

The copper whiskers were prepared by Mrs E. L. Fontanella of General Electric Co., Schenectady, New York using techniques of handling described by Fontanella & De Blois (1959). Copper, silver and gold crystals were grown by slow cooling of the molten metal in graphite moulds under vacuum ($\sim 3 \times 10^{-5}$ mm Hg), but two different procedures were used:

(*a*) Many wires of about $\frac{1}{2}$ mm diameter and 5 mm long were crystallized with random orientations and one or two selected which were sufficiently close to the desired orientation. This procedure, which was very wasteful in time because of its small yield, was later abandoned in favour of (*b*).

(*b*) An ingot of about 6 mm diameter and 1 cm long was crystallized and then several $\frac{1}{2}$ mm diameter cylinders were 'spark-cut' from it in the desired orientation.

The $\frac{1}{2}$ mm diameter crystal produced by either method was reduced by suitable chemical means (dilute nitric acid for copper, 3% hydrogen peroxide in ammonia for silver, and boiling saturated solution of ferric chloride for gold) to a diameter of order 0·1 to 0·3 mm according to circumstances. The crystal was then mounted in a thin-walled Pyrex glass tube of internal diameter 0·8 mm with a thin layer of petroleum jelly diluted in ether (or occasionally Durofix), leaving a clear space round it for good contact with liquid helium. Finally, the glass tube was glued into a cylindrical ebonite head co-axial with itself and carrying a small mirror. The normal to the mirror and the axis of the tube provided a system of axes with respect to which the orientation of the crystal was determined by X-rays.

Frequency measurement

Three techniques have been used:

(i) *Direct method*

This is illustrated by figure 3, plate 1; the frequency F is deduced as $n/(1/H_1 - 1/H_2)$ where H_1 and H_2 are the fields at the beginning and end of a series of n oscillations. The field is recorded by the second beam of the c.r.o. as the voltage across a substandard 0·01 Ω resistor carrying the main magnet current. Although the method is simple in principle, many small points must be considered if an accurate result is to be obtained:

(*a*) Since typically $\Delta H/H$ for 100 oscillations (as many as can usually be resolved) is only 2%, the voltages of the calibration lines which form the basis of the measurement of H_1 and H_2 must be very precisely and reproducibly set. This was achieved by a simple circuit suggested by Dr J. Ashmead, which provides voltage tappings at intervals of 0·1 V, adjusted to within 1 part in 10^3 of their nominal values by reference to a standard cell.

The slight differences between the nominal and true values were determined with a potentiometer.

(*b*) It was found that when a calibration voltage was applied to the input of the c.r.o. there was an appreciable drift of the line on the screen lasting several seconds. To avoid this effect the voltage was applied for only a few milliseconds before the triggering of the c.r.o. so as to reproduce the conditions in which the field signal is applied. There was also usually a long-term drift of the positions of lines put on in this way and even though the calibration lines were put on within a few seconds of the field trace, and within a few seconds of each other, the positions of the lines relative to each other (and presumably relative to the field trace) were not exactly reproducible. This gives rise to a random error in measured frequency of order 1 % for any one determination.

(*c*) The analysis of photographs was made with a travelling microscope and it was assumed that the field corresponding to any feature of an oscillation is given by the intersection of the field trace with a line perpendicular to the direction of a trace with no signal on it. However, owing to various slight imperfections of the c.r.o. this can lead to small errors. First, the lines produced by the two beams are not always exactly parallel or even exactly straight; secondly, the two beams may not start from exactly corresponding points and thirdly they may travel with different velocities.

The errors due to each of the first two imperfections can be roughly eliminated if F is taken as the average of determinations, F_R for rising and F_F for falling fields, also, of course, care was usually taken to synchronize the starting points as well as possible. The third error is not eliminated by averaging F_R and F_F. On simplifying assumptions (exactly uniform speeds, and that the regions chosen for measurement are exactly symmetrical for rising and falling fields) it can be shown that if the velocity of the oscillation signal trace is $(1+\epsilon)$ times that of the field trace, the mean of F_R and F_F is $(1+2\epsilon)$ times the true frequency F if the rising and falling traces are photographed in the same discharge, but only $(1+\epsilon)F$ if the field rises throughout one photograph and falls throughout the other. Ideally, this error could be eliminated by repeating the measurements with the functions of the traces interchanged, but this was found too lengthy a procedure for routine measurements. Instead ϵ was estimated by photographing simultaneously on both traces a signal of appropriate frequency. Unfortunately the importance of this correction was not fully appreciated till rather late and this check was not always carried out; since ϵ was found to be as much as 2 % on occasion and even its sign varied from time to time, this leads to occasional uncertainties of as much as 4 % in some of the measurements.

(*d*) The effect of eddy currents in the specimen is to modify the observed frequency slightly by an amount depending on $\mathrm{d}H/\mathrm{d}t$ (see p. 124 for a detailed discussion). Evidently a mean of F_R and F_F tends to eliminate this error too.

(*e*) For weak signals it is often essential to use resonant amplification to bring the signal above the noise. In passing through resonance, however, the amplified signal changes phase by π with respect to the input signal, so that an extra half cycle of oscillation is counted when the field is rising and a half cycle is missed when the field is falling. This makes F_R greater and F_F less than F, by a factor $(1+\frac{1}{2}n)$ for n cycles, and so can be an appreciable source of error if only a few cycles are measureable. Here, too, the error can be eliminated by averaging F_R and F_F for comparable n.

(*f*) The potential across the 0·01 Ω through which the magnet current passes contains an appreciable component proportional to $\mathrm{d}H/\mathrm{d}t$ due to inductive effects. Once again the error is eliminated by averaging F_R and F_F.

(*g*) The voltage sensitivity of the c.r.o. was found to vary appreciably (by about 3 %) over the screen. Usually only three or four calibration lines were put on (covering the necessary range of variation of the field trace) and an appropriate interpolation procedure was used to allow for the non-linearity when the required field fell between two calibration lines. It can be estimated that the roughness of the interpolation procedure should cause a random error which is unlikely to exceed 1 % in any one determination of F.

(*h*) Finally, it is essential that the wiring of the circuit which carries the potential from the 0·01 Ω to the c.r.o. is not such as to introduce any additional potentials (apart from those mentioned in (*f*)). This should hardly need mention, but was in fact the cause of a systematic error of 8·8 % which was discovered only later in the investigation (and could fortunately be allowed for). The trouble (located by Dr M. G. Priestley and Mr B. R. Watts) was that owing to a redundant earth connexion an appreciable fraction of the main magnet current flowed through the lead connecting the negative end of the 0·01 Ω to the c.r.o.; thus the potential drop recorded was always greater by 8·8 % than the drop across the 0·01 Ω.* A good check on the correctness of the wiring is to verify that there is no potential recorded by the c.r.o. if both leads to it are connected to one or other of the 0·01 Ω resistance terminals; it was this check which led to the discovery of the trouble.

(ii) *Peak-to-peak method*

This is illustrated by figure 4 (plate 1). If a suitable small condenser (typically 0·03 μF) is put across the pick-up coil system the resulting circuit resonates at a frequency f (typically 50 kc/s). It can easily be seen that the time frequency of the de Haas–van Alphen oscillations will be just f when

$$\mathrm{d}H/\mathrm{d}t = H^2 f/F. \tag{2}$$

Since $\mathrm{d}H/\mathrm{d}t$ varies approximately linearly with t, i.e. with distance on the film, it follows that the separation of the resonant blips for rising and falling fields is roughly proportional to $1/F$ (the slight variation of H being ignored). This then forms the basis of a very simple method of comparison of frequencies either in the same, or different pictures.

In comparisons between different pictures it is important to allow for any changes of f and trace speed as well as for changes of H; because of this and the difficulty of precise definition of the blip maxima, it is difficult to achieve a consistency of better than 1 %. Although this method was useful in the exploratory experiments to establish that belly frequencies did not vary greatly, it was quite inadequate to follow the actual small changes with any accuracy. Comparisons within the same picture are much more useful, particularly in the determination of the frequencies of weak signals as ratios to those of stronger signals which have been established by careful use of the direct method. The method can give accurate results only if the ratio of frequencies is not too great; thus it is suitable for comparing the rosette and dog's bone, but not the neck, with the belly. In the accurate

* This error was present in all the data reported in the preliminary publications (Shoenberg 1960*a*, *b*). Thus the previously reported periods should be increased by 8·8 % and the cyclotron masses decreased by 8·8 %.

application of the method, the ratio of the 'peak-to-peak' separations on the film must be corrected to allow for the slight differences in the values of H at which the blips occur and for the slight departure of the time variation of field from an exact parabola. Assuming the variation to be of the form $e^{-kt}\cos(\omega t-\theta)$ it can be shown by a straighforward calculation that to an adequate approximation the ratio of frequencies should be given by

$$\frac{F_1}{F_2}=\frac{d_2}{d_1}\left\{1-\frac{5}{3}\left(1-\frac{8}{5}\frac{k^2}{\omega^2}\right)\left(\frac{H_2-H_1}{H_1}\right)\right\}, \tag{3}$$

where d_1 and d_2 are the respective peak-to-peak intervals on the film and H_1 and H_2 the fields at which the respective blips appear. The ratio k^2/ω^2 can be estimated from the capacity and the inductance and resistance of the coil as about 0·11 for 4000 μF and 0·055 for 2000 μF (though there is some uncertainty in the estimate of resistance because the coil rises in temperature during the discharge); the correction to d_2/d_1 usually amounts to less than 5 %.

(iii) *Beat method*

If the frequency to be determined is F and the reference frequency is X, then the beat frequency B is given by

$$B=|F-X| \tag{4}$$

when the specimen and reference coil systems are connected in series. Thus if X is known and B is measured, F can be inferred provided it is known which of F and X is larger. Two variants of the method have been used:

(*a*) If F and X are so close that one beat contains more individual oscillations than can be followed in a single discharge (i.e. more than a few hundred) the beating is no longer visible in any one picture. It can, however, be studied in a rather tedious way by varying the peak field systematically and taking the resonant type of picture. The blip size is a measure of the combined signal at the field at which the blip occurs and if the blip size is plotted against $1/H$ as in figure 5 the beat character is revealed and the beat frequency can be measured. It is interesting to note that the minima for the left-hand and right-hand blip occur at appreciably different fields; this is probably due to the slight influence of eddy currents being different for F and X (see p. 125). This method was used in the exploratory experiments to estimate $d^2F/d\theta^2$ round a symmetry direction, by mounting two identical whiskers at a small angle to each other and observing how B varied as the field was tilted with respect to the whole mount. If the specimens are inclined to H at angles ($\theta-\frac{1}{2}\alpha$ and $\theta+\frac{1}{2}\alpha$) it is easily shown that

$$B=|\alpha\theta d^2F/d\theta^2|. \tag{5}$$

Thus $|d^2F/d\theta^2|$ may be found from a plot of B against θ (the eddy current effects are eliminated by averaging the rising and falling field data).

(*b*) If F and X differ by a few per cent the beats can be seen in single pictures such as those of figure 6, plate 1, and B measured directly. In some experiments separate pictures were taken for rising field (e.g. figure 6 (*a*)) and falling field, while in others, at some expense in accuracy but with some gain in economy, a slower time sweep was used and the beats for both rising and falling fields were recorded together (e.g. figure 6 (*b*)). In addition to the precautions and corrections already set out in (i) above, one or two new points arise.

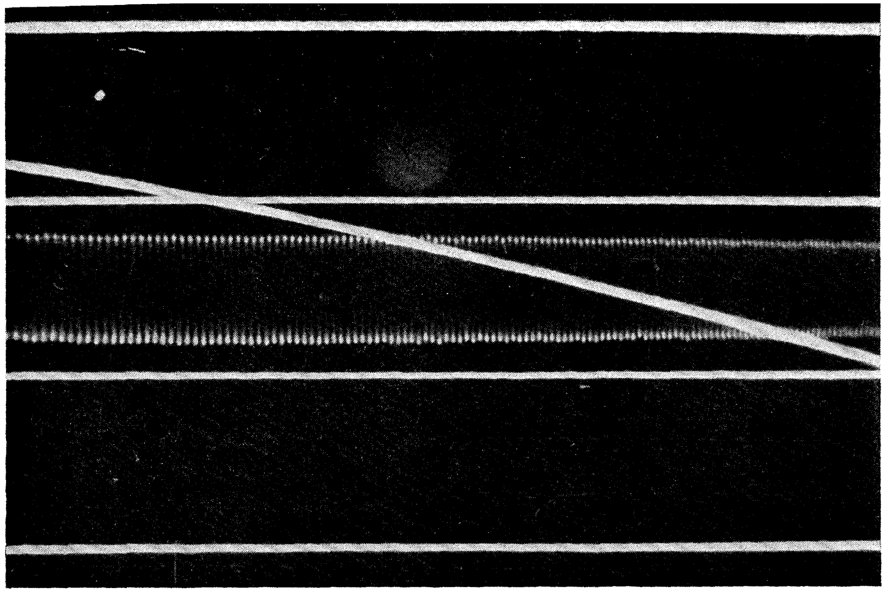

FIGURE 3. Oscillations of Cu 46, illustrating the direct method of measuring frequency. Calibration lines at $H = 1{\cdot}047$, $1{\cdot}070$, $1{\cdot}093$ and $1{\cdot}116 \times 10^5$ G; about 1 ms across picture.

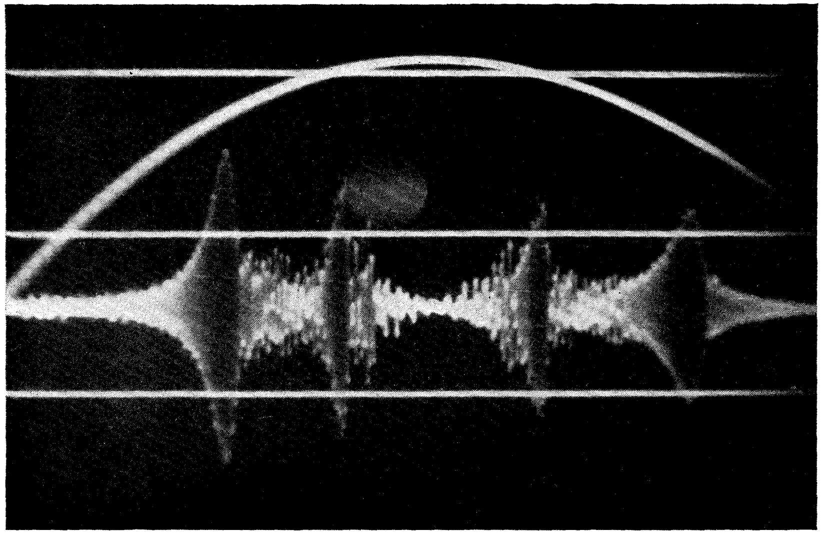

FIGURE 4. Belly and rosette blips for Au 36, illustrating the peak-to-peak method. The resonant frequency is about 44 kc/s; calibration lines at $H = 1{\cdot}05$, $1{\cdot}16$ and $1{\cdot}28 \times 10^5$ G; about 9 ms across picture.

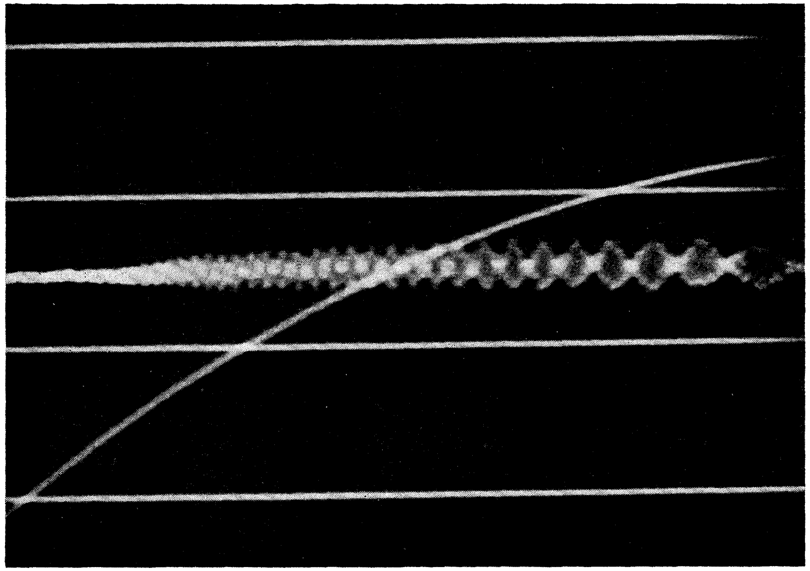

FIGURE 6. (*a*) Beats between Cu 49 set 2° off [100] in specimen coil and Cu 47 [111] in reference coil. Rising field only; calibration lines at 0·93, 1·05, 1·16 and $1{\cdot}28 \times 10^5$ G; about 5 ms across picture.

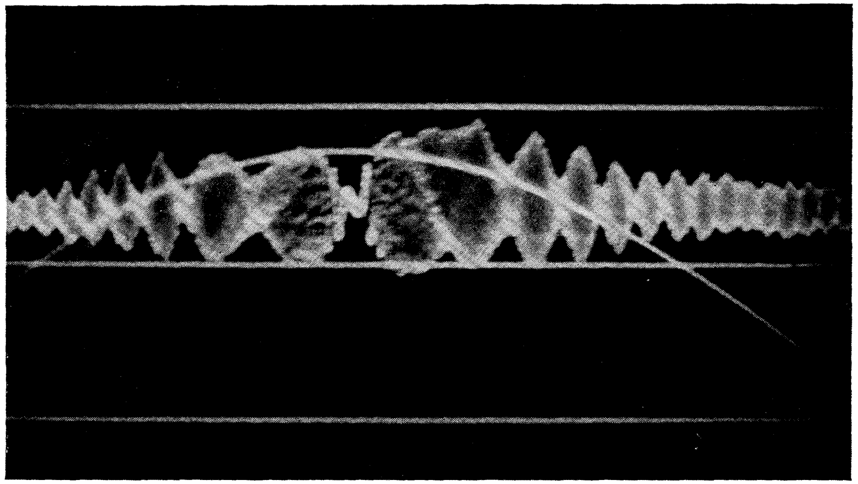

FIGURE 6. (*b*) Beats between Ag 30 set about 14° off [100] in specimen coil and Ag 27 [111] in reference coil. Calibration lines at 1·05, 1·16 and $1{\cdot}28 \times 10^5$ G; about 10 ms across picture.

(*Facing p.* 96)

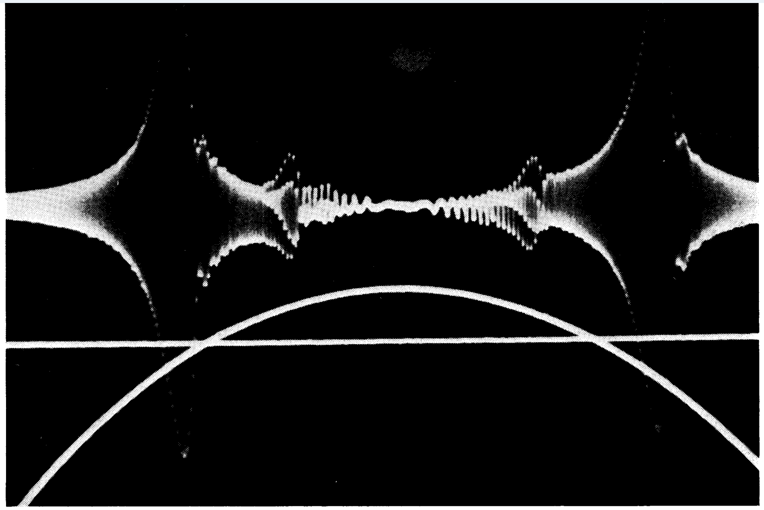

FIGURE 15. Resonant blips for Cu 46 (H along [111]) illustrating the 'ringing' effect associated with the 'gliding tone' and the presence of an appreciable first harmonic. Calibration lines at 1·07 and $1{\cdot}12 \times 10^5$ G; time across picture about 3 ms.

PHILOSOPHICAL TRANSACTIONS OF THE ROYAL SOCIETY A MATHEMATICAL, PHYSICAL & ENGINEERING SCIENCES

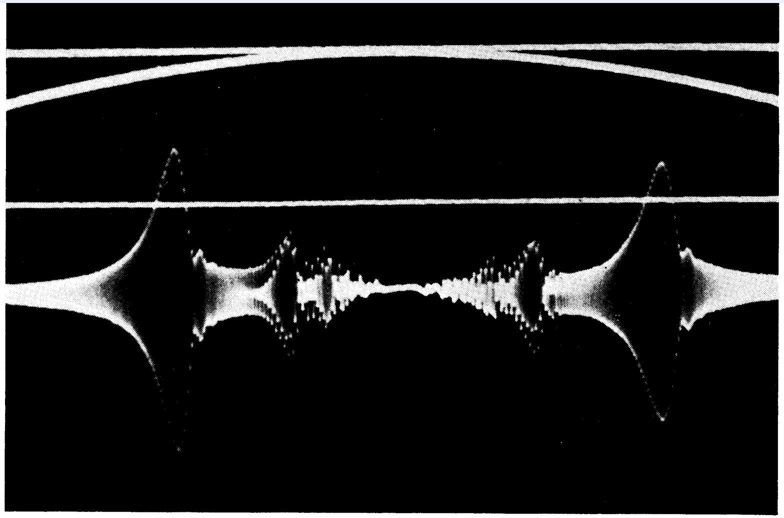

FIGURE 17. Resonant blips for Cu 46 (H close to [111]), showing strong first and second harmonics; the points marked with an arrow in figure 18 refer to this picture. Calibration lines at 1·02 and $1{\cdot}12 \times 10^5$ G; time across picture about 3 ms.

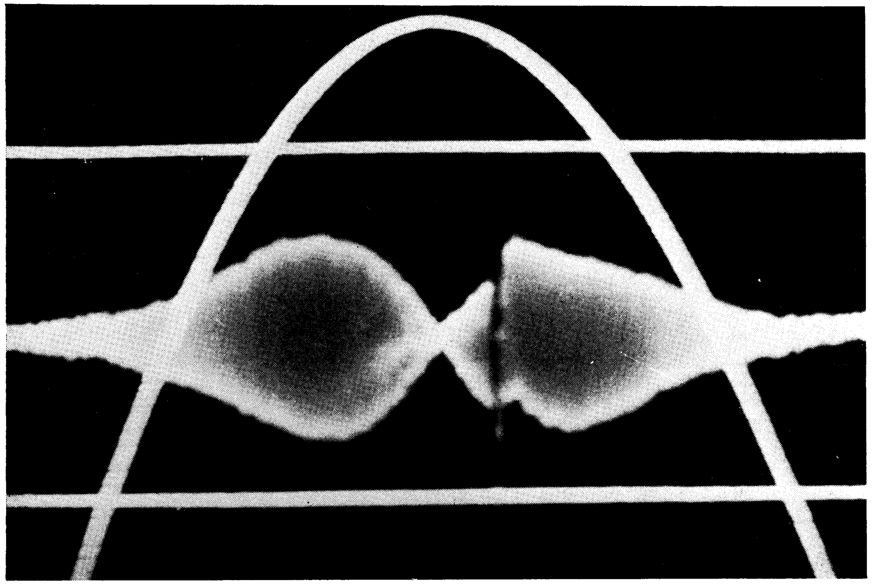

FIGURE 19. Envelope of oscillations in Cu 43 (H close to [111]) without resonance, showing smooth decay of oscillations as field falls off. The break on the right is an artefact. Calibration lines at 0·88 and $0{\cdot}98 \times 10^5$ G; time across picture about 9 ms.

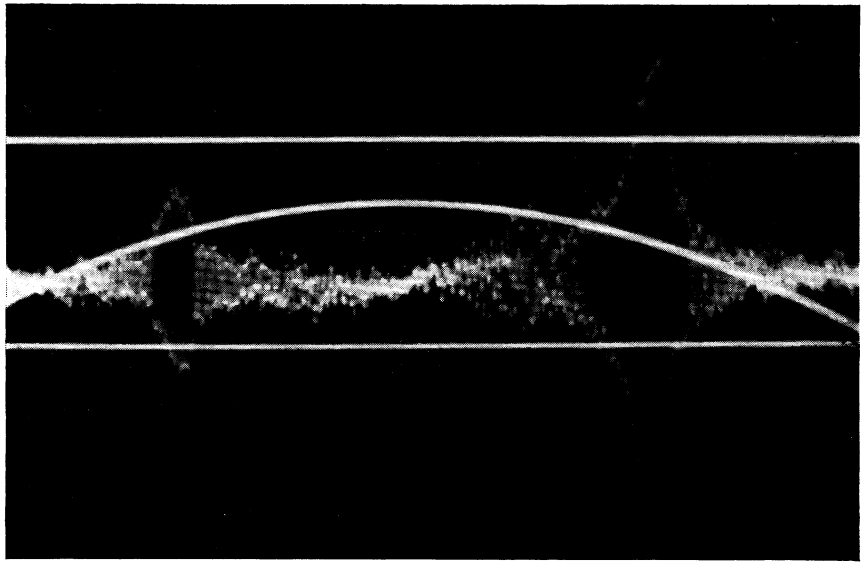

FIGURE 21. Resonant blips for Ag 7 showing unequal blips due to beats of figure 20 being slightly out of phase for rising and falling fields because of eddy current effect. The points marked with an arrow in figure 20 refer to this picture. Calibration lines at $H = 0{\cdot}79$ and $0{\cdot}84 \times 10^5$ G; time across picture about $3\frac{1}{2}$ ms.

The reference specimen must be carefully chosen to match the specimen for which the angular variation of F is to be studied. Thus, ideally, X should differ from F by at least 1 %, so that at least a few beat minima can be distinguished in the range for which there is an appreciable amplitude, but not by much more than 5 %, since with too few oscillations per beat, accuracy begins to suffer and also resolution becomes difficult. Again, the amplitudes of the two oscillations should be matched so that the beats should be as pronounced as possible, and it was sometimes found useful to shunt one or other of the pick-up coil pairs to produce this matching.

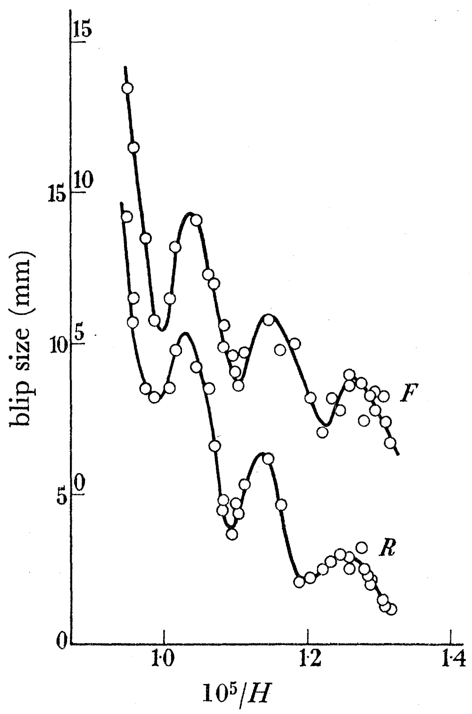

FIGURE 5. Long beats between Cu 51 and Cu 52 mounted with Cu 51 approximately parallel to the field and Cu 52 at $6\frac{1}{2}°$ to the field. R and F refer to rising and falling fields, respectively.

To achieve the best accuracy it is important that the field should lie as close as possible to a symmetry direction of the reference specimen so that any uncertainty in its precise orientation should have as little influence as possible on the value of X. The uncertainty in the value of F deduced by the beat method due to an error in X arising from an error in the determination of the angle θ between the field and the symmetry axis of the reference specimen is approximately

$$\delta F/F = (\theta\delta\theta/X)\mathrm{d}^2X/\mathrm{d}\theta^2. \qquad (6)$$

For H along [111] in silver, $(1/X)\ \mathrm{d}^2X/\mathrm{d}\theta^2$ is about 0·8, so if $\delta\theta$ is 2×10^{-2} (i.e. about 1°) and $\theta = 8\times10^{-2}$ (i.e. about $4\frac{1}{2}°$) we have $\delta F/F = 1{\cdot}3\times10^{-3}$, which is a rather larger error than any arising from the actual measurement of B itself. Unfortunately, the importance of this point was not fully appreciated at first, and in preparing specimens not enough trouble was taken to make θ much less than 5°.

A barely appreciable correction has to be made to allow for the slight inhomogeneity of the magnet which makes the field slightly different at the positions of the two specimens.

For most of the experiments this difference was only about 2 parts in 10^4, but in some of the experiments on copper where the more powerful (but less homogeneous) magnet was used, the difference was about 7 parts in 10^4.

The frequency results

To emphasize the physical significance of the experimental results, it is convenient to divide the experimental values of F for each metal by the appropriate value of F_s, the frequency for a spherical Fermi surface whose volume is exactly half that of the zone. The ratio F/F_s is just the ratio A/A_s of the area of the appropriate cross-section of the Fermi surface to the diametral cross-section area of the spherical Fermi surface and can be immediately compared with the predictions of Roaf's formulae.

It can easily be shown that

$$F_s = \frac{\pi h}{a^2(e/c)}\left(\frac{3}{2\pi}\right)^{\frac{2}{3}}, \tag{7}$$

where a is the lattice constant at 0 °K. Values of a were deduced from room-temperature values given by Pearson (1958) corrected for thermal expansion by the use of data from Landolt & Börnstein (1923) and are shown in table 2 together with the values of F_s obtained from them. Because of uncertainties in thermal expansion data and in the room temperature values, the values of a are probably reliable to only 1 part in 2000 and of F_s to 1 part in 1000.

Table 2

metal	a (10^{-8} cm)	F_s (10^8 G)
Cu	3·603	6·115
Ag	4·069	4·795
Au	4·065	4·804

To appreciate the extent and significance of the agreement between the experimentally determined frequencies and those calculated from Roaf's formulae, it is necessary first to explain briefly just what features of the experimental results have been used in determining the coefficients in each formulae. For each metal is was found that as the direction of H moved away from [100], F passed through a minimum value which will be denoted by F_{m1} in the (110) plane and F_{m2} in the (100) plane (see, for instance, figure 8). As explained more fully in the accompanying paper, the data used by Roaf in the first place were

$$\left.\begin{aligned} D = (F_{100}-F_{111})/F_s, \quad D_1 = (F_{100}-F_{m1})/F_s \quad \text{or} \quad D_2 = (F_{100}-F_{m2})/F_s, \\ N = F_{111}\,(\text{neck})/F_s. \end{aligned}\right\} \tag{8}$$

These data together with the requirement that the volume of the Fermi surface should be exactly half that of the fundamental zone are just sufficient to fix four coefficients in Roaf's formula (see II, equation (1)).

Thus in the various curves to be presented of belly frequency against orientation, the values of F_{m1}* and F_{111} relative to F_{100} are automatically in agreement with the formula because of the method of obtaining the formula, but agreement between the experimental points and the curves based on the formulae in all other respects is significant in demonstrating the validity of the formulae. So too is agreement as regards the dog's bone and

* F_{m2} instead of F_{m1} for gold.

PHILOSOPHICAL TRANSACTIONS OF THE ROYAL SOCIETY A MATHEMATICAL, PHYSICAL & ENGINEERING SCIENCES

rosette frequencies and angular variation of the neck frequencies (the neck frequency itself agrees automatically).

The values of F obtained by the beat method in any one traverse (in which F changes by only a few parts per cent) depend of course on the value assumed for X, the frequency of the reference specimen. Provided the assumed values of X are chosen consistently for different reference specimens, the precise value used is of little importance and any small change in it will merely cause an equal shift in all the F values deduced. For convenience in comparison with Roaf's formulae, the X values used in the results as presented here are based on the predictions of the formulae, rather than on experimentally determined absolute values. This avoids differences of order 1 or 2% between the experimental and calculated F values, such as would occur if the X values were 1 or 2% different from the appropriate values yielded by the formulae. Slight shifts of order 1 part in 10^3 are nevertheless sometimes necessary either because the formula had been worked out from data which have since been slightly modified or because the data used were averages of several determinations (so that an adjustment is required in considering any one determination separately). Where necessary, such adjustments have been made by a slight displacement of the origin of F for the theoretical curve, and the magnitude of each such displacement is noted. Similarly, small adjustments have been made of the origins of the angular scales so that the experimental points should fall as well as possible on the theoretical graphs (i.e. should satisfy crystal symmetry); the necessary shift rarely exceeds 2° (see p. 90).

In most of the experimental curves (but not for copper) it was possible to determine within 1 or 2° the angles at which the oscillations cease (because an extremal belly section is no longer possible) and these experimentally determined limits are marked where possible, together with the corresponding limits computed from Roaf's formulae. There is in fact no indication of any disagreement between the observed and calculated limits, greater than could be attributed to slight errors in the measurement of angle and in the setting of the plane of rotation.

The results will now be presented for each metal in turn. First, the experimental points for belly frequencies determined by the beat method traverses will be shown together with graphs calculated from Roaf's formulae. Then the absolute experimental values of belly frequencies found by the direct method will be compared with the values given by the formulae; this comparison tests the validity of the assumption that the volume of the Fermi surface is exactly half that of the zone. Next, miscellaneous features such as the dog's bone, rosette and neck frequencies and their angular variations are discussed. For simplicity of presentation, frequencies are given for exact symmetry directions, even though the measurements were sometimes made a degree or two off the exact symmetry directions; the necessary small corrections were estimated from the calculated graphs. Finally, after the individual metals have been discussed, a summary is given of the data used in fitting the formulae. The values of the coefficients in the formulae are given in II (table 1) together with a discussion of how well they agree with other experimental determinations of the Fermi surfaces and with band structure calculations.

Copper

Traverses were made by the beat method in both the (100) and (110) planes, round [100], and round [111] in a plane which was intended to be (110) but may have been unintentionally inclined by as much as 18° to (110) (see figure 7). Fortunately, for the small angular range of this last traverse the variation should be independent of the plane of rotation, so the uncertainty is unimportant.* It can be seen that there is no very significant difference between the experimental points and the curves derived from Roaf's four-term formula fitted to only three experimental data as explained above. Some

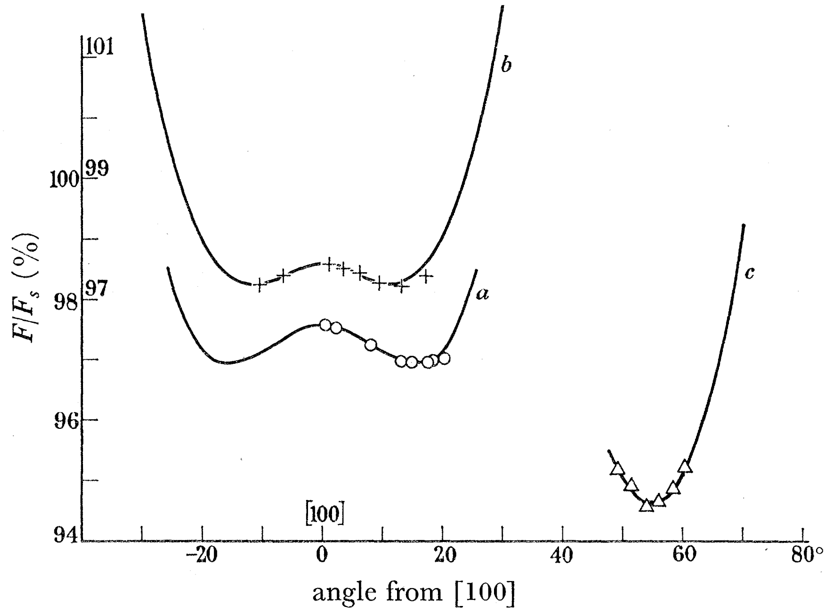

FIGURE 7. Angular variation of F/F_s for copper: (*a*) in (110) plane round [100], (*b*) in (100) plane round [100], (*c*) in plane 18° off (110) round [111]; in (*a*) and (*b*) the specimen was Cu 49 and the reference Cu 47, in (*c*) the specimen was Cu 46 and the reference Cu 51. The curves are of Roaf's Cu IV formula; the theoretical curve (*c*) is raised by 0·12. The right-hand scale of ordinates refers to (*b*).

further attempts by Roaf to fit a four-term formula showed that though a better fit could be achieved around the dip of (*a*) in figure 7, this produced little improvement at the dip in (*b*). Roaf's six-term formula, 'trimmed' to fit the anomalous skin effect data of Pippard (1957), gives appreciably lower values of F_{111} and F_{100} (see table 3) but the curves *a*, *b* and *c* if appropriately displaced, are almost exactly the same as for the four-term

* The dip in the (110) curve (*a*) of figure 7 is significantly larger than in some results obtained earlier. The earlier results had been obtained with a [111] whisker (Cu 46) tilted so that the field was in the range around [100], and it was only later realized that this could lead to considerable error if the plane of rotation was appreciably inclined to (110). In the light of the much more reliable results of figure 7, which were obtained with a [100] whisker, it seems that a 9° inclination of the plane of rotation to the (110) plane would have been enough to explain the reduced dip. The traverse of Cu 46 round [111] in figure 7 was done *after* the experiment in question and subsequently it was found that the plane of rotation had twisted by 18° from (110), so it is possible that owing to looseness in the mounting a progressive twisting of the specimen had occurred between the original time of mounting and the check that was made only at the end of a series of experiments. In the light of this experience a routine check of the mounting was made after each experiment subsequently.

formula. Probably a more perfect fit to both the de Haas–van Alphen and the anomalous skin effect could be achieved by using a formula with more than six terms, but since the present discrepancies are hardly outside experimental error the labour of computation is hardly worth while until more precise data are available.

In the application of the beat method the choice of X for the [111] reference specimen was based on the assumption that $F_{111}/F_s = 0{\cdot}945$ which is the value required to make Roaf's surface (Cu IV) have just the correct volume; the two traverses of figure 7 then agree exactly in giving $F_{100}/F_s = 0{\cdot}976$. For the traverse round [111], in which a [100] whisker (Cu 51) was used as reference, this value of F_{100} was used for X and it will be seen that the value of F_{111} comes out at 0·946, reasonably consistently with the starting assumption. In this particular experiment, however, a different magnet was used, whose calibration was not as accurately known as that of the magnet used in all the other experiments, and the field of which was much less homogeneous, so this good agreement must be regarded as a little fortuitous.

Three sets of absolute value determinations of belly frequencies were made with the results shown in table 3.

Table 3. Absolute values of F/F_s for copper

		F_{111}/F_s		F_{100}/F_s
experiment	(*a*)	0·932 ± 0·003	(*c*)	0·975 ± 0·007
	(*b*)	0·953 ± 0·004		
Roaf Cu IV		0·945		0·976
Roaf Cu VI		0·939		0·970

Notes. The ± entries are mean deviations of the means (based on ten readings for (*a*), five for (*b*) and six for (*c*)); (*a*) and (*b*) were both measured on the same whisker Cu 46, but about a year apart in the course of which the measuring technique had been a good deal modified; (*c*) was done on Cu 45 at about the same time as (*a*). Unfortunately only in (*c*) was it possible to allow for possible difference in trace speeds (see p. 94) and this may well be the main cause of the discrepancy between (*a*) and (*b*), which is larger than can reasonably be attributed to the random errors.

It can be seen that the agreement with Roaf's figures, i.e. with the assumption that the volume of the Fermi surface is exactly half that of the zone, is good in that there is no indication of any systematic disagreement in F exceeding 1% (i.e. $1\frac{1}{2}$% in volume of Fermi surface).

In copper, for reasons which are not properly understood, it has not yet been possible to observe the dog's bone oscillations and the neck oscillations are very weak. The neck frequency was observed and measured by Dr M. G. Priestley on Cu 46 by the direct method with a peak field of about $1{\cdot}5\times10^5$ G; because of the weakness of the signal it was not possible to make as accurate a measurement as usual. The value found was

$$F_{111}(N)/F_s = 0{\cdot}0402,$$

but it is possible that this might be as much as 5% in error in virtue of both random and systematic errors.

The ratio of the rosette frequency $F_{100}(R)$ to the belly frequency F_{100} was measured on Cu 52 by the peak-to-peak method and using Roaf's Cu IV value of F_{100} it was found that

$$F_{100}(R)/F_s = 0{\cdot}396$$

in each of two determinations; the random error of each determination is of order $\frac{1}{2}\%$, but systematic errors inherent in the method might be as much as 2%. The prediction of Roaf's Cu IV formula is 0·402, which can be regarded as reasonable agreement.

Silver

Traverses were made by the beat method around [100] in (110) and (100) planes, and around [111] in (110) and (211) planes (figure 8). A traverse was also made in an intermediate plane (figure 9*a*) and serves as a check that the formula is valid not only in the symmetry planes. There is again no significant difference between the experimental points and the curves derived from the Ag IV formula, even though, owing to the more

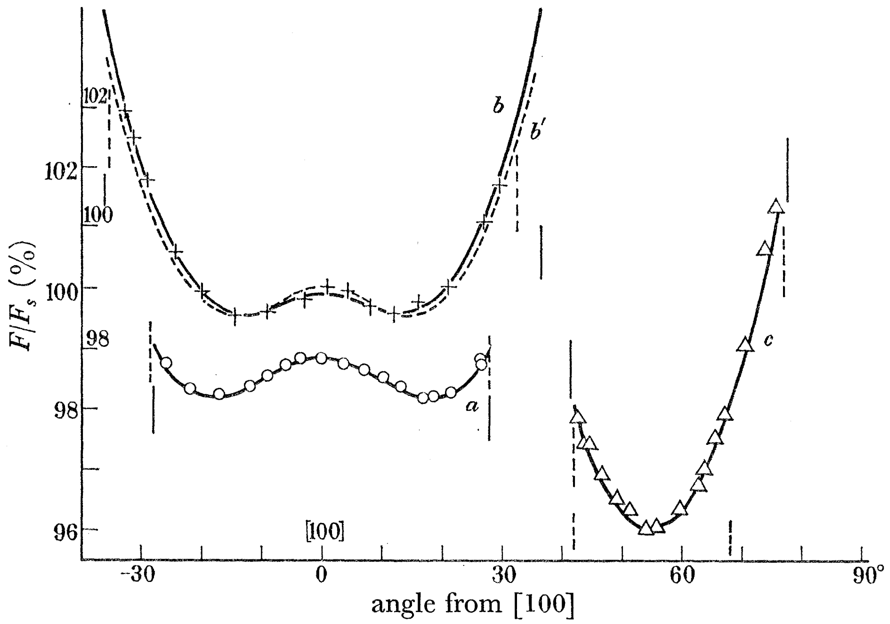

FIGURE 8. Angular variation of F/F_s for silver: (*a*) in (110) plane round [100], (*b*) in (100) plane round [100], (*c*) in (110) plane round [111]; in (*a*) the specimen was Ag 21 and the reference Ag 27, in (*b*) the specimen was Ag 30 and the reference Ag 27 and in (*c*) the specimen was Ag 27 and the reference Ag 21. The full curves are of Roaf's Ag IV formula, and the broken curve (*b*′) is for Ag VI (the curves of Ag VI for (*a*) and (*c*) are almost indistinguishable from those of Ag IV). The theoretical curves have been lowered by the following amounts: (*a*) and (*c*) 0·10, (*b*) 0·05. The broken lines indicate the approximate limits within which a signal could be observed; the lower pair of broken lines below (*c*) refer to a traverse around [111] in a (211) plane, for which the points fall well on the curve, but have been omitted to avoid confusion. The full vertical lines indicate the limits computed for Ag IV with an accuracy of about 1°. The right-hand scale of ordinates refers to (*b*) and (*b*′).

favourable conditions in silver, it was possible to make measurements over almost the whole available angular range rather than only a part as in copper. Figure 8 shows also that Ag VI, which is trimmed to fit Morton's (1960) anomalous skin effect data, while not departing from the experimental points by more than might be attributed to experimental error in the measurements of angle and frequencies, does seem to fit less satisfactorily than Ag IV. Once again, probably a formula with more than six terms would be required to obtain a more perfect fit with both sets of data.

In the application of the beat method the choice of X for the reference specimen was based on the assumption that $F_{111}/F_s = 0{\cdot}9615$ (this is Roaf's Ag IV prediction); it is then possible to estimate a value of F_{100}/F_s from each of the three traverses shown in figure 8, by demanding consistency. For instance, in the traverses round [111] where the reference specimen was close to [100] the value of X (i.e. of F_{100}) was chosen so that F_{111} came exactly to its postulated value. Appropriate corrections were of course applied for small departures of the various specimens from exact symmetry directions.

The three estimates of F_{100}/F_s were:

$$0{\cdot}9895, \qquad 0{\cdot}9907, \qquad 0{\cdot}9900 \qquad \text{mean: } 0{\cdot}9901,$$

and the fact that they are consistent within experimental error is a useful check of the reliability of the procedure.

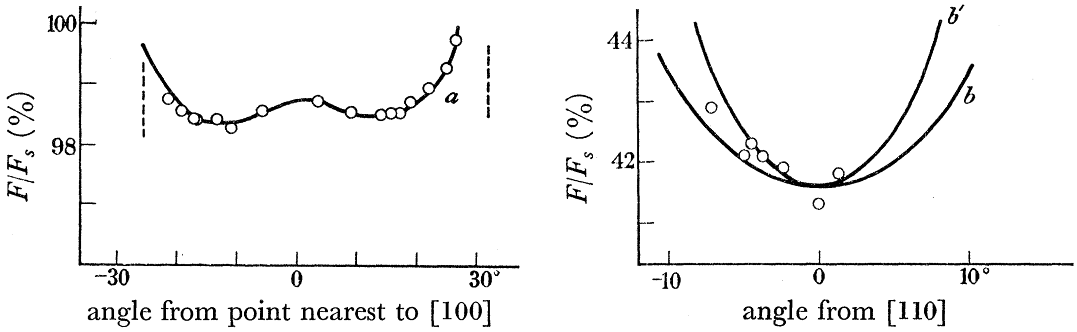

FIGURE 9. (*a*) Angular variation of F/F_s for silver in an intermediate traverse which can be defined approximately by the following pairs of values of (θ, ϕ), the polar angles about [100], (29, −68) (6, 0) (26, 84). The specimen was Ag 21 and the reference Ag 27. The full curve is for Roaf's formula Ag IV, which has been lowered by 0·10; the broken lines indicate the approximate limits within which a signal could be observed.

(*b*) and (*b′*) Angular variation of F/F_s for the silver dog's bone in a (111) plane round [110]. The theoretical variation for this plane has not been computed, but *b* and *b′* are Roaf's Ag IV curves for the (110) and (100) planes, respectively; the theoretical curves are lowered by 0·1.

Absolute values of belly frequencies were determined by the direct method and are compared with Roaf's predictions in table 4.

TABLE 4

	F_{111}/F_s	F_{100}/F_s
experiment	(*a*) 0·966 ± 0·004	(*c*) 0·980 ± 0·003
	(*b*) 0·953 ± 0·002	
Roaf Ag IV	0·9615	0·9896
Roaf Ag VI	0·9620	0·9905

Notes. The ± entries are mean deviations of means (of eight readings for (*a*), six for (*b*) and eleven for (*c*)); (*a*) and (*b*) were both done on Ag 27, but (*b*) was done by Mr B. R. Watts, using a different high-field equipment so that calibration constants were quite different; (*c*) was done on Ag 7.

The fair agreement of (*a*) and (*b*) with each other is a useful check on the reliability of the calibrations of both equipments, while the agreement of both and (*c*) with Roaf's predictions confirms with a precision of order 1% that the volume of the Fermi surface is indeed just half that of the fundamental zone.

Measurements of the neck, rosette and dog's bone frequencies are summarized in table 5 and it can be seen that they agree well with Roaf's predictions. A few measurements were also made by the peak-to-peak method of the variations of the dog's bone frequency with orientation in a (111) plane (figure 9) and these too are consistent with the predicted behaviour, though the experimental accuracy is not high enough to make this consistency very significant.

TABLE 5

	$F_{111}(N)/F_s$	$F_{100}(R)/F_s$	$F_{110}(D)/F_s$
experiment	0·0188	0·410	0·416
Roaf Ag IV	0·0187	0·408	0·418
Roaf Ag VI	0·0188	0·408	0·425

Notes. $F_{111}(N)$ is based on two determinations on Ag 27 and 28 by Mr B. R. Watts using the rather higher fields available in his equipment, and by chance the two determinations gave identical answers; the random error was $\pm 0{\cdot}2\,\%$ (M.D. of mean) but a systematic error of as much as 2 % due to calibration errors and uncertainty of the exact orientation is not excluded. The rosette data were taken rather incidentally and are not very accurate (individual results on Ag 8 and Ag 21 gave 0·404 and 0·416, respectively). The dog's bone measurements were on Ag 19 and were also not very precise as can be seen from the scatter of the points in figure 9.

Gold

Traverses by the beat method were made around [100] in (110) and (100) planes and around [111] close to a (110) plane (figure 10). The last two traverses were in fact done first and were used by Roaf to fit a formula Au IV with four terms such as had proved so successful with silver. The results of the (110) traverse, however, seemed to differ from the variation predicted by this formula by just more than seemed plausibly ascribable to experimental error. The measurements were therefore repeated with a different reference specimen and in somewhat better experimental conditions and as can be seen, proved remarkably consistent with the earlier ones. It was therefore decided to fit a five-term formula (Au V) taking account of the (110) minimum (i.e. D_1) as an extra fitting parameter. The graphs of both formulae are shown for the (110) traverse and it can be seen that the slight modification of the formula improves the fit at the minimum of this traverse; for the other traverses the graphs of Au IV and Au V are practically indistinguishable.

Once again each traverse yields a precise estimate of F for a symmetry direction relative to the value of X assumed for the reference specimen. Relative to the assumption that for silver $F_{100}/F_s = 0{\cdot}9896$ and $F_{111}/F_s = 0{\cdot}9615$, we find from the various traverses for gold: $F_{111}/F_s = 0{\cdot}9368$, $F_{100}/F_s = 1{\cdot}0080$ ((100) traverse) and $1{\cdot}0103$ ((110) traverse): mean $F_{100}/F_s = 1{\cdot}0092$. In the check (110) traverse the reference was a gold [111] crystal (Au 37) for which X was based on Roaf's (Au IV) value of F_{111} for gold; this gave $F_{100}/F_s = 1{\cdot}0097$. The appreciable discrepancy between the estimates of F_{100} from the (100) and (110) traverses may well be due to differences of oscilloscope trace speeds (see p. 94), for which no correction could be made in these particular experiments. If this is indeed the cause, the necessary correction to bring the F_{100} estimates together would make the inadequacy of the four-term formula more rather than less marked. The experimental and calculated F values are summarized in table 6.

No absolute determinations of belly frequencies were made for gold, but it should be noticed that in the beat measurements *silver* reference specimens were used, and values of the reference frequency were assumed consistent with Roaf's predictions for silver. Thus the fact that the gold belly frequencies given by the beat method are close to those predicted by Roaf for gold is not trivial, but a significant indication that (to the same degree of precision as for silver, i.e. about 1 %) the Fermi surface of gold has a volume just half that of the fundamental zone.

Measurements of the neck, rosette and dog's bone frequencies are summarized in table 6 and once again it can be seen that they agree with the predictions of both the four-term and five-term formulae.

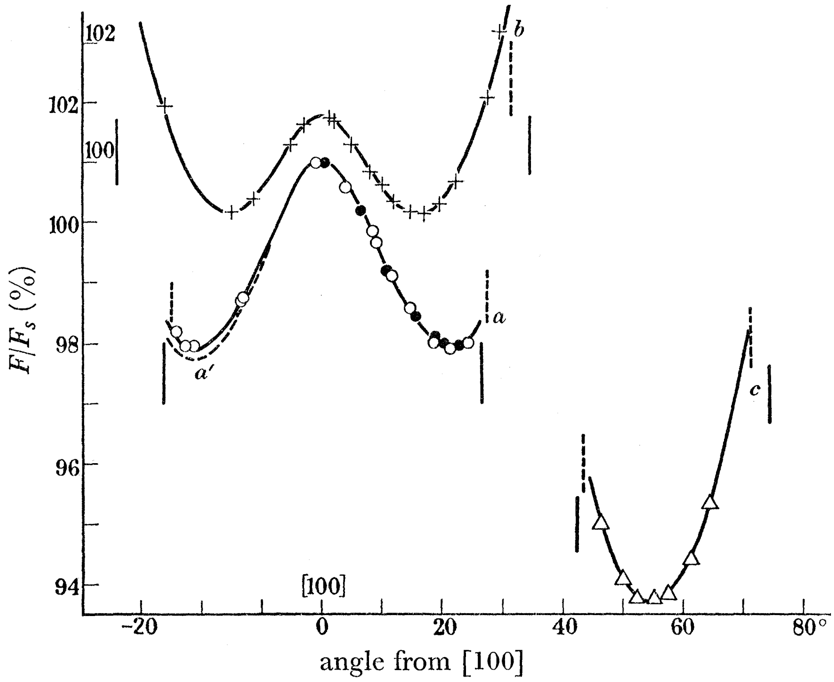

FIGURE 10. Angular variation of F/F_s for gold: (*a*) in a (110) plane round [100], (*b*) in a (100) plane round [100], and (*c*) in a (110) plane round [111]; (*a*) comprises two sets of data both with Au 36 as specimen but one set with Ag 27 as reference (○) and the other with Au 37 as reference (●), in (*b*) the specimen was Au 36 and the reference Ag 30 and in (*c*) the specimen was Au 31 and the reference Ag 30. The full curves are of Roaf's formula Au v, but (*a'*) is for Au iv, which is almost indistinguishable from Au v for (*b*) and (*c*). The theoretical curves have been lowered by the following amounts: (*a*) 0·20, (*b*) 0·42, (*c*) 0·30, but (*a'*) has been raised by 0·10. The broken lines indicate the limits over which a signal could be observed, and the full vertical lines indicate the limits computed for Au v with an accuracy of about 1°. The right-hand scale of ordinates refers to (*b*).

TABLE 6

	F_{111}/F_s	F_{100}/F_s	$F_{111}(N)/F_s$	$F_{100}(R)/F_s$	$F_{110}(D)/F_s$
experiment	0·9368	1·0092	0·0313	0·410	0·405
Roaf Au iv	0·9372	1·0092	0·0320	0·414	0·399
Roaf Au v	0·9402	1·0122	0·0313	0·413	0·400

Notes. The F_{100}/F_s experimental value is the mean mentioned in the text. $F_{111}(N)/F_s$ was measured on a number of occasions with different specimens and gave: Au 8, 0·0313, Ag-Au 17 (it is unlikely that the small silver content should have affected the frequency appreciably) 0·0316, Au 37, 0·0307; the discrepancies are probably due to uncertainties in the trace speed correction in the first two and screen distortion in the third and the estimate given above is probably within 2 % of the true value. In fitting the four-term formula, Roaf used a provisional estimate of $F_{111}(N)/F_s = 0{\cdot}0320$; the best experimental value was used in fitting the five-term formula. The rosette and dog's bone data were obtained by the peak-to-peak method and are taken from figure 11 which gives some idea of the scatter; they are also subject to the systematic error of the method which may be as much as 2 %. The rosette signal in gold was so strong in Au 36 that a measurement of F by the direct method could also be made; this gave $F_{100}(R)/F_s = 0{\cdot}422$; the slight discrepancy with the peak-to-peak result is probably due to uncertainty in trace speed (the c.r.o. was not in good adjustment at the time).

Because the amplitudes of these various features were particularly strong in gold it was possible to study the frequencies not only at the symmetry directions but also over a fair angular range. These variations are shown in figure 11 together with the corresponding calculated graphs. It can be seen that the observed variations are consistent with the predictions of Au v; the predictions of Au iv are almost identical. The rosette and dog's bone frequencies and the angular variation of the neck frequency are insensitive to variations of the formula and so are unlikely to be very useful for establishing the fine detail of the Fermi surface, unless a much greater accuracy of measurement is achieved.

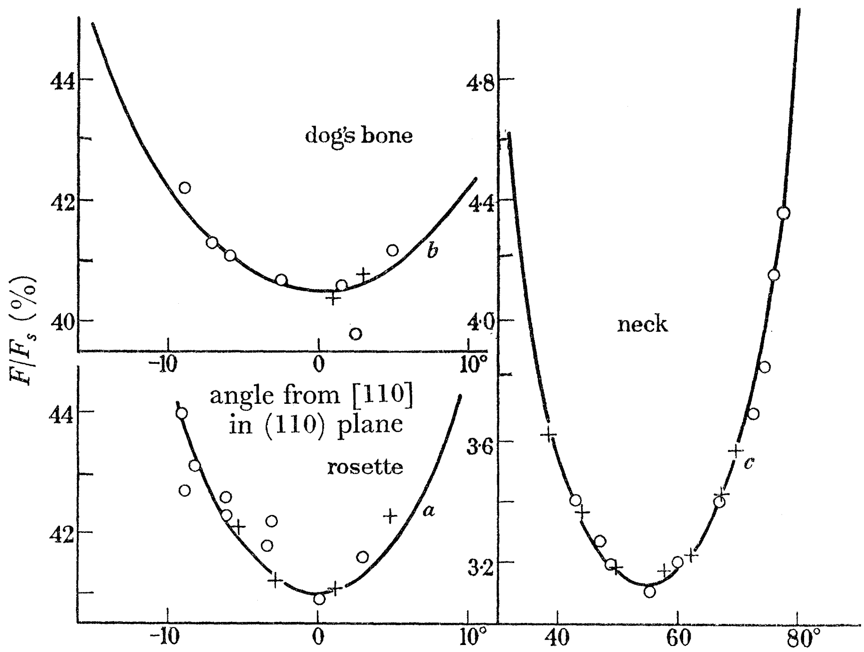

FIGURE 11. Angular variation of F/F_s for gold: (*a*) rosette in (100) plane round [100], specimens Au 29 (○) and Au 36 (+); full curve for Au v (lowered by 0·3); (*b*) dog's bone in (110) plane round [110] specimen Au 21 in two different experiments; full curve for Au v (raised by 0·5); (*c*) neck in (110) plane round [111], specimens Au 8 (○) and Ag-Au 17 (+); the full curve for Au v has not been shifted but the + points have been lowered by 0·05 to bring them into agreement with the others. A traverse in a (211) plane round [111] was also made, using Au 37; the points fall well on (*c*) but are omitted to avoid confusion.

Summary of frequency data used for determining the formulae

The best values of D, D_1, D_2 and N (see (8)) based on the above results are collected together in table 7; some of the values actually used by Roaf in arriving at the formulae were in fact slightly different (as shown) because at the time some of the experimental

TABLE 7

	Cu	Ag	Au
D	0·0305 (7, 6)	0·0286 (1, 5)	0·0722 (0, 0)
D_1	0·0062	0·0067 (4)	0·0309 (–, 7)
D_2	—	—	0·0162 (6, 1)
N	0·0402 ·	0·0188 (7)	0·0313 (20)

Note. The figures in brackets are the last significant figures of the values used by Roaf, where these differ from the data given here; the second entries refer to Cu vi, Ag vi and Au v (see ii, table 1).

data had not been completely analyzed. The differences are, however, hardly significant enough to warrant the labour of modifying the formulae; the question of how small changes in these fitting parameters influence the coefficients is discussed in II (see table 7).

Other possible oscillations

The extremal sections of the Fermi surface which have so far been discussed are not the only possible ones. First, there should be a large 'hole' section for H along [111], which has the shape of a 'six-cornered rosette', indicated schematically in figure 12*a*, and secondly, there should for many directions of H be 'extended' extremal sections which go round more than one belly (e.g. figure 12*b*).

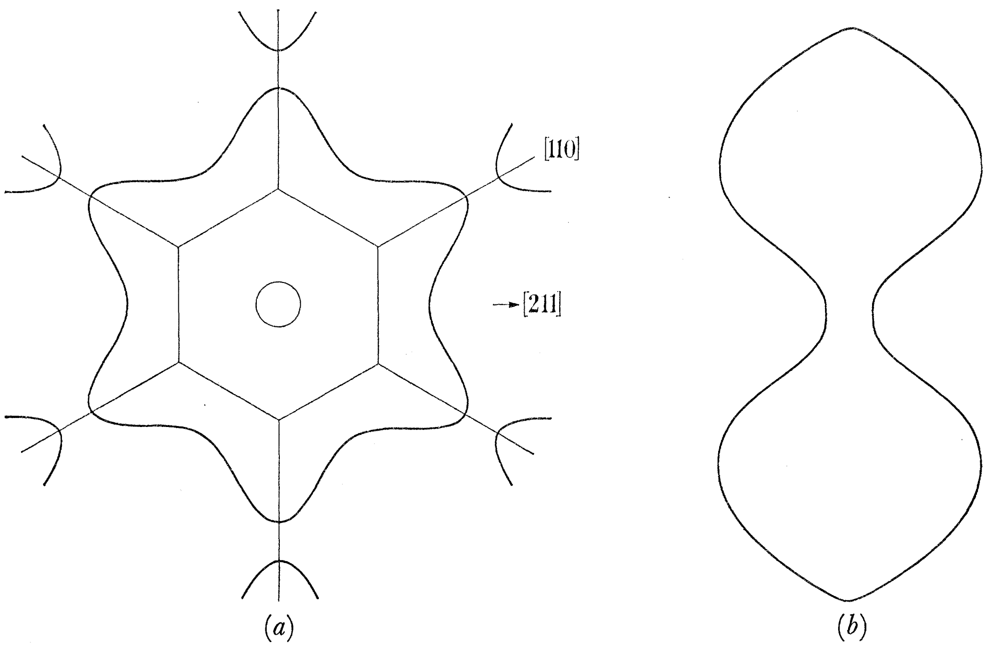

FIGURE 12. (*a*) The six-cornered rosette for gold; the sketch is based on Roaf's Au IV formula and is drawn rather schematically. The scale is exactly half that of figure 2, the lines are the intersection of the plane of the rosette with the Brillouin zone and the beginnings of neighbouring rosettes are indicated; the circle at the centre of the hexagonal face is a neck.
(*b*) An extended orbit to same scale as (*a*); the sketch is based on Au IV but is very approximate.

The six-cornered rosette should have a frequency about 1·9 times that of the [111] belly and this is very difficult to detect reliably because it is so close to the first harmonic frequency of the fundamental belly frequency. As will be discussed later (p. 118) a quite strong signal is indeed found with a frequency close to that of the first harmonic, but since this appears for [100] as well as [111] crystals, it is probably predominantly due to the first harmonic itself. Unfortunately because of inadequate resolution it is not possible to say whether or not for a [111] crystal this signal contains also a component of the six-cornered rosette frequency. In principle the rosette and the harmonic should beat together, but in practice only very few oscillations of the double frequency can, by the resonance method, be separated from the stronger fundamental.

Extended orbits can be of a variety of types, some of which have been discussed in connexion with cyclotron resonance (Kip, Langenberg & Moore 1961). The oscillations associated with most of these orbits have little chance of showing up with any appreciable amplitude because (*a*) the extremal area varies very rapidly with direction of H (so that, as explained on p. 121, specimen imperfections reduce amplitude greatly), (*b*) the extremum is a rather sharp one, and (*c*) the frequencies involved are very high. No systematic search for such oscillations has in fact been made, but on one occasion a resonant picture was obtained which can probably be attributed to an extended orbit. This was for Au 8 when the field direction was being varied in a (110) plane. When the field had been tilted about 10° away from [111] towards [100] the resonant picture showed blips corresponding to a frequency about twice that of the belly, but no blips of the belly frequency itself. The probable explanation of this observation is that for this orientation an extremal section round the belly cannot exist, but one round two bellies through a neck (figure 12 (*b*)) is possible for a narrow angular range. The study of such extended orbits might be of interest in establishing fine details of the Fermi surface, but has not been pursued because of its obvious difficulties.

Amplitude of the oscillations

Although the main object of this research was the determination of the Fermi surfaces from measurements of F quite a lot of information was obtained, rather incidentally, about the amplitude of the oscillations and its dependence on various factors. Owing to lack of time some of the interesting effects which were observed have not been thoroughly investigated, but they merit discussion, both because the underlying theory should be a useful guide to future experiments on the de Haas–van Alphen effect, and because some of them are of intrinsic interest in the new points of principle they present. We shall first give a brief resumé of the results of the conventional theory and point out an important respect in which the theory needs modification. In the light of these considerations we shall then consider the temperature variation of the amplitude and discuss observations on the absolute amplitude of the oscillations, their harmonic content and the dependence of amplitude on orientation and field, as well as the effect of eddy currents and specimen imperfections.

Theory

According to the detailed theory (Lifshitz & Kosevich 1955) the differential susceptibility of $\mathrm{d}I/\mathrm{d}H$ is given by

$$\frac{\mathrm{d}I}{\mathrm{d}H}=\frac{4kTF^2}{H^{\frac{5}{2}}}\left(\frac{2\pi e}{hc}\right)^{\frac{3}{2}}\left|\frac{1}{2\pi}\frac{\mathrm{d}^2A}{\mathrm{d}k_H^2}\right|^{-\frac{1}{2}}\left(\cos\theta+\frac{1}{F}\frac{\mathrm{d}F}{\mathrm{d}\theta}\sin\theta\right)$$

$$\times\sum_{p=1}^{\infty}\frac{p^{\frac{1}{2}}\cos\left(\frac{2\pi pF}{H}\mp\frac{1}{4}\pi-2\pi p\gamma\right)\cos\left(\frac{\pi pm}{m_0}\right)\mathrm{e}^{-4\pi^3pmckx/ehH}}{2\sinh\left(4\pi^3pmckT/ehH\right)},\tag{9}$$

where I is the oscillatory magnetization per unit volume in a direction at angle θ to the field, m is the cyclotron mass defined as

$$m=\frac{\hbar^2}{2\pi}\frac{\mathrm{d}A}{\mathrm{d}E}\tag{10}$$

(A is the extremal area and the derivative is taken at the Fermi surface), and x is an effective temperature (Dingle 1952 *b*) which takes account of the broadening of the Landau levels under certain simplifying assumptions. If level broadening is due only to collisions

$$x=h/2\pi^2k\tau,\tag{11}$$

where τ is the relaxation time. In the expression for the phase, γ depends on the form of the electronic structure ($\gamma = \frac{1}{2}$ for a quadratic $E-k$ law) and the minus or plus sign is taken according as the extremal area is a maximum or minimum respectively; we shall not, however, be concerned with the phase in our discussion. The factor $\cos(\pi pm/m_0)$ comes from spin-splitting of the energy levels (Dingle 1952*a*) and m_0 is the free electron mass if it is assumed that the spin moment is a Bohr magneton. The factor

$$(\cos\theta + (1/F)(\mathrm{d}F/\mathrm{d}\theta)\sin\theta)$$

takes account of the fact that when the axis of figure of the specimen is rotated, the pick-up coil rotates with it, and it is the component of magnetization parallel to the pick-up coil axis which is observed; in most of the experiments θ did not exceed 30°, and the second term, which arises from the magnetization perpendicular to the field, is small compared with the first, coming from the parallel component. To a sufficient accuracy then this factor may be put equal to 1.

For most of our experiments the condition

$$4\pi^3 mckT/ehH \gtrsim 1 \tag{12}$$

applies and it is then a fair approximation to retain only the first term of the summation in (9) and to replace the sinh by an exponential. The field and temperature dependence of amplitude of $\mathrm{d}I/\mathrm{d}H$ then appear only through the factor

$$TH^{-\frac{1}{2}} \exp\left(-4\pi^3 mck(T+x)/ehH\right) \tag{13}$$

so that m may be determined from the temperature variation of the amplitude A and x from the field variation.

We must now consider an important inadequacy of the theory which is relevant to the interpretation of some of the experimental observations. This inadequacy was realized only very recently as a result of thinking about the puzzlingly high observed strengths of the harmonics of the fundamental frequency of oscillation. Harmonics are indeed predicted by (9) but as will be discussed in more detail below (see p. 118) the observed amplitudes of the harmonics are a good deal larger than those predicted by (9). A possible explanation of this lies in the fact that the absolute value of the amplitude of $4\pi|\mathrm{d}I/\mathrm{d}H|$ is comparable to 1. Because of this, the field acting on the electrons in the metal may differ significantly from the applied field H. If we assume that the effective field is B it will be seen that as H varies, the effective field oscillates in sympathy with the oscillations of I, and even though I is small this 'frequency modulation' may have an appreciable effect because of the very high phase of the oscillations.

To get some idea of what happens we may simply replace H by $H+4\pi I$* in the argument of the periodic variation of I. We then have the implicit relation

$$I = I_0 \sin\left(\frac{2\pi F}{H+4\pi I}\right) = I_0 \sin\frac{2\pi F}{H}\left(1-\frac{4\pi I}{H}\right) \tag{14}$$

since $4\pi I/H \ll 1$. To solve this it is convenient to introduce the notation $y = 8\pi^2 FI/H^2$, $x = 2\pi F/H$ and it is easily seen that

$$\mathrm{d}y/\mathrm{d}x = -4\pi \mathrm{d}I/\mathrm{d}H,$$

* If the specimen has demagnetizing coefficient N, $4\pi I$ should be replaced by $(4\pi - N)I$ here and in what follows.

where it is to be understood that only terms in the periodic argument are to be differentiated (terms arising from differentiation of powers of H outside the sine are negligibly small in comparison because of the high frequency of oscillation). The implicit relation now becomes

$$y = a\sin(x-y) \tag{15}$$

and a is just the amplitude of $4\pi \mathrm{d}I/\mathrm{d}H$ for $a \ll 1$. If $a \ll 1$ the equation is easily solved in powers of a and we find, to terms in a^2,

$$y = a\{(1-\tfrac{1}{8}a^2)\sin x - \tfrac{1}{2}a\sin 2x + \tfrac{3}{8}a^2\sin 3x \ldots\}. \tag{16}$$

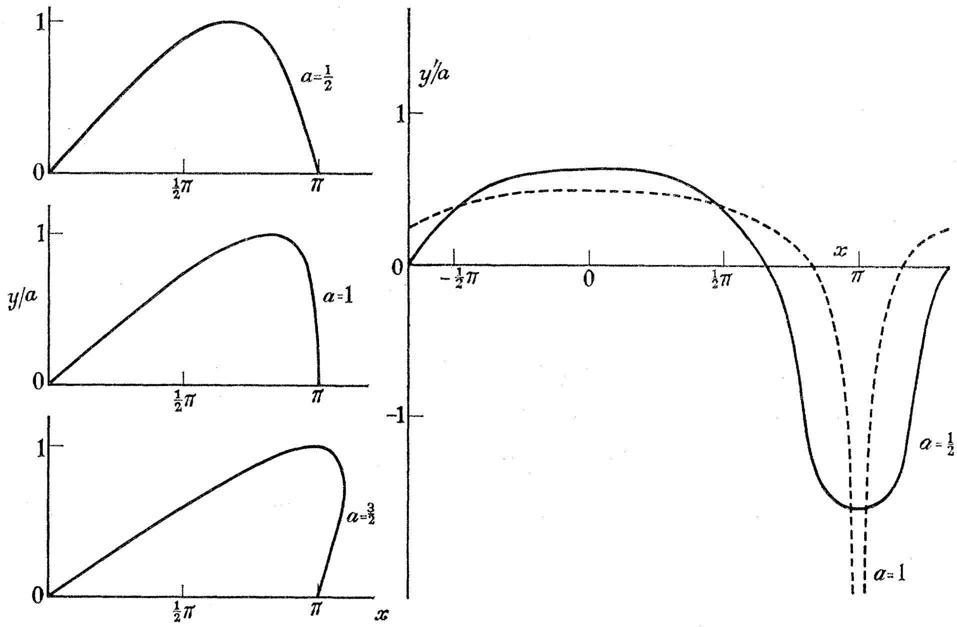

FIGURE 13. Solutions of equation (15) showing y and $\mathrm{d}y/\mathrm{d}x$ as functions of x for $a = \frac{1}{2}$, 1 and $\frac{3}{2}$. For $a > 1$ it is not clear what course the magnetization (i.e. y) would actually follow, so no attempt has been made to plot a curve for $\mathrm{d}y/\mathrm{d}x$ for $a = \frac{3}{2}$.

The value of $4\pi \mathrm{d}I/\mathrm{d}H$ is then given by

$$\frac{\mathrm{d}y}{\mathrm{d}x} = a\{(1-\tfrac{1}{8}a^2)\cos x - a\cos 2x + \tfrac{9}{8}a^2\cos 3x \ldots\}. \tag{17}$$

For larger values of a (15) can be solved by an obvious graphical procedure and solutions for $a = \frac{1}{2}$, 1 and $\frac{3}{2}$ are shown in figure 13. It can be seen that interesting novel features appear for $a \geq 1$; since, however, it is unlikely that this simplified theory is valid, particularly for $a > 1$, consideration of these features will not be pursued here. The important points which are relevant are that for $a \sim \frac{1}{2}$ (which is something like the actual value) harmonics are produced which are much stronger than those predicted by the usual theory (equation (9)) and moreover there is an appreciable reduction of the amplitude of the fundamental.

Probably the procedure of replacing H by B only in the final theoretical expression is too simple-minded. It is necessary really to go back to the basic assumptions of the theory and consider what happens to the energy levels of the electronic motion in a magnetic field when the magnetic interaction of the electrons is taken into account. This may well prove to be a many-body problem for which the kind of 'self-consistent field' treatment envisaged here is inadequate. The investigation of this problem clearly merits further attention, but for the present we shall use our admittedly crude treatment as a basis for discussion. It should, however, be borne in mind that the harmonics and the reduction of the fundamental given by a more complete theory may prove to be even stronger than given by (17). We shall indeed see below that such an enhanced reduction of the fundamental amplitude is needed to explain anomalies observed in the temperature and field variation of amplitude.

Before leaving this frequency modulation effect, it should be noticed that if more than one frequency of oscillation is present, we shall get not only harmonics of the separate frequencies but also 'combination tones', and in particular, if a low-frequency component has very high amplitude it will cause a modulation with its own frequency of the amplitude of a high-frequency component. This may be the cause of a peculiar modulation observed by Gold (1958, figure 1 h and p. 92) of a high-frequency oscillation by a low one, and also of some observations in the present work, in which the low-frequency neck oscillations in gold seemed sometimes to modulate the high-frequency belly oscillations. A detailed discussion, is however, hardly worth while until more systematic experimental evidence is available. Another effect of this combination tone effect is that the first harmonic in (9) which, as discussed on p. 119, might have an amplitude of as much as a few parts per cent of that of the fundamental, will be combined with the fundamental and modify slightly the strengths of the fundamental and of the second harmonic. It is unlikely that this effect should modify the fundamental as much as does the $\frac{1}{8}a^2$ term in (17) and, in any case, any detailed estimate will depend critically on the rather uncertain relative phase of the first harmonic and fundamental as given by (9).

Temperature variation of amplitude

If for the moment we ignore the complications of the frequency modulation effect, it can be seen from (13) that a plot of log A/T against T should be linear and the cyclotron mass m can be derived from the slope. This method of obtaining m is tedious—practically a whole helium run is needed for a good determination at any one orientation—and subject to considerable inaccuracies unless great care is taken, so only a few measurements of m were in fact made.

Since at higher temperatures the amplitudes become much smaller it was essential to use the resonant technique and the amplitude at any given temperature was taken as being proportional to the blip size. As will be discussed later, the amplitude is very sensitive to a number of factors and some of these may vary slightly in the course of a series of measurements in which only the temperature is intended to vary. Thus inaccuracies may be caused by variation in the peak field at which each shot is taken, by variation of the pick-up coil lead resistance as the liquid helium level falls (this can reduce the effective Q of the resonant circuit) and by slight changes in specimen orientation due to slight movement of the whole suspension as the pressure is lowered to reduce temperature (or perhaps to slight mechanical shocks produced by each discharge). Allowance was of course made for variations of what was intended to be a reproducible peak field, but inaccuracies in estimating this correction, together with the other two errors, were probably responsible for the rather appreciable scatter of points in a typical plot such as that shown in figure 14 (b).

PHILOSOPHICAL TRANSACTIONS OF THE ROYAL SOCIETY A MATHEMATICAL, PHYSICAL & ENGINEERING SCIENCES

Evidence for another source of error comes from the observation that two different copper [111] whiskers gave systematically non-linear plots (figure 14 (*a*)). It was at first thought that this might be due to the temperature of the specimen being above that of the bath by an amount which increased as the temperature was lowered. Such an effect might come from eddy current heating of the specimen by the varying field or from a magneto-caloric effect in the glass specimen mount, but the theoretical problem of the thermal state of a specimen in the experimental conditions is not straightforward and it is difficult to decide whether or not any appreciable temperature difference really occurs. On the whole the discussion on p. 129 suggests that there should be no appreciable rise of temperature below the λ-point, but a rise of order 0·1 °K above the λ-point, which would

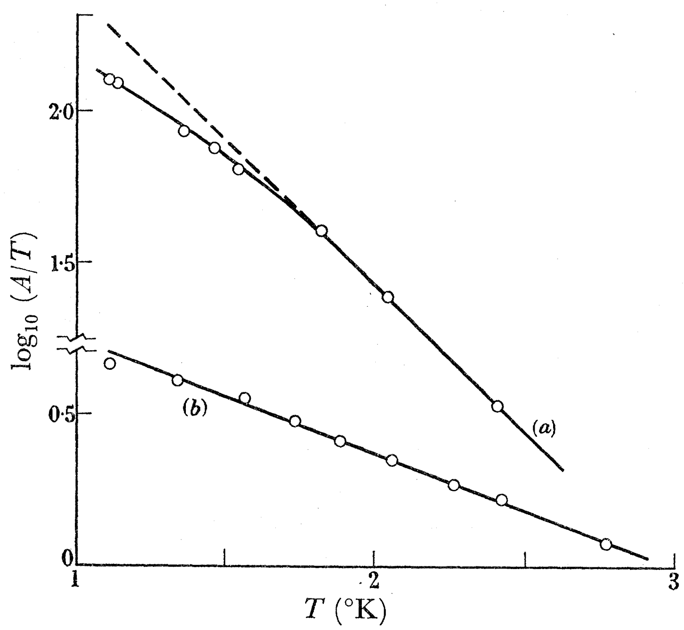

FIGURE 14. Plot of $\log_{10} A/T$ against T (*a*) Cu 41 for H along [111], (*b*) Ag 7 for H 13° off [100] in a plane 5° off (110). The units of the amplitude A are arbitrary.

increase slightly with increase of temperature. It can be seen, however, that the break in the plot occurs rather below the λ-point (at about 1·8 °K both in figure 14 (*a*) and in a series of measurements on Cu 43 in which the region of the break was more closely covered), so it is unlikely that heating is the main cause of the change of slope.

Another possible cause of the non-linearity is the frequency modulation effect discussed above. It can be seen from (17) that if a is large enough, the temperature variation of the fundamental (which is picked out by the resonant technique) comes not only through the factor a, which varies as (13), but also from the factor $(1-\frac{1}{8}a^2)$. If we conjecture that the true theory gives a coefficient of a^2 a good deal larger than $\frac{1}{8}$, say 0·5, we see that if a at the lowest temperature is as high as 0·6 (see p. 118) the blip size might be reduced by as much as 20 % below the size predicted by extrapolation of the plot of figure 14 (*a*) from high temperatures. Allowance for this depression would raise the lowest temperature point in the logarithmic plot of figure 14 (*a*) by 0·08 and go a long way to bridge the gap. The gap might perhaps be closed by supposing (as is plausible) that the eddy current or magneto-caloric heating effect is relevant for temperatures *above* the λ-point and that the point at

2·4 °K needs shifting appreciably to the right: a shift of less than 0·1 °K would be enough to lower the slope of the high-temperature line sufficiently.

Further evidence supporting this interpretation comes from the logarithmic plot of field variation (see figure 16) which was studied in the same helium experiment on the same whisker, and which also showed a non-linearity at high amplitudes. The significant point is that the 'break' both in figure 14 (*a*) and in figure 16 comes at about the same amplitude (about half the maximum amplitude). This is consistent with the above interpretation but would be rather a coincidence if the non-linearity were mainly due to heating.

According to this interpretation, then, the low temperature part of the plot should give too low a value of m because of the frequency modulation effect while the high temperature part of the plot might give too high a value of m because of slight heating effects. On the whole, however, the value of m deduced from the high-temperature plot is probably nearer to the true value. This is consistent with the fact that the 'high' value of cyclotron mass for [111] in copper comes less above the value of Kip *et al.* (1961) than the 'low' value comes below (see table 8).

TABLE 8

metal and orientation	values of m/m_0 and temperature range (°K)		Kip *et al.* (1961)
Cu 41 [111]	1·45 (2·0 to 2·9)	1·19 (1·1 to 2·0)	
	1·48 (1·8 to 2·4)	1·04 (1·1 to 1·6)	1·36
Cu 43 [111]	1·49 (1·7 to 2·4)	1·18 (1·1 to 1·7)	
Cu 38 [100]	1·27 ± 0·1 (1·1 to 1·6)		1·39
Cu 45 [100]	1·28 ± 0·07 (1·1 to 2·0)		
Cu 51 10° from [100] in plane 10° off (100)	1·28 ± 0·05 (1·2 to 2·0)		
Cu [111] neck	—		0·6
Ag 7 13° from [100] in plane 5° off (110)	0·63 ± 0·03 (1·1 to 2·8)		
Ag 28 [111] neck	0·35 ± 0·01 (1·2 to 2·1)		
Au 29 [100] belly	1·19 ± 0·03 (1·1 to 2·1)		
Au 16 [111] belly	1·09 ± 0·10 (2·0 to 4·2)		
Au 16 [111] neck	0·44 ± 0·04 (2·0 to 4·2)		
Au 29 [100] rosette	1·09 ± 0·07 (1·1 to 2·1)		
Au 9 [100] dog's bone	0·98 ± 0·1 (1·1 to 2·1)		
Au 21 [110] dog's bone	1·00 ± 0·1 (1·1 to 2·1)		

Note. The ± are intended only as rough indications of the possible inaccuracies. The two entries for Cu 41 refer to two separate determinations probably at slightly different orientations.

No appreciable non-linearity was observed in the plots for any of the other specimens,* but this may be merely because (owing to insufficient amplitude) measurements were not made over as wide a temperature range as for Cu 41 and Cu 43. It is possible then that some of the estimates of m in which the temperature was not taken above 2·1 °K may be appreciably low.

The results for m (expressed as a ratio to m_0 the free electron mass) are summarized in table 8; where necessary a correction has been applied to take account of the fact that the exponential factor in (13) is only an approximation to the exact variation (9) (see Shoenberg 1952*a*, p. 15).

Possible reasons for the discrepancies between the m/m_0 values for copper and those obtained by Kip *et al.* (1961) from cyclotron resonance have already been mentioned, but

* Except perhaps for Ag 7; figure 14 (*b*) does show an indication of the same effect as figure 14 (*a*).

even if there were no experimental error in either experiment it would not be too surprising if the agreement were imperfect. The mass m in both types of experiment is defined as proportional to dA/dE (see (10)), and in the de Haas–van Alphen experiments, because of the very high phase of the oscillations, the A concerned is just the extremal area of cross-section normal to the field. In the cyclotron resonance experiments, however, the phase is very much smaller and consequently contributions from sections other than ones very close to the extremal one do not cancel each other at all completely and the A concerned is a suitably weighted average over all sections normal to the field. Calculations by Kip *et al.* (1961) on a simplified model of the electronic structure suggest that the m observed in cyclotron resonance may well differ by a few parts per cent from the extremal value observed in the de Haas–van Alphen effect, and this may account for at least a small part of the discrepancies between the estimates by the two methods.

Although in principle the electron velocity at each point of the Fermi surface could be deduced if the cyclotron mass were known for every direction of H, nothing very detailed can be deduced from the rather meagre data of table 8. It is, however, possible to estimate an *average* of the electronic velocity v round some extremal sections of the Fermi surface, for it is easily seen from the definition of m that

$$V/V_s = (m_0/m)(\bar{r}/r_s), \tag{18}$$

where V is a harmonic mean of the velocity round the section (i.e. $1/(\overline{1/v})$), $\bar{r}$ is the mean radius of the section (i.e. perimeter/2π) and r_s and V_s are the radius and velocity for the free electron Fermi sphere of volume half that of the zone. We then deduce the rather rough values of V/V_s shown in table 9.

TABLE 9. VALUES OF V/V_s

	[100]	[111]	neck [100]	rosette [100]	dog's bone [110]
Cu	0·77 (0·71)	0·66 (0·71)	(0·33)	—	—
Ag	1·57	—	0·39	—	—
Au	0·85	0·89	0·40	0·58	0·87

Notes. The values in brackets are based on the cyclotron masses of Kip *et al.* (1961); for Cu [111] the result 0·66 assumes $m/m_0 = 1{\cdot}45$.

Field variation of amplitude

Some attempts were made to study the field variation of amplitude in order to obtain an estimate of x, but because of the difficulty that the field variation is controlled as much by field inhomogeneity (see p. 119) and specimen imperfections (see p. 120) as by the intrinsic factors in (9), only rather qualitative indications have been obtained. In principle the field variation can be studied either by examining a single picture or by taking a succession of pictures with varying peak fields. The first method did not seem practicable because of the limited range of fields over which the oscillations can be seen in a single picture, and because of the difficulty of allowing adequately for the variation in sensitivity of the detecting circuits as the time-frequency of the oscillations rises (to frequencies of order 200 kc/s where the oscillations fade out).

In the second method, resonance is used to increase sensitivity and a series of pictures is taken at varying peak fields and we must consider how this affects the field dependence.

The e.m.f. fed into the resonant circuit is proportional to $(\mathrm{d}I/\mathrm{d}H)(\mathrm{d}H/\mathrm{d}t)$ and if the resonant frequency of the circuit is f the resonant blip will occur for $\mathrm{d}H/\mathrm{d}t = H^2f/F$ (see (2)). Thus if H is varied by altering the condenser voltage the blip size A should be proportional to

$$H^{-\frac{1}{2}} \exp\left(-4\pi^3 mck(T+x)/ehH\right). \tag{19}$$

This argument, however, does not take account of the fact that the resonance is dynamic rather than static, i.e. that we are applying a signal of rather rapidly varying time frequency so that the resonance may not have time to develop fully.

The problem is similar to that of the 'gliding tone' considered by Barber & Ursell (1948) and can be solved exactly under the simplifying assumptions that the resonance is undamped, and that the field varies parabolically with time. The calculation (see appendix) shows that the resonant blip should be larger than the response without resonance by a factor proportional to $H^{\frac{1}{2}}$. The calculation also predicts a 'ringing' effect after the resonance, and this can be clearly seen in figure 15, plate 2; the beats can be distinguished from genuine beats due to two de Haas–van Alphen frequencies by the fact that they occur only *after* each blip in time. The relevance of the calculation to the present argument is that it modifies the expected field dependence of the blip size to simply

$$\exp\left(-4\pi^3 mck(T+x)/ehH\right).$$

It should, however, be mentioned that the calculation ignores damping of the resonance, and it is not certain whether the $H^{\frac{1}{2}}$ factor is still required in the actual conditions in which the static Q of the circuit is of order 5 or 10. The effect of omitting the extra $H^{\frac{1}{2}}$ factor is to increase slightly the deduced value of x.

Evidently to get useful results it is desirable that field dependence due to specimen bending should be avoided, and since a small degree of bending is almost inevitable this can be best achieved by setting the field rather accurately along a symmetry axis as can be seen from the calculations of p. 121. In the experiments with Cu 41 (a [111] whisker) the field variation was at first similar to that of figure 20 (but with much slower beats), probably because the field was 2° or 3° off parallel to [111], but when the specimen was remounted more carefully parallel, the plot of log A against $1/H$ shown in figure 16 was obtained.

The break in the plot has already been discussed (p. 113) in connexion with the interpretation of the temperature variation of the same specimen, and it was suggested that both breaks might be due to the frequency modulation effect becoming appreciable at the higher amplitudes. On this interpretation, it is the lower part of the plot which should conform to the usual theory, and the slope of this part then gives $x = 1{\cdot}7$ °K if m/m_0 is taken as 1·36 (Kip *et al.* 1961) or $x = 1{\cdot}5$ °K if m/m_0 is 1·48 as indicated by the temperature variation if possible heating effects are ignored. If the 'gliding tone' effect is ignored and log $AH^{\frac{1}{2}}$ is plotted rather than log A, these estimates of x are increased by about 0·2 °K. All these estimates, however, are likely to be exaggerated, because field inhomogeneity may well be responsible for an appreciable extra reduction of amplitude as the field is reduced (see p. 119); an extra reduction factor of 1·5 might well occur over the relevant range without appreciably affecting the linearity of the plot, and this would reduce all the estimates of x by about 0·4 °K. There is thus considerable uncertainty in the value of x, though it is probably within the range 1 to 2 °K and rather nearer to 1 than to 2 °K.

If x is due to collision broadening alone its value can be estimated as 0·5 °K from (11), using the relation

$$\frac{1}{\tau} = 4\frac{e^2}{c^2}\frac{\mathscr{A}}{\mathscr{A}_s}\frac{V}{V_s}\frac{\rho}{m_0 a^3}, \tag{20}$$

where ρ is the resistivity in e.m.u. (assumed the same as for Cu 43 (table 1)), a is the lattice constant (table 2) and $\mathscr{A}$ and $\mathscr{A}_s$ are the surface areas of the Fermi surface and the free electron Fermi sphere, respectively; V/V_s is taken as 0·71 (table 9) and $\mathscr{A}/\mathscr{A}_s$ is close to 1 (see II, table 1). Thus, as has been found for other metals before, the observed value of x is somewhat higher than that due to collisions alone, but in view of the considerable uncertainties in interpretation not too much significance need be attributed to this discrepancy.

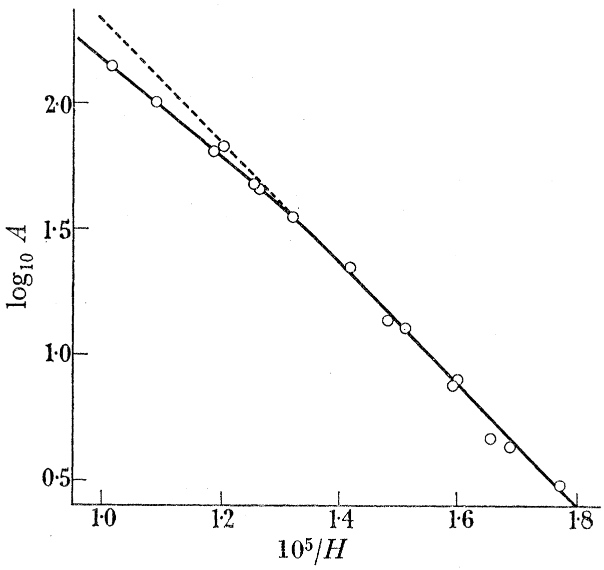

FIGURE 16. Plot of $\log_{10} A$ against $1/H$ for Cu 41 (H along [111]).

A rough estimate of x for Ag 7 can be made from the data to be discussed later (see figure 20) if it is assumed that the envelope curve to the beat maxima represents the true variation of a perfect specimen. This gives $x = 1{\cdot}9$ °K if the gliding tone effect is allowed for, but this might come down to 1·0 °K if field inhomogeneity is considered. The value based on collision broadening alone is 1·1 °K and the discrepancy is in the usual sense.

An interesting possibility is to use measurements of x to study how the relaxation time at particular parts of the Fermi surface depends on addition of impurities or defects. Experiments on tin (Shoenberg 1952 *a*) showed the feasibility of the idea, and a preliminary experiment has been made on a [111] crystal of an alloy of gold with 0·3 % silver. This still gave quite large neck oscillations, though the belly oscillations had an amplitude below noise level. It was possible to see the neck oscillations down to $H = 0{\cdot}45 \times 10^5$ G and a good linear plot of log A against $1/H$ was obtained (neck oscillations are less sensitive to specimen distortion because of the lower value of F'' (see table 10)), from which it was deduced that $x = 1{\cdot}5$ °K, on the assumption that m/m_0 was the same as for pure gold. Field inhomogeneity is much less important for the neck oscillations because of their low frequency, so this estimate of x is not likely to err on the high side, though it might be as much as 0·5 °K too low if the allowance made for the gliding tone effect is not soundly based.

If we substitute into (20) the resistivity of the alloy from table 1 and the value of V/V_s for the neck from table 9 (this assumes effectively that the mean free path round the neck is the same as the average over the Fermi surface which determines the resistivity), we find $x = 2{\cdot}7$ °K, which is appreciably higher than the observed value. This suggests, then, that the mean free path on the neck may be appreciably longer than over the belly. Evidently, however, more experiments (with varying amounts of alloying) are needed before any definite conclusions can be drawn and these are being pursued as a separate investigation.

Absolute amplitude of the oscillations

Comparison of the absolute amplitude predicted by (9) with that experimentally observed is complicated by insufficiently precise knowledge of some of the parameters in the theoretical formula, by uncertainties in the reduction of the observed amplitude on the c.r.o. screen to an absolute amplitude of $\mathrm{d}I/\mathrm{d}H$ and perhaps most seriously by various effects discussed in more detail later which tend to reduce the observed amplitude below its theoretical value. In principle, if all these difficulties could be overcome (and with enough trouble they could be) such a comparison would determine the value of the dimensionless factor $|(1/2\pi)\mathrm{d}^2A/\mathrm{d}k_H^2|^{-\frac{1}{2}}$ (which is 1 for a spherical surface) and thus provide a check on the form of the Fermi surface determined from the frequency data. On the information available we can, however, make only a rather qualitative comparison to get some idea of the validity of the formula.

The amplitude of the e.m.f. developed across the pick-up coil is

$$E = 4\pi SN\left|\frac{\mathrm{d}I}{\mathrm{d}H}\right|\frac{\mathrm{d}H}{\mathrm{d}t}\times 10^{-8}\,\mathrm{V},$$

where S is the area of cross-section of the specimen and N is the effective number of turns of the pick-up coil which surround the specimen. The evaluation of $|\mathrm{d}I/\mathrm{d}H|$ from the amplitude is complicated by uncertainties in estimating the effective amplification of the e.m.f. across the pick-up coil, and the effective number of turns. Typical figures for a [111] whisker (Cu 47) for $H = 1{\cdot}13\times10^5$ G and $T = 1{\cdot}2$ °K were $E = 2{\cdot}1\times10^{-4}$ V, $S = 0{\cdot}8\times10^{-4}\,\mathrm{cm}^2$, $N \sim 200$, $\mathrm{d}H/\mathrm{d}t = 7{\cdot}5\times10^6\,\mathrm{G\,s^{-1}}$, giving

$$4\pi\,|\mathrm{d}I/\mathrm{d}H| \sim 0{\cdot}18, \qquad (21)$$

but this estimate might well be out by 50%.

In the theoretical estimate for these conditions, the main uncertainties are in the values of x, $\mathrm{d}^2A/\mathrm{d}k_H^2$ and m/m_0. The determination of x is subject to considerable uncertainties as has already been explained and though a value of 1·7 °K was obtained (for a different [111] whisker) this may be a good deal too high. The value of $|(1/2\pi)\mathrm{d}^2A/\mathrm{d}k_H^2)|^{-\frac{1}{2}}$ given by Roaf's formula Cu VI is 3·4 (see II, table 6), but this could be computed only roughly and in any case Roaf's formula is probably hardly a precise enough representation of the true surface to reproduce such a fine detail faithfully. A value above 1 is of course plausible because of the proximity of the bulges round the necks to the (111) section; for the (100) section

Roaf's formula gives 0·9, which is not unreasonable.* For m/m_0 we take 1·36, the value of Kip *et al.* (1961), because of the uncertainties in the interpretation of the de Haas–van Alphen data. The theoretical formula then gives

$$4\pi|\mathrm{d}I/\mathrm{d}H| = 56\exp(-5{\cdot}1 \text{ or } -3{\cdot}9) = 0{\cdot}32 \quad \text{or} \quad 1{\cdot}1 \qquad (22)$$

according as x is taken as 1·7 or 1·0 °K (the lowest estimate of p. 115).

Either estimate is consistent with the experimental estimate (21) bearing in mind all the uncertainties and in particular that the observed value might be expected to be lower than the theoretical one, and to this extent the validity of the theoretical formula is confirmed. These calculations also bring out the important point that $4\pi|\mathrm{d}I/\mathrm{d}H|$ is quite appreciable compared with 1 (this is, of course, because of the extra factor $2\pi F/H$, which is $\sim 10^4\pi$, involved in going from I/H to $\mathrm{d}I/\mathrm{d}H$); it is because of this very high value of $4\pi|\mathrm{d}I/\mathrm{d}H|$ that the frequency modulation effects discussed above are of practical importance.

For silver and gold the absolute amplitudes of the belly oscillations, which were comparable to that of Cu 47, are also in qualitative agreement with the theory, and so too are the neck, dog's bone and rosette oscillations. Though only rough measurements were made, it may be noted that for silver and gold the dog's bone amplitudes were $\frac{1}{5}$ or $\frac{1}{10}$ those of the belly, the rosette was somewhat stronger (particularly in gold) and the neck was comparable to the belly in gold but about $\frac{1}{5}$ as strong in silver. The behaviour of copper is, however, anomalous; the rosette has a reasonable enough amplitude (of order $\frac{1}{5}$ of that of the belly), but the dog's bone has not been observed at all and the neck is much weaker than in silver and than the theory predicts with the same value of x as assumed above. It might be that the value of x is particularly high in copper for orbits which pass close to the neck, but then it is puzzling why the rosette oscillations are not also very weak. Another mystery about copper is why it has not been possible to obtain any de Haas–van Alphen effect at all with crystals grown from the melt. In the light of the residual resistance measurements (table 1) it is not surprising that no effect was found with Cu 68 since from collisions alone, x should have been as high as 6·5 °K; Cu 72 and 73 had a much lower residual resistivity than the whiskers and it is just possible that the eddy current heating effect discussed later may have caused a large temperature rise (the orientation was, however, varied over 10° or so round [111] in small steps to make sure that the negative result was not due to low magneto-resistance at exactly [111]). Cu 75, however, appears to be very comparable to a typical whisker and it is very puzzling why no oscillations were observed.

Harmonic content of the oscillations

As already mentioned, strong harmonics were observed in the de Haas–van Alphen oscillations. This can be seen both from the resonant blips of pictures such as figures 15 and 17 (plate 2) and from the shape of the individual oscillations off resonance (near the centre of figure 15). To estimate the strengths of the harmonics relative to the fundamental in the Fourier analysis of $\mathrm{d}I/\mathrm{d}H$ allowance must be made for the fact that the harmonics resonate at values of $\mathrm{d}H/\mathrm{d}t$ smaller than that for the fundamental and also for the fact that the

* Note that A is a maximum for (100), but a minimum for (111).

passage through resonance is rapid, which further reduces the resonant amplitude. The analysis of this 'gliding tone' effect given in the appendix shows that the net effect is to reduce the relative amplitude of the pth harmonic resonant blip by $p^{\frac{3}{2}}$ compared with its relative amplitude in the Fourier analysis of dI/dH. Allowance must also be made for the 'tails' of the main resonance in estimating the contribution of a harmonic to the blip it produces. We then find that in figure 17 the amplitudes of the first and second harmonics (i.e. $p = 2$ and 3) relative to the fundamental of dI/dH are about 0·9 and 0·8, respectively, while in figure 15 the first harmonic is about 0·3 of the fundamental. Whatever the cause of the variation in harmonic content between the two pictures (some suggestions will be discussed later), the significant fact is that the harmonics are much stronger than the prediction of (9), which is that the ratio of the amplitude of the pth harmonic to that of the fundamental should be approximately

$$p^{\frac{1}{2}}|\cos(\pi pm/m_0)/\cos(\pi m/m_0)|\exp-(p-1)(4\pi^3mck(T+x)/ehH). \tag{23}$$

Even if we take $x = 1$ °K, the argument of the exponential is $-3\cdot9(p-1)$, which for $p = 2$ gives a ratio 0·04 and for $p = 3$, 0·0016 (assuming $m/m_0 = 1\cdot36$ as in (22)). At first sight it might seem that the strong first harmonic might be a consequence of m/m_0 being close to 1·5, for then $\cos(\pi m/m_0)$ becomes small compared with $\cos 2\pi m/m_0$, but this cannot explain a strong second harmonic since $\cos 3\pi m/m_0$ would also be small. Subsidiary tests showed also that the observed harmonics were not due to any non-linearity of the amplifying circuit.

Most probably the harmonics are due mainly to the frequency modulation effect discussed earlier which for an amplitude a of $4\pi dI/dH$ of order 0·1 to 0·5 (such as obtained here) should produce harmonics of the right order of magnitude. Since, however, the theory needs to be more fully worked out and only a few isolated observations of harmonic content were made in the course of measurements for other purposes, it is hardly worth attempting any detailed discussion. Some possible causes of the irreproducibility of the effects (e.g. the difference between figures 15 and 17) will become apparent below when the influence of field inhomogeneity and specimen imperfections is discussed. It should be mentioned that appreciable harmonics were noticed not only for the [111] copper whiskers, but also in other specimens whenever the absolute amplitude of $4\pi dI/dH$ was of the same order as in the [111] whiskers.

We shall now discuss a number of effects which can reduce the amplitude below its theoretical value.

Reduction of amplitude by field inhomogeneity

The magnet was designed to have a very homogeneous field, and measurements with a differential search coil system showed that over the region of 4 mm occupied by the specimen, the field varied by only about 1 part in 15000. Even this small inhomogeneity, however, is enough to make the phase $2\pi F/H$ vary by about $\frac{1}{2}\pi$ between the ends and the middle of the specimen and this might well be the cause of an appreciable reduction of the theoretical amplitude. If we assume a parabolic variation of field round the centre of the specimen, i.e. $H = H_0(1-\frac{1}{2}cz^2)$ the integration over phase gives the result (26) below with $v = (2Fc/H)^{\frac{1}{2}}z$ (see Shoenberg 1952*a*, p. 28). Substituting $c = 1/300$ (to give a drop of 1/15000 2 mm from $z = 0$) we find that for $F = 5\cdot8\times10^8$ G and $H = 10^5$ G

$v_1 - v_2 = 2{\cdot}4$ and the reduction factor is 0·79; if, however, H is reduced to 5×10^4 G the reduction factor becomes about 0·38.

These figures are of course only rough estimates since the exact amount and form of the inhomogeneity have not been accurately enough determined, but they serve to show not only that the absolute amplitude may be appreciably reduced, but also that in studies of the field variation appreciable errors may arise because of the field dependence of the reduction factor. Field inhomogeneity may also be the cause of quite appreciable irreproducibility of amplitude, since displacement of the specimen by as little as 1 mm even in the most homogeneous parts of the field can change the amplitude by 10% or so, while a cm or so from the magnetic centre the amplitude falls off rapidly and fluctuates more and more wildly as the specimen embraces more and more 'half period zones'. Even though the specimen is supposed to be fixed, some variation of position (of order $\frac{1}{2}$ mm) occurs as the liquid helium level falls and the mounting undergoes thermal expansion; also in the trifilar suspension (see p. 91) change of orientation of the specimen inevitably involves slight change of its position.

Reduction of amplitude due to specimen imperfections

We shall assume that the effect of imperfections is due only to the variation of orientation through the specimen it involves, i.e. we ignore possible effects due to lattice imperfections such as dislocations. We shall, moreover, consider only the following idealized types of specimen distortion which lend themselves to simple analysis in the hope that they will give some idea of the effect of actual (and more complicated) distortions, (1) the specimen consists of two equal crystals inclined at angle β, (2) the specimen is bent through an angle β into the arc of a circle, and (3) the specimen consists of many crystallites with a Gaussian distribution of orientations about some mean orientation, so that the proportion of the specimen for which the field is at an angle between ϕ and $\phi + \mathrm{d}\phi$ from its mean direction with respect to the crystal axes is $(2/\phi_0^2)\,\mathrm{e}^{-(\phi/\phi_0)^2}\,\phi\,\mathrm{d}\phi$.

For each type of variation we consider two limiting cases: (*a*) the mean orientation (specified by θ, the mean angle between the field and the symmetry axis) is close to a symmetry direction, so that the contours of F on a spherical plot of field directions will be circles centred on the symmetry direction, and (*b*) the mean orientation is arbitrary, so that the contours of F are approximately parallel straight lines. A straightforward integration of $\cos(2\pi F/H)$ over the specimen (regarding F as varying with the varying orientation, specified by ϕ) then shows that the amplitude is reduced by a factor f as follows:

1 (*a*).
$$f = |\cos(\pi F''\theta\beta/H)|. \tag{24}$$
*

(This is the basis of the method of measuring F'' mentioned on p. 96).

1 (*b*). We assume for simplicity that the plane of the two pieces is perpendicular to the plane of the contours and find
$$f = |\cos(\pi F'\beta/H)|. \tag{25}$$

If θ, though much larger than β, is not so large as to invalidate a parabolic approximation, then $F' \simeq F''\theta$, and (25) becomes identical with (24). Effectively this is the

* Here, and in what follows, F' means $\mathrm{d}F/\mathrm{d}\theta$ taken at the mean value of θ, the angle between the field and the symmetry axis, while F'' means $\mathrm{d}^2F/\mathrm{d}\theta^2$ taken at $\theta = 0$.

PHILOSOPHICAL TRANSACTIONS OF THE ROYAL SOCIETY A MATHEMATICAL, PHYSICAL & ENGINEERING SCIENCES

approximation of supposing the contours are still circles but of such large radius that they can be considered as locally straight.

2 (*a*).

$$f = \frac{1}{v_1 - v_2}\left\{\left(\int_{v_1}^{v_2} \cos \tfrac{1}{2}\pi v^2 \, dv\right)^2 + \left(\int_{v}^{v_2} \sin \tfrac{1}{2}\pi v^2 \, dv\right)^2\right\}^{\frac{1}{2}}, \tag{26}$$

where $v = (2F''/H)^{\frac{1}{2}}\phi$, ϕ is the angle between the field and the symmetry axis at any part of the specimen, and the subscripts 1 and 2 refer to the two ends of the specimen (i.e. $\phi_1 - \phi_2 = \beta$); f is just the ratio of the chord to the arc of a Cornu spiral and becomes appreciably less than 1 only if $(v_1 - v_2)$ becomes comparable to or greater than 1.

2 (*b*). We assume for simplicity that the plane of the circular arc is perpendicular to the plane of the contour of F through the mean orientation and find

$$f = \left|\frac{\sin(\pi F'\beta/H)}{\pi F'\beta/H}\right|. \tag{27}$$

If as above, we assume $F' \simeq F''\theta$, (27) can be derived from (26) as a limiting case valid for $v \gg v_1 - v_2$, in precise analogy with the change-over from Fresnel to Fraunhofer diffraction in optics.

3 (*a*). The integration is now more complicated, since the orientation varies in two dimensions, rather than one; we find

$$f = (1 + (\pi\phi_0^2 F''/H)^2)^{-\frac{1}{2}} \exp - \frac{(\pi\phi_0\theta F''/H)^2}{1 + (\pi\phi_0^2 F''/H)^2} \tag{28}*$$

For $\pi\phi_0^2 F''/H \ll 1$, but $\theta > \phi_0$, (28) becomes

$$f = \exp(-\pi\phi_0\theta F''/H)^2, \tag{29}$$

while for $\pi\phi_0^2 F''/H \gg 1$, we have

$$f = (H/\pi\phi_0^2 F'') \exp - (\theta^2/\phi_0^2). \tag{30}$$

If the mean orientation is not along a symmetry direction but is such that F has an extremum, the contours will be ellipses rather than circles and the calculation is more complicated, since F'' will then depend on the azimuth of ϕ, but evidently f still gives a measure of the reduction factor if F'' is taken as some appropriate average.

3 (*b*). If we assume that F'' is small (i.e. $\pi\phi_0^2 F''/H \ll 1$), we find

$$f = \exp(-\pi F'\phi_0/H)^2 \tag{31}$$

and if we put $F' \simeq F''\theta$ this reduces, as it should, to (29).

It will be seen that in all cases f begins to fall appreciably below unity when $\pi F''\beta\theta/H$ (or $\pi F''\beta^2/H$ if the field is exactly along a symmetry direction) is comparable to 1, where β is a characteristic angle which specifies the spread of orientation, and the fall is particularly rapid for a Gaussian spread of orientations.

Some rough estimates of F'' are shown in table 10 (based on Roaf's formulae and consistent with the experimental data) and it can be seen that they set high demands on crystal perfection. If we take $F'' = 4 \times 10^8$ as typical, we find that for $H = 1{\cdot}2 \times 10^5$, $\pi F''\beta^2/H = 1$ for $\beta \sim 10^{-2}$ (i.e. $\frac{1}{2}°$); thus if the field is exactly along a symmetry direction amplitude will begin to fall off for a spread of orientation of order $\frac{1}{2}°$, but if we are say 5°

* I am indebted to Dr M. G. Priestley for the derivation of this result (Priestley 1962).

away from a symmetry direction $\frac{1}{20}°$ will already be sufficient to reduce amplitude, and moreover the reduction will be drastic for a random spread of twice as much.

No detailed study of the substructure of the specimens was made by X-ray methods (e.g. fine beam technique) though the size of the Laue spots indicates that the random spread ϕ_0 was certainly less than $\frac{1}{2}°$; often, however, especially when a specimen had been in use for some time, a bending of order 1° or 2° was evidenced by the drawing out of the spots into streaks. Some idea of the size of ϕ_0 can, however, be obtained from a study of the variation of amplitude with orientation.

Table 10. Values of $10^{-8} F''$ (G)

	belly [100]	belly [111]	rosette	dog's bone		neck
Cu VI	−2·1 (1·6)	8·0 (5·8)	11	6	11	0·9
Ag IV	−1·4	3·9	10	5	11	0·4
Au V	−5·9	6·1	9	5	10	0·6

Note. The figures in brackets were very rough experimental determinations by the beat method described on p. 96 (see Shoenberg 1960*a*). The two columns for the dog's bone refer to the two planes of rotation (110) and (100). The estimates from Roaf's other formulae are mostly within 10 % of those given here.

Orientation dependence of amplitude

Some typical results for Cu 46 (a [111] whisker) are shown in figure 18. If we disregard for a moment the considerable fluctuations in amplitude, it can be seen that for $\theta \sim 4°$, the amplitude falls to something like $\frac{1}{10}$ of its peak value. If we assume that this drop is entirely due to the random substructure (i.e. case 3(*b*) above), it would mean that for $\theta \sim \frac{1}{15}$, $\pi F''\theta\phi_0/H \sim 1{\cdot}5$, and putting $F'' = 7\times10^8$ G, $H = 10^5$ G, we find $\phi_0 \sim 10^{-3}$, i.e. $\frac{1}{20}°$.

No detailed study of angular amplitude variation has been made for silver and gold, but in the measurements of frequencies an appreciable amplitude (say $\frac{1}{50}$ of the value for the symmetry direction) was still observable for F' as high as 10^8, and this again suggests that ϕ_0 is something like $\frac{1}{20}°$. Evidently, these estimates of ϕ_0 are only rough upper limits, since part of the amplitude reduction may well be due to other kinds of specimen distortion and to other causes, such as increase of m away from [111] (Kip *et al.* (1961)), variation of d^2A/dk_H^2 and perhaps eddy current effects (see below); but probably the random substructure is the main factor which reduces amplitude whenever F' approaches 10^8. It should be noticed, however, that if ϕ_0 is only $\frac{1}{20}°$, (28) predicts no appreciable reduction for H along a symmetry direction.

Owing partly to difficulties of precise angular control and measurement, the points of figure 18 are rather irregularly scattered but there does seem to be a periodic variation with θ, which suggests that the specimen is bent either into a continuous arc or several segments. If we identify the period of about 1·1° for $\theta > 2°$ with $H/F''\beta$ (ignoring the fact that the minima are not zeros, which is probably due to the fact that the specimen distortion is more complicated than envisaged in any of the simple cases discussed above) we find $\beta = 0{\cdot}4°$, which is a plausible result. Probably the oscillations are due more to bending into a small number of straight pieces rather than a circular arc, since (26) predicts a rather more rapid fall off in general level of amplitude than is suggested by figure 18. Thus with $\beta = 0{\cdot}4°$, $(v_1 - v_2) \sim 0{\cdot}8$, and (26) predicts that the first off-centre maximum should come at about $1\frac{1}{2}°$, and be only about 20 % of the central one. Whatever the exact interpretation may be, figure 18 illustrates the important point that the least bending of the specimen can cause considerable fluctuations of amplitude for quite small changes of specimen orientation.

The angular variation of the amplitude of the first harmonic is also shown in figure 18 and this makes clear what is probably the main reason for irreproducibility in observations of relative harmonic strength (e.g. the differences between figures 15 and 17). It is simply that both the harmonic and the fundamental fluctuate rapidly with slight changes of orientation and the fluctuations are not in step, so that for some orientations a maximum of the harmonic curve coincides with a minimum of the fundamental and vice versa. Thus quite small changes of orientation can alter drastically the apparent relative harmonic

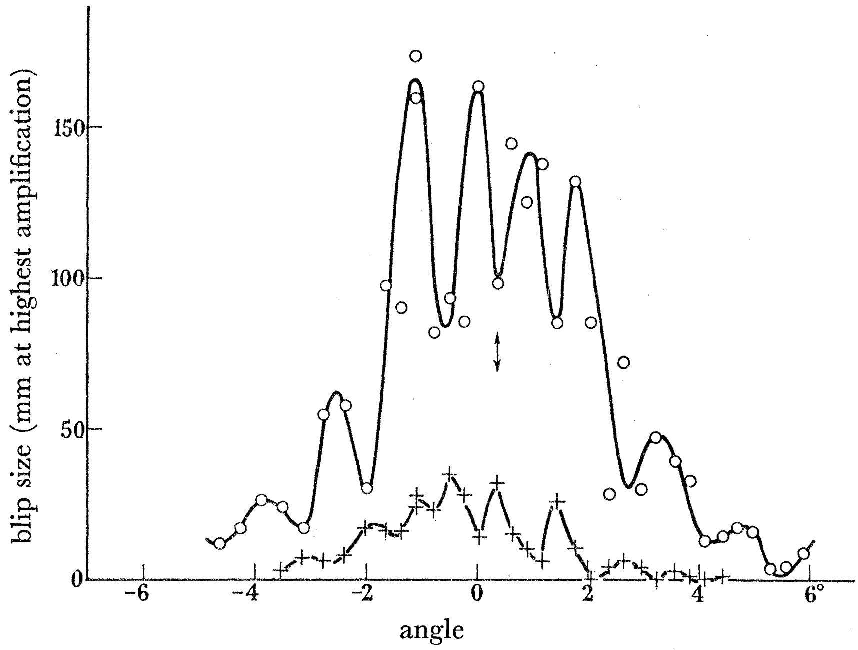

FIGURE 18. Variation of amplitude with orientation for Cu 46 round [111]. ○, fundamental; +, first harmonic. The zero of the angular scale is close to [111] (probably within 1°), but the plane of rotation may not pass exactly through [111]. The angles were obtained by interpolations between monitored orientations several degrees apart, using the setting of the screw in the trifilar suspension as an indicator; they may be appreciably wrong, and occasionally not even in correct sequence. The curve has been drawn somewhat schematically, bearing this in mind. The units of blip size are mm on the film scaled to the conditions of highest amplification. The arrow indicates the points taken from figure 17.

strengths. It should in principle be possible to decide whether (24) or (27) is the more applicable by noting the phase of the variations in the harmonic relative to that of the fundamental, but the angular resolution of figure 18 is hardly adequate for the purpose, and it is quite possible that the real bending of the specimen conforms to neither of the simple assumptions considered. Moreover, if as seems probable, the harmonics come from the frequency modulation effect, the proper theory for an imperfect specimen might be very complicated, since B must be kept continuous through the specimen in spite of the variations in I due to the varying orientation.

Before leaving the subject of angular variation of amplitude it may be noted that the above discussion referred to variation round [111]. For all three metals it was found that on tilting away from [100] the amplitude rises rather than falls. The biggest amplitudes (as much as 10 times those at [100]) were usually observed close to the 'dip' in the curves of figures 7, 8 and 10. Since as we saw above, random substructure should not be relevant for a symmetry direction (particularly at [100] where F'' is smaller than at [111]), the vanishing of F' at the 'dip' cannot explain an increase of amplitude over that at [100], though it might explain why it is greater than at intermediate points, where F' is appreciable. A possible partial explanation is that the factor $|(1/2\pi)\mathrm{d}^2A/\mathrm{d}k_H^2|^{-\frac{1}{2}}$ in (9) increases and Roaf's formulae do in fact have just this property (see II, table 6). For gold, for instance, this factor increases from 0·7 to 1·4 as the orientation goes from [100] to the dip in the (110) plane and to 0·9 for the dip in the (100) plane. This can explain only part of the observed increase and probably other causes, such as variation of m (Kip *et al.* (1961) report a drop of 7% in m at 9° off [100] in a (110) plane), and low magneto-resistance at [100] (see p. 125) may also be responsible.

Effect of inhomogeneity due to eddy currents

The general problem of field distortion due to eddy currents induced by the time variation of H has been discussed by Kosevich (1957); here we discuss only a simple special case to give an idea of the physical principles and orders of magnitude. This is the case of a cylinder of radius a and resistivity ρ (which depends on H) in a field parallel to its axis, with the field varying so slowly that its value on the axis is only slightly different from that at the outside (this approximation is certainly valid for our conditions). Faraday's law then shows that the field H at radius r in the cylinder is given by

$$H(r) = H(1-\alpha(1-r^2/a^2)), \tag{32}$$

where $$\alpha = \pi a^2 \mathrm{d}H/\mathrm{d}t/H\rho \quad \text{and} \quad \alpha \ll 1.$$

If the oscillatory susceptibility at any point is $\cos(2\pi F/H)$, the observed susceptibility will be

$$\frac{1}{\pi a^2}\int_0^a 2\pi r\,\mathrm{d}r\cos\left[\frac{2\pi F}{H}\left\{1+\alpha\left(1-\frac{r^2}{a^2}\right)\right\}\right]$$

which reduces to $$\frac{\sin(\pi F\alpha/H)}{\pi F\alpha/H}\cos\left\{\frac{2\pi F}{H}(1+\tfrac{1}{2}\alpha)\right\}. \tag{33}$$

There are then two effects: a reduction in amplitude and a very slight change of frequency. The reduction in amplitude will be appreciable as $F\alpha/H$ approaches 1 and should show oscillations with zeros whenever $F\alpha/H$ has an integral value (for other shapes of specimen oscillations should still occur but the minima might no longer be zeros). When $F\alpha/H \gg 1$ it will be noticed that the amplitude varies as $H/\pi F\alpha$, but since the observed signal is also proportional to πa^2 and $\mathrm{d}H/\mathrm{d}t$, it will vary as $\pi a^2 H\,\mathrm{d}H/\mathrm{d}t/\pi F\alpha$, i.e. as $\rho H^2/\pi F$. In this extreme limit, then, the signal becomes independent of specimen size and of $\mathrm{d}H/\mathrm{d}t$. However, in our conditions it is probable that we are at just the opposite extreme, i.e. $F\alpha/H < 1$.

An upper limit to α can be estimated from the fact that there is no evidence for any appreciable beats over several hundred oscillations in oscillograms such as figure 19, plate 2 in which α increases steadily from zero because of the variation of $\mathrm{d}H/\mathrm{d}t$. Presumably $F\alpha/H$ is still less than 1 at the furthest point at which there is still an appreciable amplitude of de Haas–van Alphen effect, (since no appreciable modulation of the envelope is evident as $\mathrm{d}H/\mathrm{d}t$ increases smoothly from zero up to this point). This shows then that $\alpha < H/F$, i.e. $< 2\times10^{-4}$, and we deduce from the known values of $\mathrm{d}H/\mathrm{d}t$ and specimen radius a, that $\rho > 100$ e.m.u. Similar observations on a silver specimen (Ag 7) gave $\rho > 50$. Since the zero-field residual resistivities of Cu 43 and Ag 7 were about 12 and 18 e.m.u., respectively, only a modest magneto-resistance is needed to make ρ large enough and the required magneto-resistance is reasonably in accord with the data of Alekseevski & Gaidukov (1959). It is just possible that when H is very close to [111] or

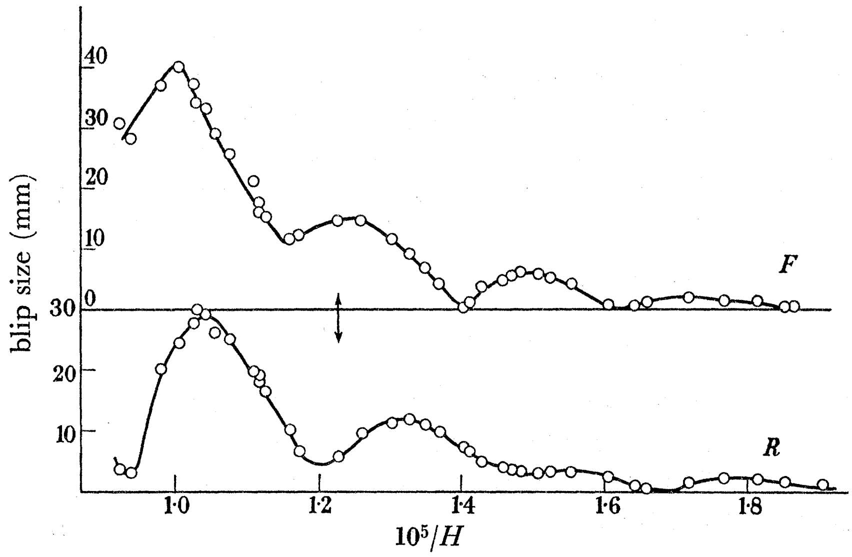

FIGURE 20. Variation of blip size (mm on film) with $1/H$ for Ag 7 showing beats due to specimen bending. R and F refer to rising and falling fields, respectively. The arrow indicates the points taken from figure 21.

to [100], where the magneto-resistance has deep minima, ρ falls to a value low enough to make $F\alpha/H > 1$, and this might be responsible for some of the dips in figure 18 and for the low amplitude at [100]. In general, however, it seems that the specimens are thin enough and ρ high enough, so that reduction of amplitude due to eddy current inhomogeneity is not a serious effect for our conditions of working.

There is some evidence that the slight change of frequency of order 1 part in 10^4 suggested by (33) can show up in rather a subtle way when long beats are being measured. Detailed measurements were made of the field variation of amplitude (by the resonant blip technique) for Ag 7 with the field set at about 13° off [100] in a plane 10° off (110)*, and the well-defined beats of figure 20 were observed. At first sight it might be thought that these beats are just due to the modulating factor of (33), but this would mean $\alpha \sim 1100$ and contradict the observation that no beats are observed when $\mathrm{d}H/\mathrm{d}t$ is increased from zero (see above). The most likely explanation is that this specimen is by an accident an almost perfect example of one of the ideal cases considered above, i.e. of either a circular arc or two equal segments inclined at a small angle β, and from the observation that

* At that time the angle monitor was reading erroneously and this setting was made under the wrong impression that the field was along [100]; this was a lucky mistake because the observed effects should not occur along a symmetry axis.

PHILOSOPHICAL TRANSACTIONS OF THE ROYAL SOCIETY A MATHEMATICAL, PHYSICAL & ENGINEERING SCIENCES

$F\Delta(1/H)$ is about 1100 it can be deduced that β is about 2° (taking $F'/F \sim 0{\cdot}03$ from figure 8). An X-ray photograph taken subsequently confirmed this interpretation almost exactly by showing that the specimen did in fact consist mainly of two single crystals inclined to each other at just about 2° in roughly the expected plane.

The evidence for the slight change in period due to eddy currents comes from the observation that the beat minima come at appreciably higher values of $1/H$ for the rising field resonant blip than for the falling field one. This shows itself strikingly by the inequality of blip sizes at appropriate fields, as for instance in figure 21, plate 2; such unequal blips have also been seen with many other specimens. If indeed F should be replaced by $F(1+\frac{1}{2}\alpha)$ for rising field and $F(1-\frac{1}{2}\alpha)$ for falling field, then F' in (25) should also be modified, approximately to $F'+\frac{1}{2}\alpha' F$ and $F'-\frac{1}{2}\alpha' F$, respectively, which implies that the beat frequencies should be slightly different for the rising and falling blips. The difference in beat frequency, $\alpha' F\beta$ is too small to show up directly, but the difference of phase is appreciable. It can easily be shown that if Δ is the interval in $1/H$ of neighbouring beat minima and δ is the difference between the values of $1/H$ for which the same minimum occurs for rising and falling blips, then

$$\delta/\Delta = -F\beta\alpha'/H = F\alpha\beta\rho'/\rho H.$$

Thus if we put $\alpha < 2\times 10^{-4}$, $\beta = 3\times 10^{-2}$, $F/H = 6\times 10^{3}$ we find $\delta/\Delta < 0{\cdot}036\rho'/\rho$. To fit the observed value of δ/Δ of about 0·15 we should have to suppose $\rho'/\rho > 4$, i.e. a variation of ρ of more than 7% per degree, which is quite consistent with the rate of change to be expected on the basis of the data* of Alekseevski & Gaidukov (1959).

Possible heating effects

Careful consideration suggests three possible sources of heat production which might cause the temperature of the specimen to rise appreciably above that of the bath. In descending order of total heat produced during the time the field rises to its peak, these are (*a*) eddy current heating in the windings of the pick-up coil, (*b*) reversible magneto-caloric effect in the glass specimen holder, and (*c*) eddy current heating in the specimen itself. We shall first estimate for each process the total energy E produced, the initial power, and the power per unit area at the time the oscillations are observed, and then estimate the temperature rise at the time the resonant blip occurs in experiments on temperature variation of amplitude.

In (*a*) the problem is essentially that of the eddy currents produced in a long cylinder of length l, radius a and resistivity ρ (e.m.u.) transverse to the field and it is easily shown that the power W produced is given by

$$W = \tfrac{1}{4}\pi l a^4 (\mathrm{d}H/\mathrm{d}t)^2/\rho. \tag{34}$$

The result for a longitudinal cylinder (i.e. for (*c*)) is just half as big. To obtain E, (34) must be integrated over the time τ taken from the beginning of the discharge to the time the resonant blip is observed, and it will be assumed for simplicity that H varies as $H_0 \sin\omega t$

* The published data are too meagre to permit an exact comparison for the orientation of Ag 7, but suggest that ρ'/ρ should be positive and of order 10% per degree.

PHILOSOPHICAL TRANSACTIONS OF THE ROYAL SOCIETY A MATHEMATICAL, PHYSICAL & ENGINEERING SCIENCES

and that τ is $\pi/2w$. For the 47 s.w.g. copper windings of the pick-up coil, ρ varies nearly linearly with H, and if we assume $\rho = \rho_0(1+\gamma(H/H_0))$ we find for $\gamma \geqslant 1$

$$E = \frac{4}{\pi}W_0\tau\{1-\gamma\ln 2-((\gamma^2-1)/\gamma)\ln(\gamma+1)+(\gamma^2-1)^{\frac{1}{2}}\ln(\gamma+(\gamma^2-1)^{\frac{1}{2}})\}, \qquad (35)$$

where W_0 is the initial power. For $\gamma = 0$ (no magneto-resistance) the result is $\frac{1}{2}W_0\tau$. For the wire used $\rho_0 \sim 20$ e.m.u. (90 times less than at room temperature) and from the magneto-resistance data of Chambers (1956) it can be deduced that $\gamma \sim 2{\cdot}5$, for which (35) gives $E = 0{\cdot}25\, W_0\tau$. Putting $a = 2{\cdot}5\times10^{-3}$ cm, $l = 800$ cm, $\mathrm{d}H/\mathrm{d}t = 1{\cdot}4\times10^7\,\mathrm{G\,s^{-1}}$ we have $W_0 = 2{\cdot}5\times10^5$ ergs s^{-1}, and $E = 600$ ergs for $\tau = 10^{-2}$ s. The power per unit area of the ebonite wall of the coil (area 0·16 cm^2) at the time of the blip is roughly $W_0/50$ ($\mathrm{d}H/\mathrm{d}t$ is 10 times smaller than initially and ρ 3·5 times larger).

For case (c) we assume that $\rho = \rho_0(1+\alpha(H/H_0)^2)$ since for a single crystal the variation is usually quadratic rather than linear, and find

$$E = W_0\tau/\{1+(\alpha+1)^{\frac{1}{2}}\}. \qquad (36)$$

For the specimen which showed the non-linearity of figure 14, $\rho_0 = 12$ e.m.u., $l = 0{\cdot}5$ cm, $a = 8\times10^{-3}$ cm and we may guess that $\alpha \sim 3$, and we find $W_0 \sim 2\times10^4$ ergs s^{-1} and $E \sim 70$ ergs; the power per unit area (area $2{\cdot}5\times10^{-2}$ cm^2) at the time the blip is observed is something like $W_0/10$ (here ρ is increased four times).

The magneto-caloric effect is reversible and the total heat liberated is

$$E = \tfrac{1}{2}\chi H^2 V, \qquad (37)$$

where χ is that part of the susceptibility which obeys Curie's law and V is the volume of glass. Assuming that the Pyrex glass is similar to that studied by Salinger & Wheatley (1961), $\chi \sim 4\times10^{-5}/T$, $V \sim 1{\cdot}5\times10^{-3}$ ml. and for $H = 10^5$ G we find E is 500 ergs at 1·2 °K and 250 ergs at 2·5 °K. The power production is $(2E\mathrm{d}H/\mathrm{d}t)/H$ and is zero initially; at the time of the blip it is per unit area (inside plus outside area $\sim 0{\cdot}3$ cm^2) roughly $80E$, and this is positive for rising field but negative for falling field, since the magneto-caloric effect is reversible.

We must now consider for each case how the heat would spread and what temperature rise is produced in the specimen. If the specimen is bathed in liquid helium II, the high speed of second sound ensures that the heat which gets into the liquid helium is spread over such a large volume that the temperature rise is negligible. The only effect to be considered is the effect of the instantaneous power in the rise of temperature it causes due to the Kapitza boundary-layer resistance; this resistance is not very reliably known but a typical estimate is $10^{-6}/T^3$ °K erg^{-1} s cm^2. Only the instantaneous power in (b) and (c) need be considered, since the glass is not in good contact with the ebonite wall of the pick-up coil; the relevant power per unit area at the time of the blip is thus $\frac{1}{10}W_0\pm80E$ or $2\times10^3\pm4\times10^4$ (the $\pm$ according as the field is rising or falling), though in fact it is very doubtful if the larger contribution from the magneto-caloric effect should really be included, since thermal contact with the specimen is probably far from perfect. At 1·2 °K this power should produce a rise of roughly $0{\cdot}001\pm0{\cdot}02$ °K in the specimen, though initially, when the eddy current power is 400 times bigger, the rise should be 0·5 °K. Probably the $\pm0{\cdot}02$ °K is an over-estimate of the magneto-caloric effect, and unless some instability occurs for the high initial power, such that local evaporation occurs, it is fairly safe to assume that below the λ-point the specimen is effectively at bath temperature at the time of the blip, though there is not a very large safety margin and for thicker and purer specimens an appreciable temperature rise might occur.

Above the λ-point, all three modes of heating must be considered, and the temperature rise of the specimen can be estimated roughly by supposing that the total heat produced up to the time of observation spreads over a distance of order L given by

$$L = (\kappa\tau/C)^{\frac{1}{2}}, \tag{38}$$

where κ is the thermal conductivity and C the heat capacity per ml. of the medium, and that the temperature rise is determined by the heat capacity of the source, together with that of a thickness L of the surrounding medium. This almost certainly exaggerates the temperature rise, since it assumes effectively that all the heat is produced instantaneously at the moment the discharge starts, and moreover it ignores numerical coefficients which would appear in a detailed calculation. The heat produced in the pick-up coil has first to pass through a thin wall (0·2 mm thick) of ebonite; since for typical plastics at 2·5 °K $\kappa \sim 3000$ and $C \sim 3000$ (erg units throughout), $L \sim 1$ mm for $\tau = 10^{-2}$ s, and the ebonite wall can be ignored. For liquid helium at 2·5 °K, $\kappa \sim 2000$, $C \sim 3 \times 10^6$ so $L \sim 2{\cdot}5 \times 10^{-3}$ cm and the heat capacity of a layer of liquid helium of this thickness round the inside of the hole in the pick-up coil (1 mm diameter, 5 mm long) is of order 1200 erg/deg K. The heat capacity of the copper wire itself and the ebonite which is penetrated by the heat waves is small in comparison ($\sim$ 100 ergs/deg K) and can be ignored. Thus the liquid helium within $2{\cdot}5 \times 10^{-3}$ cm of the inside ebonite wall may rise by 0·4 °K but it is unlikely that the specimen rises by anything like as much since the glass specimen tube is probably separated from the ebonite wall by more than L. The construction of the coil is such that it is difficult to know whether or not its outer turns are also in contact with liquid helium; if they are, the effective heat capacity would be greatly increased (say five times) and the rise of temperature would be correspondingly reduced. Once again then, there is a rather small safety margin, but probably there is no appreciable temperature rise due to eddy current heating the coil.

The 250 ergs produced by the magneto-caloric effect in the glass tube is more dangerous because the specimen is in direct contact with it. The heat is again spread through a thin layer of liquid helium, but this time it is the layer of liquid helium in direct contact with the specimen and the temperature rise of order 0·2 °K should be that of the specimen. It should be noticed that in these conditions the temperature varies as $C^{-\frac{1}{2}}$ and because of the rapid rise of C near the λ-point the temperature rise increases as T increases from the λ-point to about 2·5 °K.

The 70 ergs produced in the specimen itself, although the smallest figure of the three considered, is the most dangerous of all because it is generated in the specimen itself. The layer of liquid helium of thickness L surrounding the specimen has a much smaller volume than the layers discussed above because of the small diameter of the specimen and its heat capacity is only about 200 erg per °K, so that the temperature rise should be 0·3 °K.

Although it is unlikely that the heat developed by any of the heating processes is sufficient to produce a gas bubble of any appreciable size around the specimen, it should be pointed out that if the specimen is in immediate contact with an appreciable thickness of vapour rather than liquid, the temperature rise may become quite serious. For helium vapour at 1·2 °K, $\kappa \sim 400$ and $C \sim 2500$, so for $\tau = 10^{-2}$ s we find $L \sim 4 \times 10^{-2}$ cm which is nearly as much as the radius of the specimen tube. The heat capacity of the vapour into which the heat spreads is of order $\pi L^2 lC$, i.e. $\pi\kappa l\tau$ which is only 6 ergs/deg K, which suggests a temperature rise of 12 °K. Obviously this is a much exaggerated estimate since it ignores the heat flow into the surrounding ebonite which would add appreciably to the heat capacity and it ignores the changes of the parameters in the calculation which would occur as the temperature rose. None of the experimental results suggest a temperature rise of anything like this order so probably the conditions envisaged never really occur.

One other possibility which needs consideration is that a temperature rise occurs as a result of a poorly conducting layer round the specimen, such as the petroleum jelly or Durofix used to hold the specimen in place. The thermal conductivity of such a layer is unlikely to be less than 1000 and assuming it to be as thick as 10^{-2} cm, we find that for the power per unit area of 2×10^3 ergs s^{-1} cm^{-2} produced at the time of the oscillations, the temperature rise should be only of order 0·02 °K at most. The propagation distance L in such a material is of order 1 mm for 10^{-2} s (taking C as 500) so there is no question of such a layer storing up an appreciable fraction of the energy released earlier. Unless the value of κ has been much exaggerated it seems that even a fairly thick petroleum jelly layer should not be important.

To sum up then, it seems that the various sources of heat production considered are unlikely to produce any appreciable temperature rise in the specimen as long as the liquid helium is below the λ-point, but above the λ-point a rise of perhaps a few tenths of a degree might occur. The exact magnitude of this rise cannot be calculated without a more detailed discussion for which many of the required parameters are uncertain, but the evidence of the temperature variation of the amplitude of oscillations suggests that the rise is in fact hardly more than 0·1 °K. The calculations show, however, that all the effects considered have only a small margin of safety and that quite slight modifications of the experimental conditions might well lead to a much larger temperature rise.

Appendix. The 'gliding tone' effect

Since H varies parabolically with time around the maximum of the field and the e.m.f. developed in the pick-up coil is proportional to $\mathrm{d}H/\mathrm{d}t$, this e.m.f. is proportional to $t \sin \beta t^2$, (t is measured from the time of maximum field) and, ignoring damping, the e.m.f. y across the condenser of the resonant circuit (resonant angular frequency ω) satisfies the differential equation

$$\mathrm{d}^2y/\mathrm{d}t^2 + \omega^2 y = bt \sin \beta t^2. \tag{A 1}$$

The instantaneous angular frequency of the 'driving' e.m.f. is $2\beta t$, so if resonance occurs at time τ (we consider only the case of falling field) we have

$$\beta = \omega/2\tau. \tag{A 2}$$

It is convenient to introduce the notation

$$T = \omega t, \quad \alpha = \beta/\omega^2 = 1/2\omega\tau, \quad a = b/\omega^3; \tag{A 3}$$

(A 1) then becomes

$$\mathrm{d}^2y/\mathrm{d}T^2 + y = aT \sin \alpha T^2$$

and resonance occurs for $T = 1/2\alpha$.

We are interested only in the particular integral and this is given by

$$y = \int_0^T av \sin \alpha v^2 \sin (T-v)\,dv \tag{A 4}$$

which reduces to

$$y = \frac{a}{2\alpha}\sin T - \frac{a}{4\alpha}\left(\frac{\pi}{2\alpha}\right)^{\frac{1}{2}} \{(C(s+\epsilon)-C(\epsilon))\cos(T+1/4\alpha)+(S(s+\epsilon)-S(\epsilon))\sin(T+1/4\alpha)$$
$$+(C(s-\epsilon)+C(\epsilon))\cos(T-1/4\alpha)-(S(s-\epsilon)+S(\epsilon))\sin(T-1/4\alpha)\} \tag{A 5}$$

where $$C(u) = \int_0^u \cos\tfrac{1}{2}\pi u^2 du, \quad S(u) = \int_0^u \sin\tfrac{1}{2}\pi u^2 du,$$

$$u = (2\alpha/\pi)^{\frac{1}{2}}v, \quad s = (2\alpha/\pi)^{\frac{1}{2}}T, \quad \epsilon = (2\alpha/\pi)^{\frac{1}{2}}/2\alpha. \tag{A 6}$$

For $u \gg 1$ and u positive, the asymptotic forms of $C(u)$ and $S(u)$ are

$$C(u) = \tfrac{1}{2} + \frac{1}{\pi u}\sin\tfrac{1}{2}\pi u^2, \quad S(u) = \tfrac{1}{2} - \frac{1}{\pi u}\cos\tfrac{1}{2}\pi u^2 \tag{A 7}$$

and it should be noted that $C(-u) = -C(u)$ and $S(-u) = -S(u)$. For the approach to resonance, $s-\epsilon$ is negative and for $s-\epsilon \ll -1$ (i.e. for $\tau - t \gg (\pi\tau/\omega)^{\frac{1}{2}}$) using (A 7), (A 5) reduces to

$$y = (bt/(\omega^2-4\beta^2t^2))\sin\beta t^2. \tag{A 8}$$

This is of course exactly the result for the growth towards an infinite amplitude for slow variation of a driving frequency $2\beta t$, i.e. the fact that the driving frequency is time dependent becomes irrelevant.

For $s = \epsilon$ (i.e. $t = \tau$), where resonance would occur if the gliding tone effect were ignored, we find

$$y = \tfrac{1}{2}b(\tau/\omega)^{\frac{3}{2}}\,(\tfrac{1}{2}\pi)^{\frac{1}{2}}(\sin(\tfrac{1}{2}\omega\tau-\tfrac{1}{4}\pi)+(2\pi\omega\tau)^{-\frac{1}{2}}\sin\tfrac{1}{2}\omega\tau). \tag{A 9}$$

The second term can be neglected in our conditions, since τ is many times the period of the resonancy frequency.

For $s-\epsilon \gg 1$, we find

$$y = (bt/(\omega^2-4\beta^2t^2))\sin\beta t^2 + b(\tau/\omega)^{\frac{3}{2}}(\tfrac{1}{2}\pi)^{\frac{1}{2}}\sin(\omega t - \tfrac{1}{2}\omega\tau - \tfrac{1}{4}\pi). \tag{A 10}$$

To get a better idea of the meaning of (A 10) it is helpful to measure $t-\tau$ in units of $(\pi\tau/\omega)^{\frac{1}{2}}$, i.e. to put

$$t = \tau + \mu(\pi\tau/\omega)^{\frac{1}{2}}$$

so that (A 10) becomes

$$y = -\tfrac{1}{2}b\frac{(\tau/\omega)^{\frac{3}{2}}}{\pi^{\frac{1}{2}}\mu}\sin(\tfrac{1}{2}\omega\tau+\mu(\pi\omega\tau)^{\frac{1}{2}}+\tfrac{1}{2}\pi\mu^2)+b(\tfrac{1}{2}\pi)^{\frac{1}{2}}\,(\tau/\omega)^{\frac{3}{2}}\sin(\tfrac{1}{2}\omega\tau+\mu(\pi\omega\tau)^{\frac{1}{2}}-\tfrac{1}{4}\pi). \tag{A 11}$$

Although (A 11) is valid only for $\mu \gg 1$, it will still apply roughly even for μ only slightly greater than 1 and it can be seen that a maximum amplitude should occur for μ a little less than $(\tfrac{3}{2})^{\frac{1}{2}}$, where the first term is just in phase with the second (a little less, because μ appears in the denominator of the first term). This maximum amplitude will be somewhat larger than its value for $\mu = (\tfrac{3}{2})^{\frac{1}{2}}$ i.e.

$$|y| = b(\tau/\omega)^{\frac{3}{2}}(\tfrac{1}{2}\pi)^{\frac{1}{2}}\{1+1/(3^{\frac{1}{2}}\pi)\}. \tag{A 12}$$

This will be followed by a minimum amplitude approximately for $\mu = (\frac{7}{2})^{\frac{1}{2}}$ and so on, and the first minimum is approximately

$$|y| = b(\tau/\omega)^{\frac{3}{2}}(\tfrac{1}{2}\pi)^{\frac{1}{2}}\{1-1/(7^{\frac{1}{2}}\pi)\}. \tag{A 13}$$

There should, then, be rather more than $\frac{1}{2}(7^{\frac{1}{2}}-3^{\frac{1}{2}})(f\tau)^{\frac{1}{2}}$ or $0{\cdot}46(f\tau)^{\frac{1}{2}}$, periods of oscillation between the maximum and the first minimum (where $f = \omega/2\pi$).

The predicted 'ringing' effect is clearly visible in oscillograms such as figure 15, plate 2, though because of damping, the second term in (A 11) evidently decays fairly rapidly with time. In figure 15 $f \sim 10^5\,\text{s}^{-1}$ and $\tau \sim 10^{-3}$ s, so there should be only about five oscillations between the maximum and the first minimum; the individual peaks of the oscillations are clearly visible in figure 15 and there are in fact about seven; probably this slight discrepancy can be ascribed to insufficient accuracy of the formula for μ so close to 1, and perhaps, also to the effects of damping. The fact that the blip for rising field is of very similar size and appearance to that for falling field suggests that the above calculations are at least approximately valid for the case of resonance approached from the side of high rather than low frequencies, a case which is more difficult to treat mathematically.

The main relevance of these calculations is not only in explaining semi-quantitatively some of the curious features in resonant pictures, which seemed at first rather puzzling, but also in showing that the amplitude of a resonant blip is larger than the amplitude would be at the same time without resonance by a factor M, which is easily shown to be approximately

$$M = 2ft_{\text{max.}}\,(H/F)^{\frac{1}{2}}(1+1/3^{\frac{1}{2}}\pi), \tag{A 14}$$

where $t_{\text{max.}}$ is the time from the start of the discharge to the peak field. For $f \sim 10^5\,\text{s}^{-1}$, $t_{\text{max.}} \sim 10^{-2}$ s, $H \sim 10^5$ G, $F \sim 5\times10^8$ G, we have $M \sim 30$. The actual magnification is a good deal smaller because of damping; the static Q of the resonant circuit was only about 5 or 10, so it is not surprising that the real value of M was only of order 3 or 4. In our discussions of amplitude effects we have assumed that even with damping, the gliding tone effect still involves a factor $(H/F)^{\frac{1}{2}}$ in the effective magnification over non-resonant conditions, but without a detailed calculation and further experiments it is difficult to be certain that this is sound. It is possible that if the static Q is as small as 5 or 10, i.e. much less than the theoretical M for infinite static Q, that the magnification would be just approximately Q and that no factor $(H/F)^{\frac{1}{2}}$ is required.

[*Note added in proof* 30 *July* 1962.] T. D. Holstein (private communication) has shown that a strict application of the self-consistent field method does indeed lead to the replacement of H by B in the conventional formula for magnetization, as conjectured in the discussion of the 'frequency modulation' effect. A. B. Pippard (*Proc. Roy. Soc.* A, to be published) has also justified this conjecture by an argument based on the assumption that the replacement of H by B must be correct in the formula for entropy, and he has considered what happens for $a > 1$ (see equation (15)), showing that the actual course of the magnetization curve is profoundly influenced by eddy currents. Pippard points out also that the discussion of eddy currents leading to equation (33) is incomplete, because it assumes that the observed oscillatory e.m.f. comes only from the oscillatory part of the magnetization and leaves out of account the contribution from the oscillatory part of H (which proves to be of comparable importance when the de Haas–van Alphen effect is considered in working out the field distribution associated with eddy currents). For a slab specimen the correct treatment leads to a considerable enhancement in the effect of eddy currents in cutting down amplitude, but the more complicated problem of a cylindrical specimen has not yet been worked out.

The development of the impulsive high-field method owes much to the ingenuity and skill of the late Mr E. Laurmann who designed and built most of the original equipment and assisted in the preliminary experiments between 1952 and his death in 1954, also to Dr R. G. Chambers and Dr D. V. Osborne who gave invaluable help with electronic problems in the early stages. Mr H. L. Davies built most of the new equipment described in this paper, and invented the ratchet wheel rotating system which was vital for the definitive experiments. He also prepared some of the copper and all the silver and gold crystals and assisted in the experiments, and I should like to acknowledge gratefully his willing and patient collaboration throughout. This study of the noble metals was opened up by the use of copper whiskers and I am very grateful to the General Electric Company of Schenectady, New York, and in particular to Mrs E. Fontanella, for their generosity in preparing and supplying all the whiskers used in these experiments. Throughout the work I have benefited greatly from many discussions particularly with Professor A. B. Pippard, F.R.S., and also with Dr V. Heine, Dr V. M. Morton, Dr W. F. Vinen and Dr J. M. Ziman. Dr M. G. Priestley and Mr B. R. Watts carried out a few of the measurements on their equipment and have contributed a number of valuable suggestions in discussion. Mr R. J. Balcombe carried out the resistivity measurements of table 1. My understanding of the frequency modulation effect has been much helped by discussions with Professor A. B. Pippard, Dr P. W. Anderson, Mr B. D. Josephson, Dr D. J. Thouless and Mr H. P. F. Swinnerton-Dyer, and Professor F. Ursell showed me how to calculate the gliding tone effect. Dr J. Ashmead, Dr C. J. Adkins and Mr H. V. Beck have given valuable help in connexion with particular items of the measuring equipment, and Mr F. T. Sadler and his staff have supplied liquid helium on some 140 occasions, often at the sacrifice of their own convenience. To all these I should like to express my warmest thanks. Finally, it is a pleasure to acknowledge gratefully the vital part played by Mr D. J. Roaf, whose skill and patience in calculation has made possible an interpretation far more complete than I could have hoped for when results first began to emerge.

References

Alekseevski, N. E. & Gaidukov, Yu. P. 1959 *J. Exp. Theor. Phys. U.S.S.R.*, **37**, 672.
Barber, N. F. & Ursell, F. 1948 *Phil. Mag.* **39**, 345.
Chambers, R. G. 1956 *Proc. Roy. Soc.* A, **238**, 344.
Dingle, R. B. 1952*a* *Proc. Roy. Soc.* A, **211**, 500.
Dingle, R. B. 1952*b* *Proc. Roy. Soc.* A, **211**, 517.
Fontanella, E. L. & De Blois, R. W. 1959 *Rev. Sci. Instrum.* **30**, 982.
Gold, A. V. 1958 *Phil. Trans.* A, **251**, 85.
Kip, A. F., Langenberg, D. N. & Moore, T. W. 1961 *Phys. Rev.* **124**, 359.
Kosevich, A. M. 1957 *J. Exp. Theor. Phys., U.S.S.R.*, **33**, 735.
Landolt, H. H. & Börnstein, R. 1923 *Physikalisch-Chemische Tabellen* (5th ed.), vol. II.

Lifshitz, I. M. & Kosevich, A. M. 1955 *J. Exp. Theor. Phys., U.S.S.R.*, **29**, 730.
Morton, V. M. 1960 Ph.D. Thesis, Cambridge University.
Onsager, L. 1952 *Phil. Mag.* **43**, 1006.
Pearson, W. B. 1958 *Lattice spacings and structures of metals and alloys.* London: Pergamon.
Pippard, A. B. 1957 *Phil. Trans.* A, **250**, 325.
Priestley, M. G. 1962 *Phil. Mag.* **7**, 1205
Salinger, G. L. & Wheatley, J. C. 1961 *Rev. Sci. Instrum.* **32**, 872.
Shoenberg, D. 1952*a* *Phil. Trans.* A, **245**, 1.
Shoenberg, D. 1952*b* *Nature, Lond.*, **170**, 569.
Shoenberg, D. 1953 *Physica*, **19**, 791.
Shoenberg, D. 1957 *Progr. Low. Temp. Phys.* **2**, 226.
Shoenberg, D. 1959 *Nature, Lond.*, **183**, 171.
Shoenberg, D. 1960*a* *Phil. Mag.* **5**, 105.
Shoenberg, D. 1960*b* *The Fermi surface*, p. 74. New York: John Wiley and Sons, Inc.
Shoenberg, D. 1962 *Proc. Phys. Soc.* A, **79**, 1.

PHILOSOPHICAL TRANSACTIONS OF THE ROYAL SOCIETY A MATHEMATICAL, PHYSICAL & ENGINEERING SCIENCES

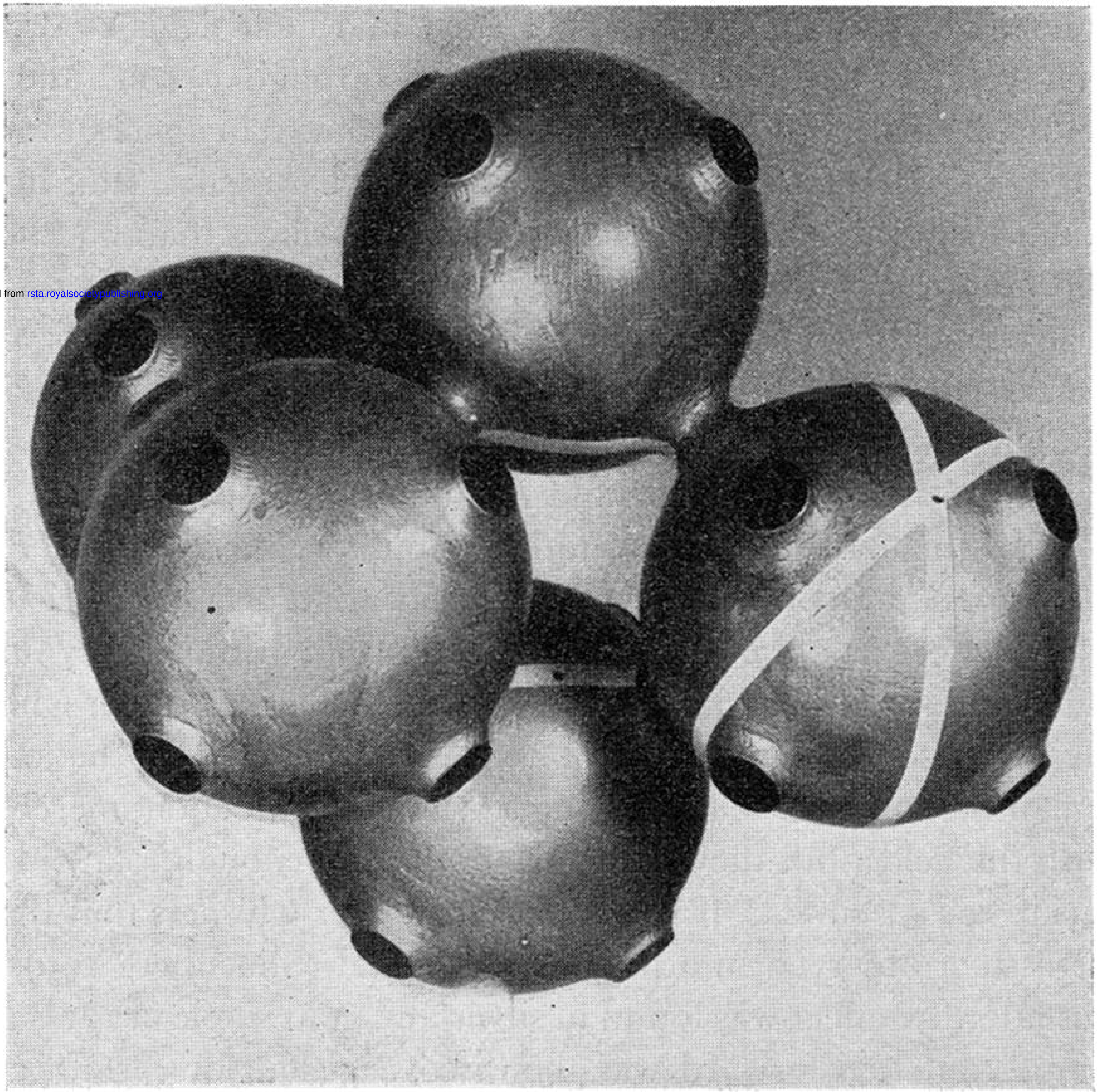

FIGURE 1. Schematic model of Fermi surface; the real surfaces are much less spherical (a photograph showing the shape of the gold surface appears in Shoenberg (1962) and sections of the various surfaces are shown in figure 3 of II). The white bands pick out the (100) and (111) 'belly' sections (vertical and oblique, respectively), and part of the 'four-cornered rosette'.

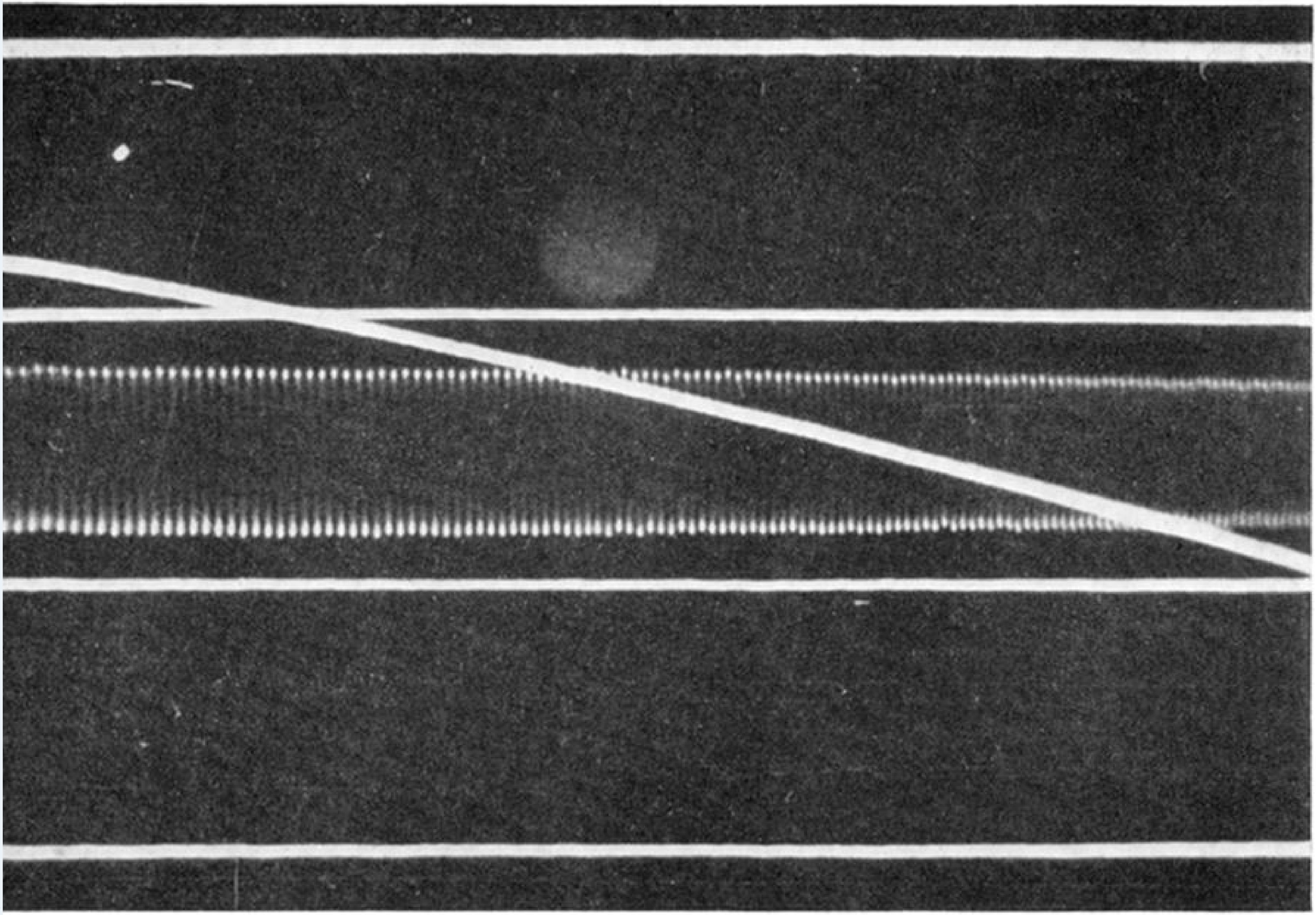

FIGURE 3. Oscillations of Cu 46, illustrating the direct method of measuring frequency. Calibration lines at $H = 1{\cdot}047$, $1{\cdot}070$, $1{\cdot}093$ and $1{\cdot}116 \times 10^5$ G; about 1 ms across picture.

PHILOSOPHICAL TRANSACTIONS OF THE ROYAL SOCIETY A MATHEMATICAL, PHYSICAL & ENGINEERING SCIENCES

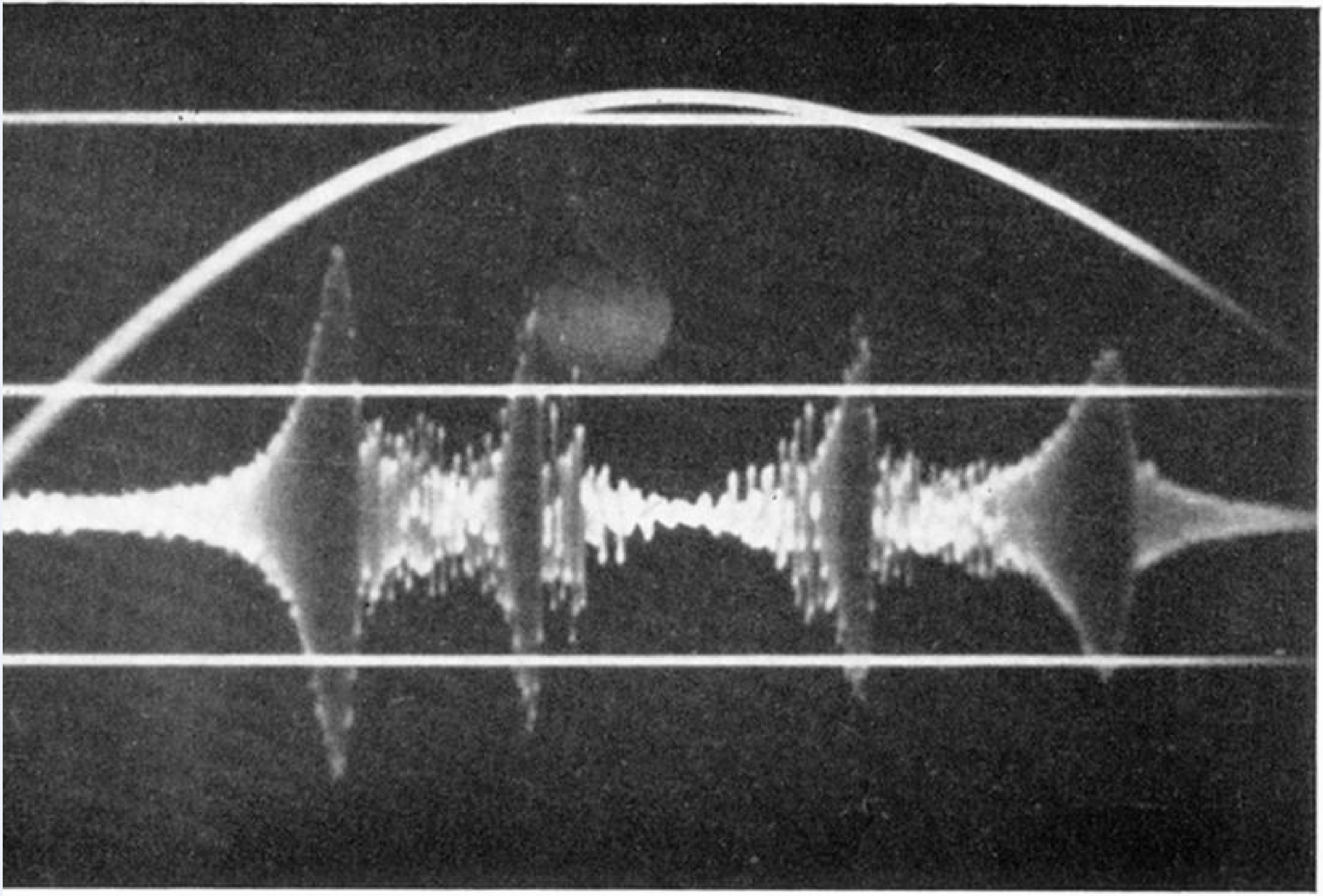

PHILOSOPHICAL TRANSACTIONS OF THE ROYAL SOCIETY A MATHEMATICAL, PHYSICAL & ENGINEERING SCIENCES

IGURE 4. Belly and rosette blips for Au 36, illustrating the peak-to-peak method. The resonant frequency is about 44 kc/s; calibration lines at $H = 1{\cdot}05$, $1{\cdot}16$ and $1{\cdot}28 \times 10^5$ G; about 9 ms across picture.

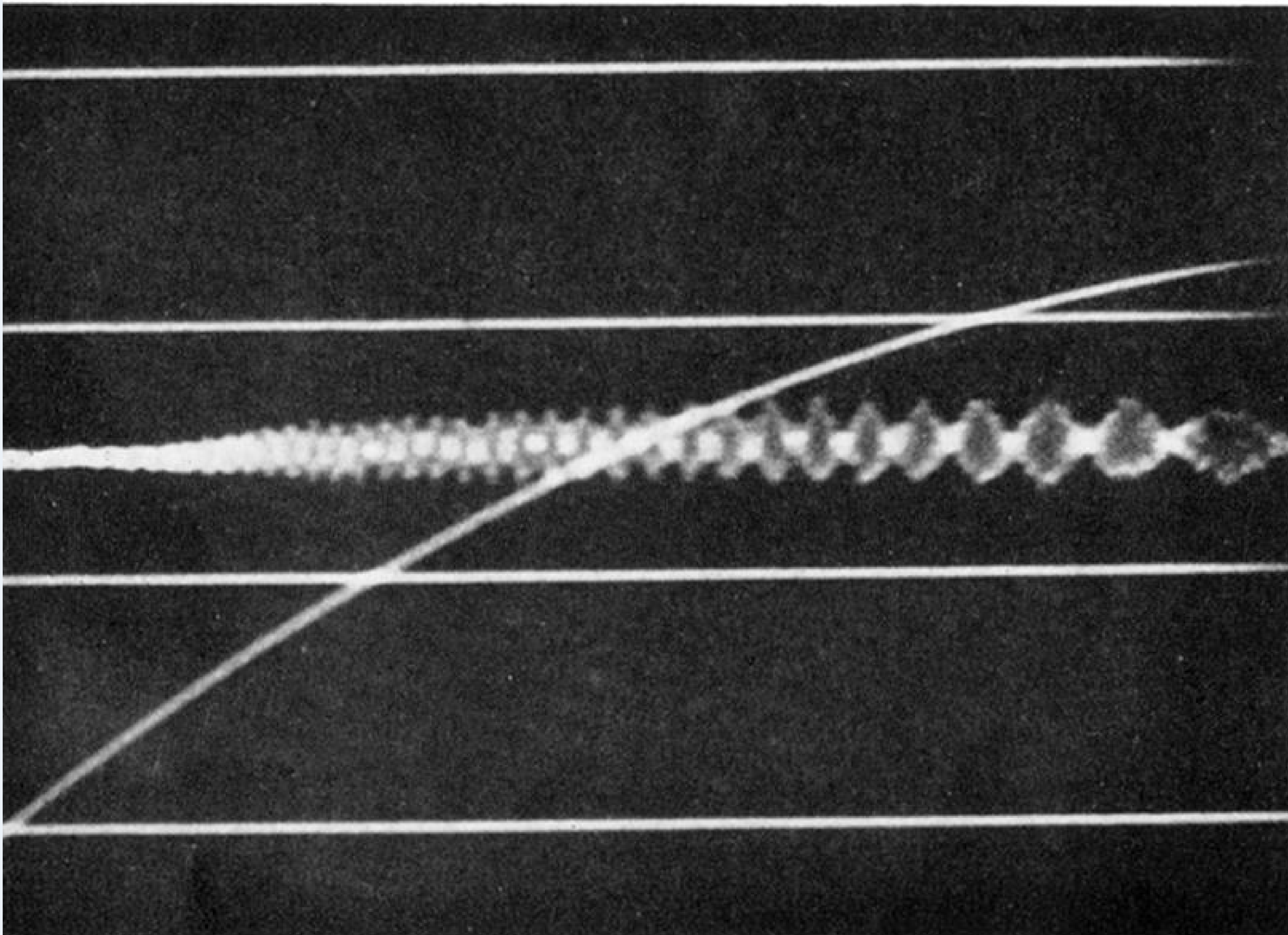

FIGURE 6. (*a*) Beats between Cu 49 set 2° off [100] in specimen coil and Cu 47 [111] in reference coil. Rising field only; calibration lines at 0·93, 1·05, 1·16 and $1{\cdot}28 \times 10^5$ G; about 5 ms across picture.

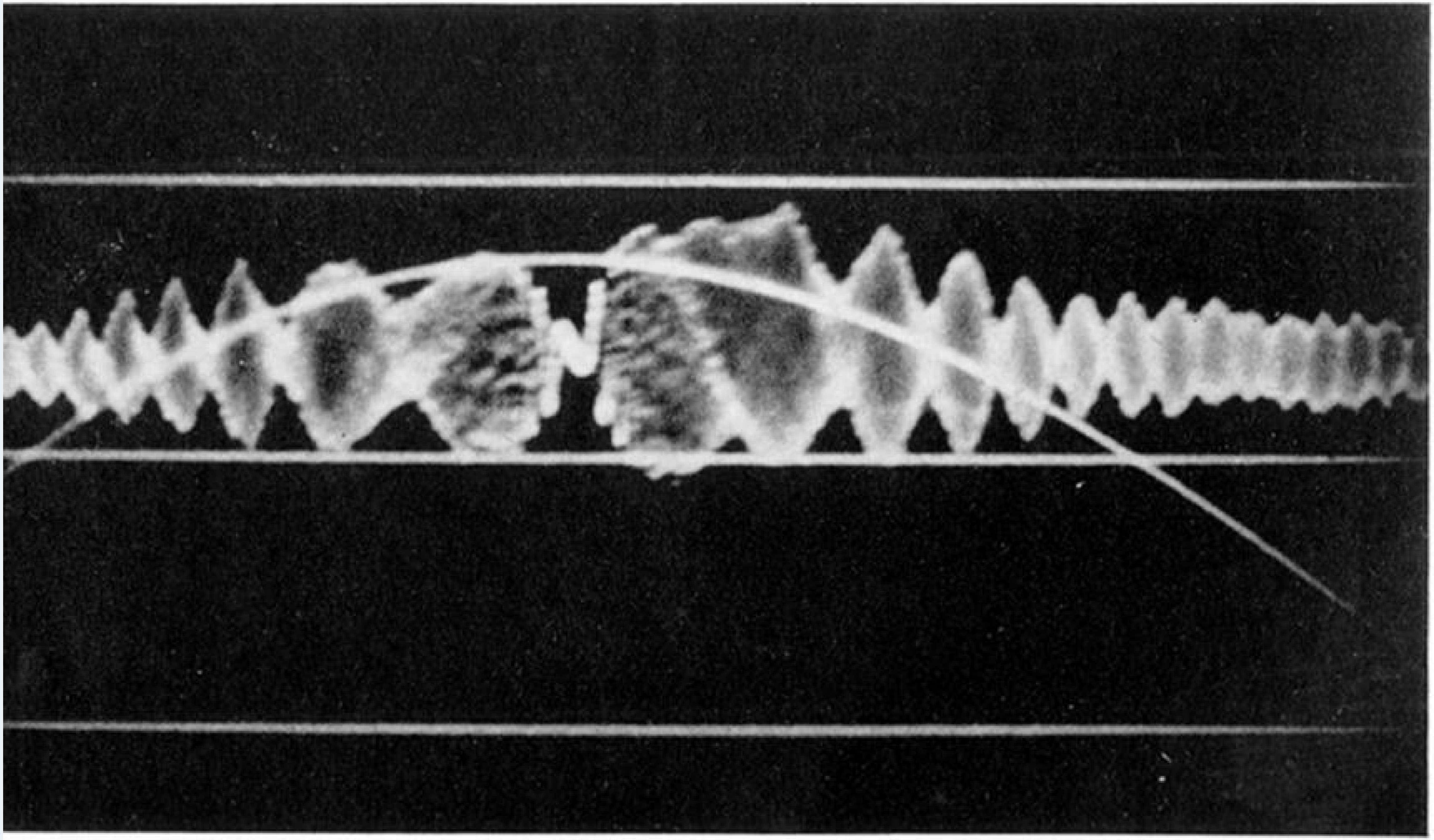

IGURE 6. (*b*) Beats between Ag 30 set about 14° off [100] in specimen coil and Ag 27 [111] in reference coil. Calibration lines at 1·05, 1·16 and $1{\cdot}28 \times 10^5$ G; about 10 ms across picture.

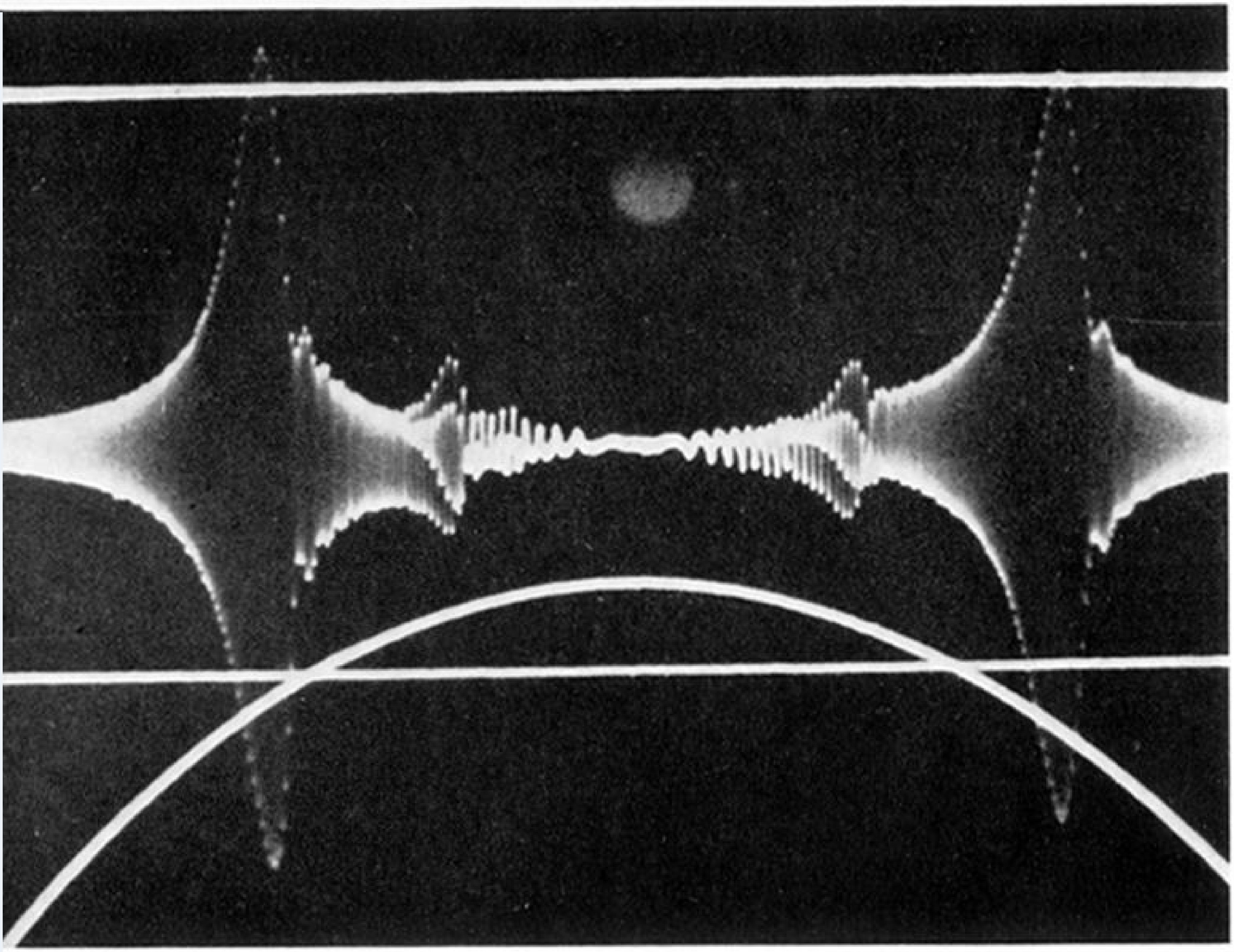

IGURE 15. Resonant blips for Cu 46 (H along [111]) illustrating the 'ringing' effect associated with the 'gliding tone' and the presence of an appreciable first harmonic. Calibration lines at $1{\cdot}07$ and $1{\cdot}12 \times 10^5$ G; time across picture about 3 ms.

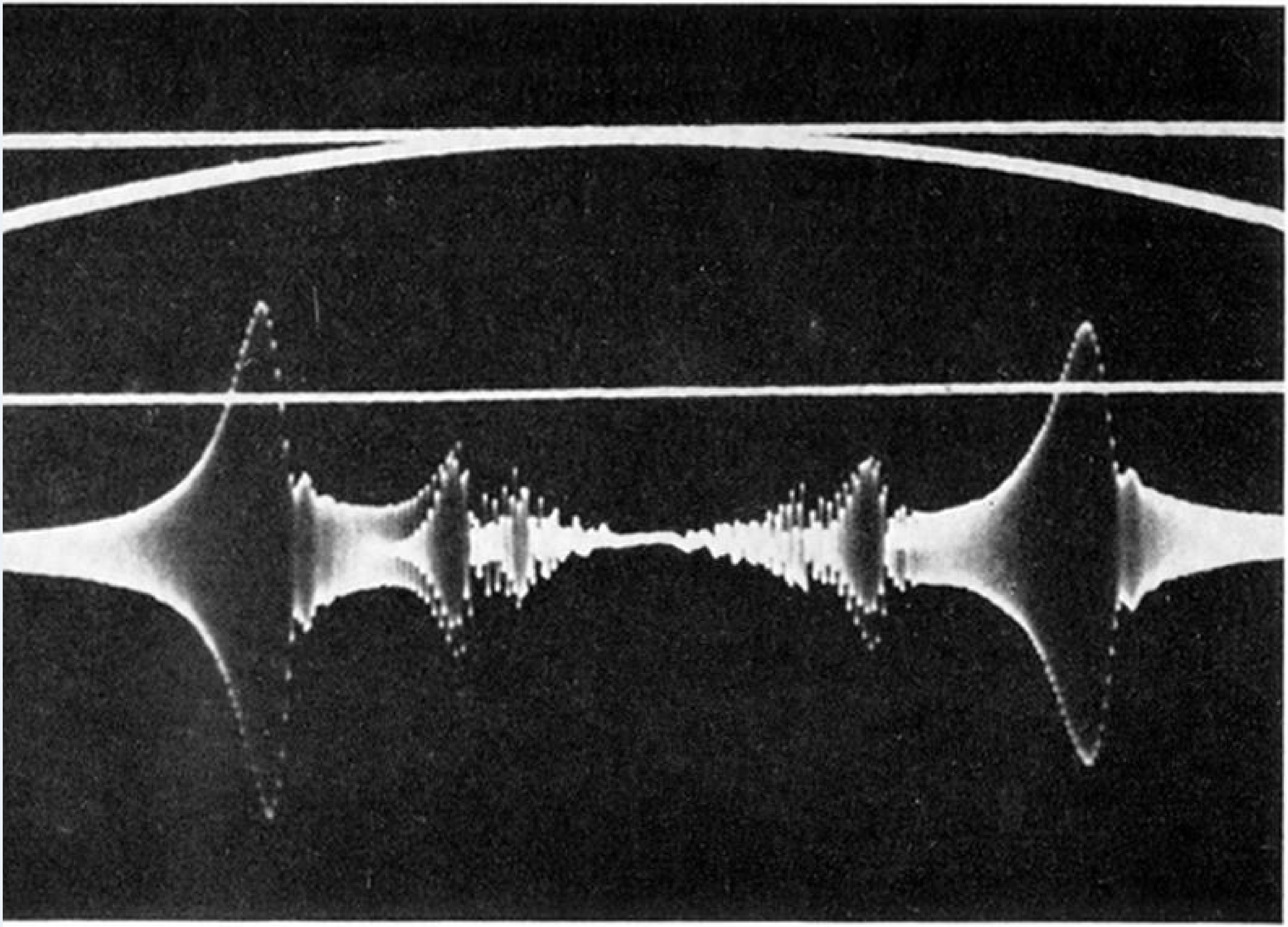

FIGURE 17. Resonant blips for Cu 46 (*H* close to [111]), showing strong first and second harmonics; the points marked with an arrow in figure 18 refer to this picture. Calibration lines at 1·02 and $1{\cdot}12 \times 10^5$ G; time across picture about 3 ms.

MATHEMATICAL, PHYSICAL & ENGINEERING SCIENCES
THE ROYAL SOCIETY A
PHILOSOPHICAL TRANSACTIONS OF

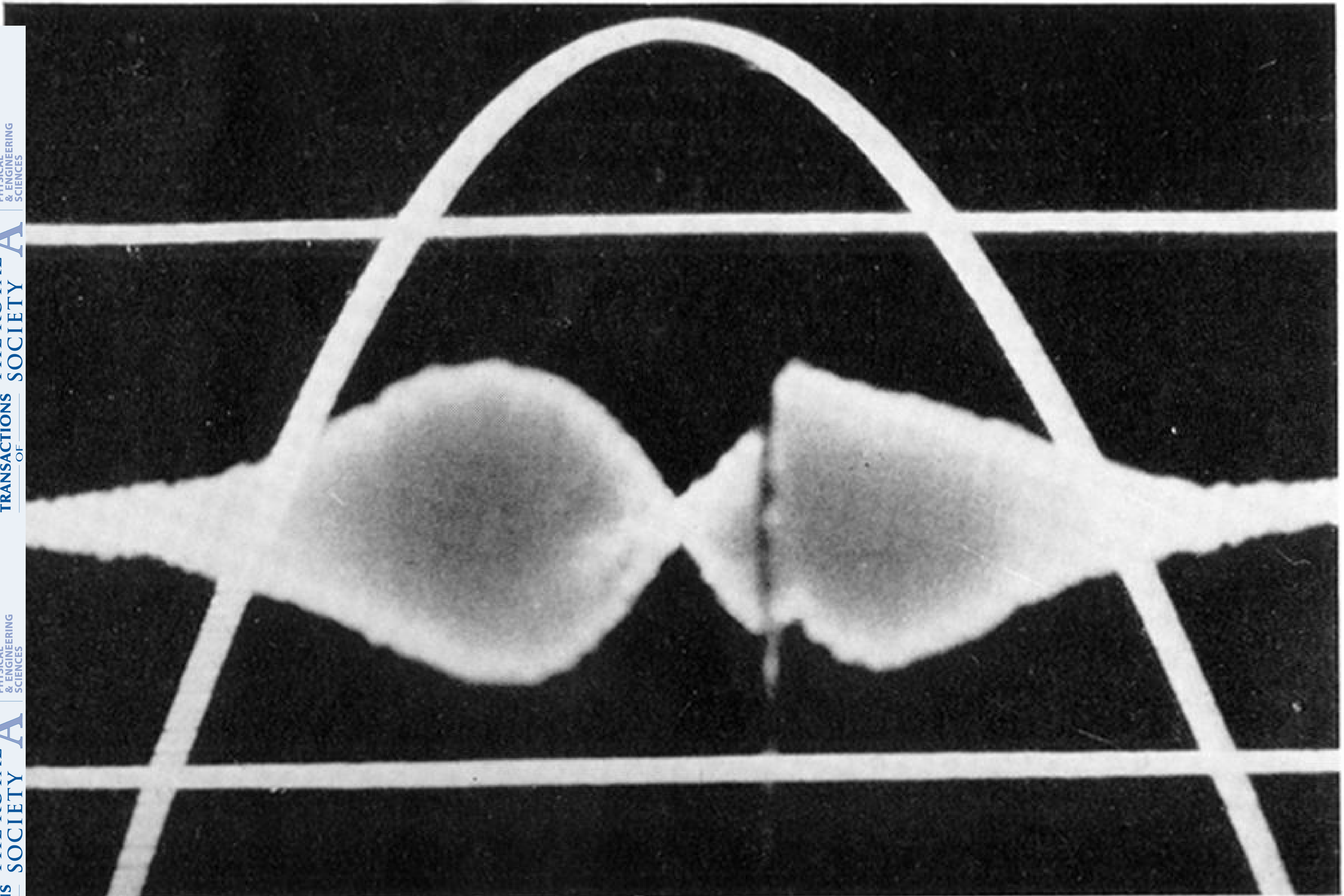

Figure 19. Envelope of oscillations in Cu 43 (H close to [111]) without resonance, showing smooth decay of oscillations as field falls off. The break on the right is an artefact. Calibration lines at 0·88 and $0{\cdot}98 \times 10^5$ G; time across picture about 9 ms.

PHILOSOPHICAL TRANSACTIONS OF THE ROYAL SOCIETY A MATHEMATICAL, PHYSICAL & ENGINEERING SCIENCES

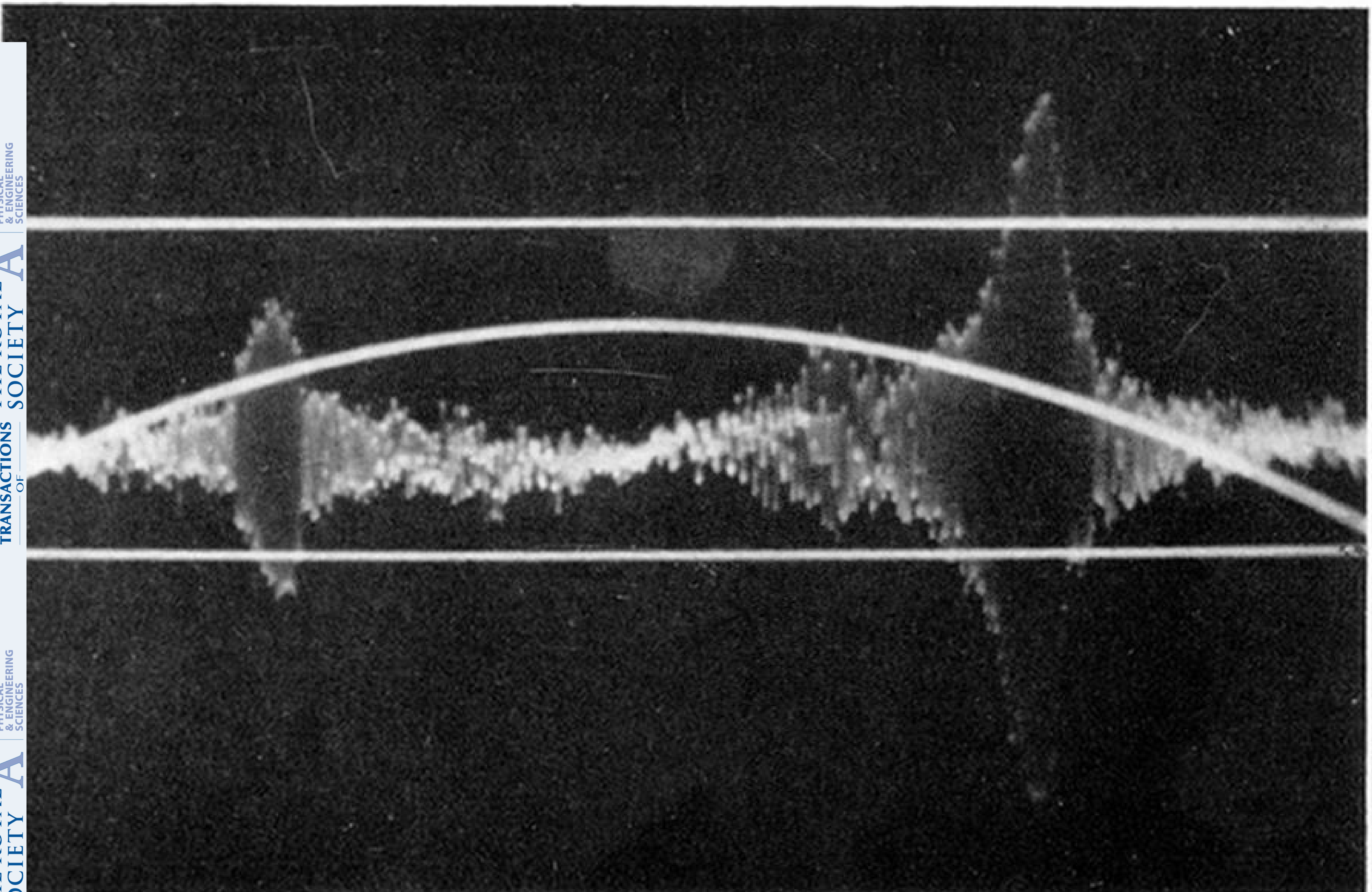

FIGURE 21. Resonant blips for Ag 7 showing unequal blips due to beats of figure 20 being slightly out of phase for rising and falling fields because of eddy current effect. The points marked with an arrow in figure 20 refer to this picture. Calibration lines at $H = 0{\cdot}79$ and $0{\cdot}84 \times 10^5$ G; time across picture about $3\frac{1}{2}$ ms.

PHILOSOPHICAL TRANSACTIONS OF THE ROYAL SOCIETY A MATHEMATICAL, PHYSICAL & ENGINEERING SCIENCES